AD-A192 270 HIGH LATITUDE IONOSPHERIC RADIO STUDIES(U) LOWELL UNIV 1/2
MA CEOTER FOR ATMOSPHERIC RESEARCH B W REINISCH ET AL.
JAN 88 ULRF-439/CAR AFGL-TR-87-0056 F19628-83-C-0092
UNCLASSIFIED FFG 4/1 NL

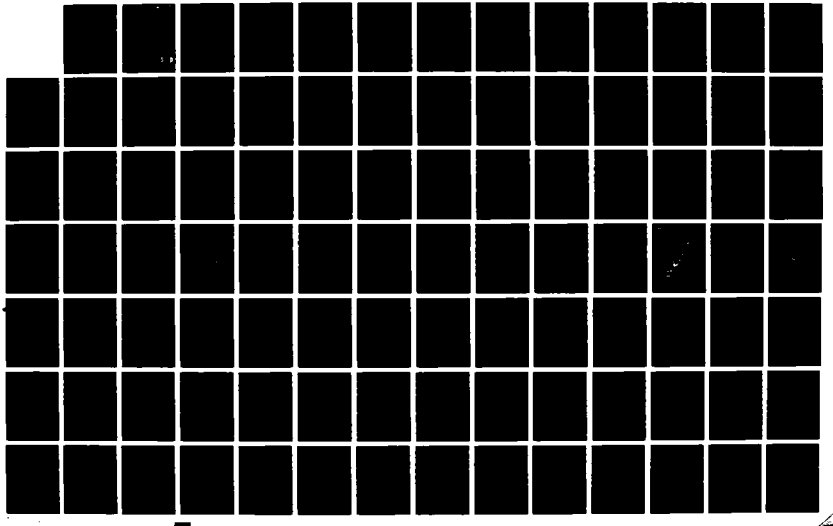

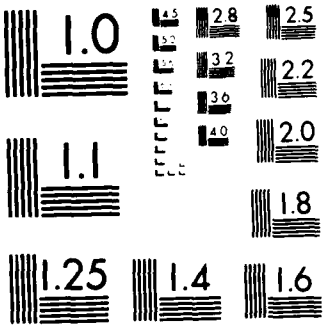

AFGL-TR-87-0056

HIGH LATITUDE IONOSPHERIC RADIO STUDIES

Bodo W. Reinisch
Klaus Bibl
Claude G. Dozois
Robert R. Gamache
David F. Kitrosser
Siu Wing Li
Gary S. Sales
Sau-Har Tang

University of Lowell
Center for Atmospheric Research
450 Aiken Street
Lowell, Massachusetts 01854

January 1988

Final Report

3 May 1983 - 30 September 1986

AIR FORCE GEOPHYSICS LABORATORY
AIR FORCE SYSTEMS COMMAND
UNITED STATES AIR FORCE
HANSCOM AFB, MASSACHUSETTS 01731

UNCLASSIFIED

SECURITY CLASSIFICATION OF THIS PAGE (When Data Entered)

REPORT DOCUMENTATION PAGE		READ INSTRUCTIONS BEFORE COMPLETING FORM
1. REPORT NUMBER AFGL-TR-87-0056	2. GOVT ACCESSION NO.	3. RECIPIENT'S CATALOG NUMBER
4. TITLE (and Subtitle) HIGH LATITUDE IONOSPHERIC RADIO STUDIES		5. TYPE OF REPORT & PERIOD COVERED Final May 3, 1983- September 30, 1986 6. PERFORMING ORG. REPORT NUMBER ULRF-439/CAR
7. AUTHOR(s) Bodo W. Reinisch, David F. Kitrosser, Klaus Bibl, Siu Wing Li, Claude G. Dozois, Gary S. Sales, Robert R. Gamache, Sau-Har Tang		8. CONTRACT OR GRANT NUMBER(s) F19628-83-C-0092
9. PERFORMING ORGANIZATION NAME AND ADDRESS University of Lowell, Center for Atmospheric Research, 450 Aiken Street, Lowell, Massachusetts 01854		10. PROGRAM ELEMENT PROJECT, TASK AREA & WORK UNIT NUMBERS 62101F 464306AJ
11. CONTROLLING OFFICE NAME AND ADDRESS Air Force Geophysics Laboratory Hanscom AFB, MA 01731 Contract Monitor: J. B. Waaramaa (LIS)		12. REPORT DATE January 1988 13. NUMBER OF PAGES 164
14. MONITORING AGENCY NAME & ADDRESS (if different from Controlling Office)		15. SECURITY CLASS. (of this report) UNCLASSIFIED 15a. DECLASSIFICATION DOWNGRADING SCHEDULE

16. DISTRIBUTION STATEMENT (of this Report)

Approved for public release; distribution unlimited.

17. DISTRIBUTION STATEMENT (of the abstract entered in Block 20, if different from Report)

18. SUPPLEMENTARY NOTES

19. KEY WORDS (Continue on reverse side if necessary and identify by block number)

Ionosphere
Digital High-Frequency Sounding
Dynamics
Drift
Main F-Layer Trough

20. ABSTRACT (Continue on reverse side if necessary and identify by block number)

Structure and dynamics of the ionosphere are explored under this contract by digital high-frequency sounding techniques. The research emphasizes the investigation of the auroral and subauroral ionosphere, but also includes studies on the polar cap and mid-latitude ionosphere.

DD FORM 1 JAN 73 1473 EDITION OF 1 NOV 65 IS OBSOLETE

UNCLASSIFIED

SECURITY CLASSIFICATION OF THIS PAGE (When Data Entered)

TABLE OF CONTENTS

TABLE OF CONTENTS (Continued)

TABLE OF CONTENTS (Continued)

TABLE OF CONTENTS (Continued)

LIST OF FIGURES

LIST OF FIGURES (Continued)

LIST OF FIGURES (Continued)

LIST OF FIGURES (Continued)

LIST OF FIGURES (Continued)

LIST OF FIGURES (Continued)

LIST OF FIGURES (Continued)

LIST OF TABLES

1.0 INTRODUCTION

Better understanding of the structure and dynamics of the ionosphere is important for the improvement of radio wave propagation system performance that depends upon or is affected by the Earth's upper atmosphere. Heretofore, instrumentation and data processing limited the information that was available to investigate systematically the detailed spatial and temporal characteristics of the ionosphere. It has been the objective of this research contract to deploy modern instrumentation i.e., the Digisondes 256 and 128PS with associated, improved data processing capabilities to enable comprehensive, efficient study of the ionosphere. The past three years have been significant in the realization of these objectives.

The maturation of the Digisonde 256 for ionospheric drift measurements, provides an alternative to satellites and incoherent scatter facilities for investigating the dynamics of the ionosphere. Results from this contract demonstrate convincingly that ionospheric drift measurements are consistent with the conclusions derived from other instrumentation. The Digisonde has the further advantage of not being restricted in local time (as is a low orbiting satellite) and an economy and efficiency of operation (compared to the few incoherent scatter facilities). This opens new opportunities to investigate the dynamics of larger, synoptic ionospheric patterns both in area and in time.

Previously, ionospheric sounding equipment has been labor intensive to operate if real time information was to be derived. With the development of microcomputer analysis methods for digital ionograms, it is now possible to derive detailed real time information. This capability has been

developed and extended under this contract, such that it is now accurate and reliable and is used for the real time frequency management of radar and communication systems.

Vital to the realization of the real time capability has been the development and improvement of the Automatic Real Time Ionogram Scaler with True Height (ARTIST). Results from this microcomputer based program compare favorably with those obtained through manual scaling by experienced personnel. The ARTIST provides a reliable, accurate data base for true height N(h) real time analysis. Automatic N(h) profile inversion techniques were developed and extended under this contract. These also run within the Digisonde ARTIST computer and the key data are made available in real time to the operational communities that manage radar and communication systems. The results are also significant for the research community as a new data base can be routinely available to assess ionospheric variability in response to solar and geomagnetic stimuli.

During the course of this contract, these new instrumentation and data analysis capabilities have been used in a number of scientific experiments. These are described in Sections 5.0 through 12.0. Unquestionably, two of the most significant results obtained from these experiments are confirmation from airborne and ground observations of:

a. the two-cell convection pattern that dominates the nighttime ionospheric plasma motions in the polar cap and in the auroral region.

b. the plasma flow from the dayside cusp across the polar cap into the nightside auroral zone in form of large patches of ionization when B_z is southward.

These results demonstrate the utility of the Digisonde for the systematic study of ionospheric plasma motions and their interrelationships with solar and geomagnetic phemomena.

Several experiments have demonstrated the utility of the aforementioned instrumentation and data processing techniques. The Precision Targeting Experiment (Section 10.0) was conducted to better understand frequency management of an OTH-B radar, and the Battle TOAD (Section 14.0) experiment was conducted for a detailed assessment of HF communication networks operating in a relatively limited area. Upper atmospheric chemical releases were also observed and reported during this contractual period (Section 15.0).

In the past, the archival of ionospheric data has not been in a convenient form for rapid survey and assessment. The film or paper copy ionograms contain valuable information that the eye and mind lose in scanning a data set. The scaled, tabulated parameters omit detail that is needed for the research scientist or the operational community conducting a post analysis of system performance related to ionospheric conditions. To alleviate this situation, relevant ionogram data have been selected, compressed and recorded on microfiche. The result is a convenient, comprehensive, integrated visual record of ionospheric data.

This contract period has been especially significant in terms of instrumentation development, real time data processing and use of these capabilities in the systematic study of ionospheric structure and dynamics. It is from this perspective that we confidently predict that the next few years will be an exciting time in gaining a new and broader understanding of the near-Earth space environment and its relationship to the dominant extraterrestrial processes in our solar system.

2.0 IONOSPHERIC DRIFT OBSERVATIONS

Observations of the polar cap F region convection were conducted in the center of the polar cap at Thule and Qanaq and at the subauroral stations at Goose Bay and Argentia. Reinisch et al (1987) discuss the Digisonde-Doppler-Drift technique and the drift observations. The current report provides a survey of the processed data.

2.1 Review of the Digisonde Doppler Drift Technique

The use of the Doppler shift imposed on radio waves by moving reflectors to detect the motion of the ionosphere has been discussed previously in Reinisch and Bibl (1983) section 4.0 and references therein. When operating in the drift mode, the Digisonde measures the full Doppler spectrum of the echo signals received at each of four or seven antennas. The data processing technique is illustrated in Figure 2.1. A cross-correlation of the complex spectra (amplitude and phase) yields the locations of multiple reflection points ("sources") and the Doppler shifts which are imposed on these sources. The "map data" (source amplitudes, locations and Doppler frequencies) are used in printing skymaps which illustrate the locations of the reflection areas in the sky. The skymap in Figure 2.1 shows the locations of the strongest sources calculated from a 16-second drift measurement. The sources with negative-Doppler frequencies are labeled 1, 2, 3, ... and the positive-Doppler sources are labeled A, B, C, ... (1 and A representing the lowest Doppler frequencies). The locations and frequencies of these sources indicate motion of the ionosphere towards the northeast. An automated computer analysis of a series of skymaps uses a least-squares-fit procedure to calculate drift velocities and

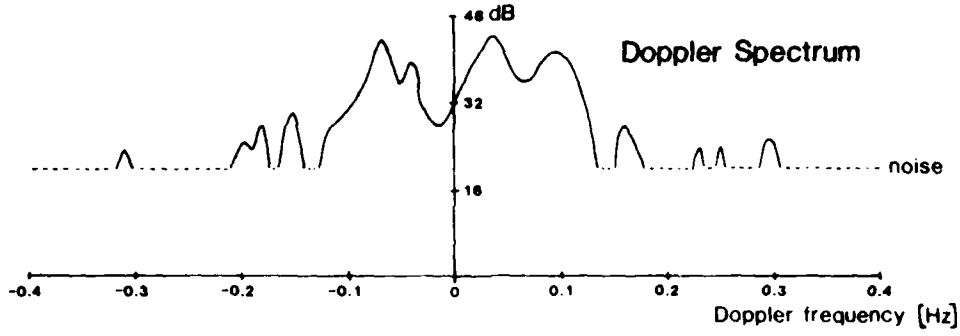

Cross-correlation P of complex Doppler spectrum F from 4 antennas:

$$P_{k\ell} = \sum_{j} \sum_{j'} F_{j\ell} \, F^{*}_{j'\ell} \, \exp -i \, \underline{k} \cdot \left[\underline{a}_{j} - \underline{a}_{j'} \right]$$

ℓ = spectral line
j = antenna
$\underline{a}$ = antenna position

yields angle of arrival of each reflected spectral line.

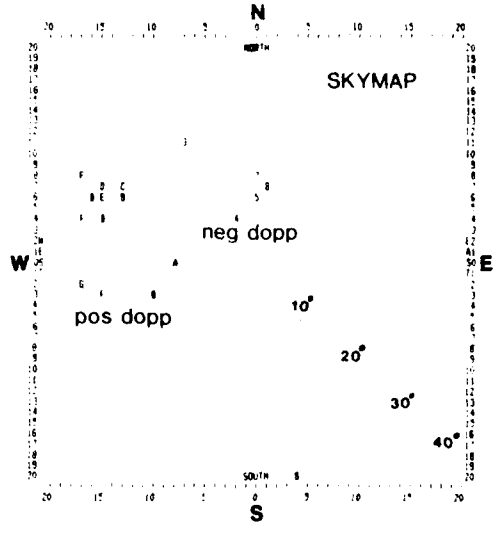

Least Squares Fit for Drift Velocity V:

$$\varepsilon^{2} = \frac{\sum_{s} w_{s} \left(\underline{V} \cdot \underline{R}_{s} - \frac{1}{2} \frac{\Delta f_{s}}{f} c \right)^{2}}{\sum_{s} w_{s}}$$

$\underline{R}_{s}$ = unit position vector of reflector s
Δf_{s} = Doppler frequency of reflector s
f = sounding frequency
w_{s} = weighting factor
c = speed of light in vacuo

DOPPLER DRIFT TECHNIQUE

Figure 2.1

generate a time-sequence of smoothed velocity curves (Figures 2.2-2.8). The observational techniques and methods of analysis used until 1983 have been described by Dozois (1983). Since that report, the installation at Qanaq and Argentia of the later generation Digisonde 256 has made possible better sidelobe suppression through the use of seven receiving antennas instead of four (Bibl et al, 1981). In addition, the implementation of new software for automatic frequency/range bin selection in the ARTIST microcomputer (Section 2.2) assures reliable tracking of the F region echoes. Analysis of the drift data has also been perfected with methods for better separation of source data from the noise and improved smoothing of the velocity curves.

2.1.1 Drift Observations at the Goose Bay Ionospheric Observatory

Since the Goose Bay January 1982 drift measurements discussed in the 1983 Final Report (Reinisch and Bibl, 1983), drift measurements have been made with the Digisonde 128PS in Goose Bay in January, March and December 1983, January-February and September 1984, and January and March 1985. Since April 1985, routine drift measurements are made at Goose Bay during the three regular monthly World Days. Analysis of several days of these drift measurements yields further evidence of a midnight drift reversal from West to East which would be expected if the Goose Bay F region is coupled to the polar cap two-cell convection pattern. Figure 2.2 is a graph of F region drifts at Goose Bay on 14/15 January 1983. The bottom panel shows the azimuth (horizontal direction) of the drift velocity, and the upper panel shows its magnitude, with the vertical velocity component shown as + (up) and - (down) symbols. Each velocity shown is a median

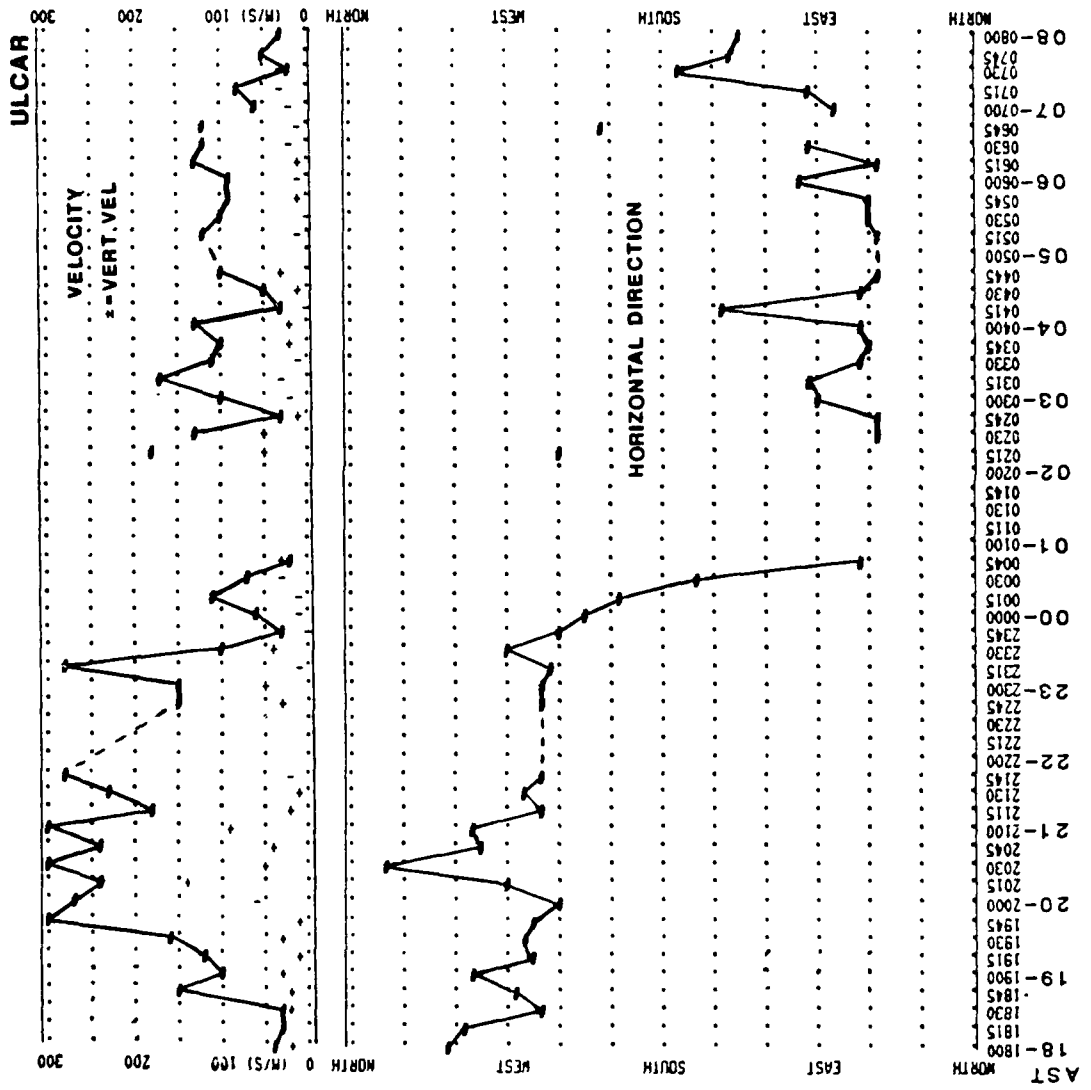
ULCAR
VELOCITY
±=VERT.VEL
300
200
100 (M/S) 0
NORTH
WEST
SOUTH
EAST
HORIZONTAL DIRECTION
AST
F - REGION DRIFT
DIGISONDE OBSERVATIONS AT GOOSE BAY, LABRADOR
14/15 JAN 83 18:00 TO 08:00 AST

Figure 2.2

of about 20 to 25 separate drift cases over a 15-minute period (a case is a 16-second drift measurement made at three different heights simultaneously). The drift reversal from west to east around midnight is very well defined, as would be expected at local (magnetic) midnight when the station leaves the western polar cap convection cell and rotates underneath the dawn cell. It has been observed repeatedly in the Goose Bay data that a distinct change in drift direction is usually accompanied by a decrease in the magnitude of the velocities. We see in Figure 2.2 that the velocity decreases from about 275 m/s to 100 m/s or below as the drift reversal takes place. Also, when the velocities are low, the drift direction tends to be random, whether or not a drift reversal takes place. This randomness is not evident in Figure 2.2, but it has been observed on many other velocity graphs.

Figure 2.3 shows the F-region drift velocities at Goose Bay on 21/22 March 1985. The format of this graph is slightly different from that of the previous one; here, the 15-minute (median) velocities are shown for three simultaneous measurements made at different heights, using three different transmit frequencies. The median of the three simultaneous velocities is indicated by a "#" symbol; the other two velocities are indicated by a number or letter (1, 2, 3, ..., 9, A, B, C, ...) indicating the standard deviation σ over 15 minutes. The standard deviations for the horizontal directions are in 5-degree increments. The magnitudes of the horizontal velocities V_h are plotted with symbols representing σ/V_h in 5% increments. Only the median values of the three simultaneously observed vertical velocity components are shown (+ or -). Below the local time (AST) the corrected geomagnetic local time (CGLT) is also indicated. For several hours before midnight, the median drift is predominantly westward, turning towards the east after midnight. Again,

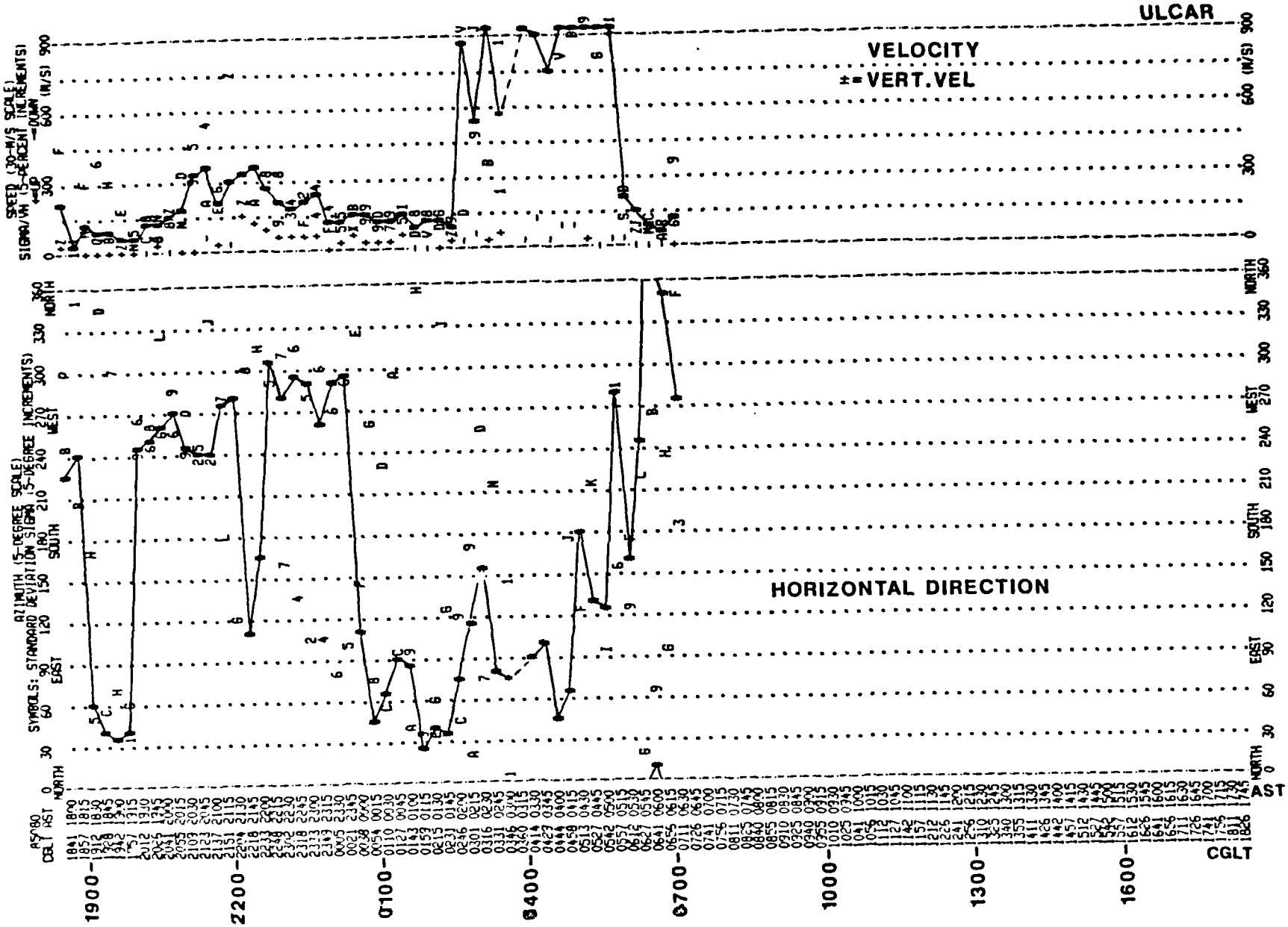

Figure 2.3 F-Region Drift, Goose Bay, Labrador, 21/22 March 1985, 1800 - 1615 AST

the velocity decreases from about 300 m/s to about 100 m/s as the drift changes direction. (Note that the magnitude scale goes to 900 m/s on this graph, as opposed to 300 m/s on the previous graph.)

During periods of high magnetic activity the auroral oval, which bounds the polar cap, expands to lower latitudes and, at night, Goose Bay may be under or poleward of the oval. During more quiet periods Goose Bay is south of the equatorward edge of the oval. The ionospheric drift motion is, of course, affected by arcs and travelling ionospheric disturbances. The polar cap convection pattern appears to be dominant during the time periods involved in Figures 2.2 and 2.3. The printing of the three simultaneous measurements on Figure 2.3 shows that before midnight one of the measurements yields velocities towards the southeast, with the other two velocities being towards the west. On other days, the polar cap convection pattern is not so dominant. Figure 2.4 is an example of this. Although it could be argued that there is a predominance of north-east velocities after magnetic midnight, the directions are random before midnight. The magnitudes of the drift velocities are quite small before midnight; in that case our method of determining the drift direction is less accurate.

2.1.2 Drift Observations at Thule and Qanaq

Drift measurement campaigns were conducted with the DGS 128PS on the AFGL Airborne Ionospheric Observatory parked on the Thule airstrip. These campaigns were in December 1983, January-February 1984 and January and March 1985. After the installation of the Digisonde 256 in Qanaq, drift measurements were made there in April and July 1986. The positions of Thule (86° CGL) and Qanaq (86.8° CGL) relative

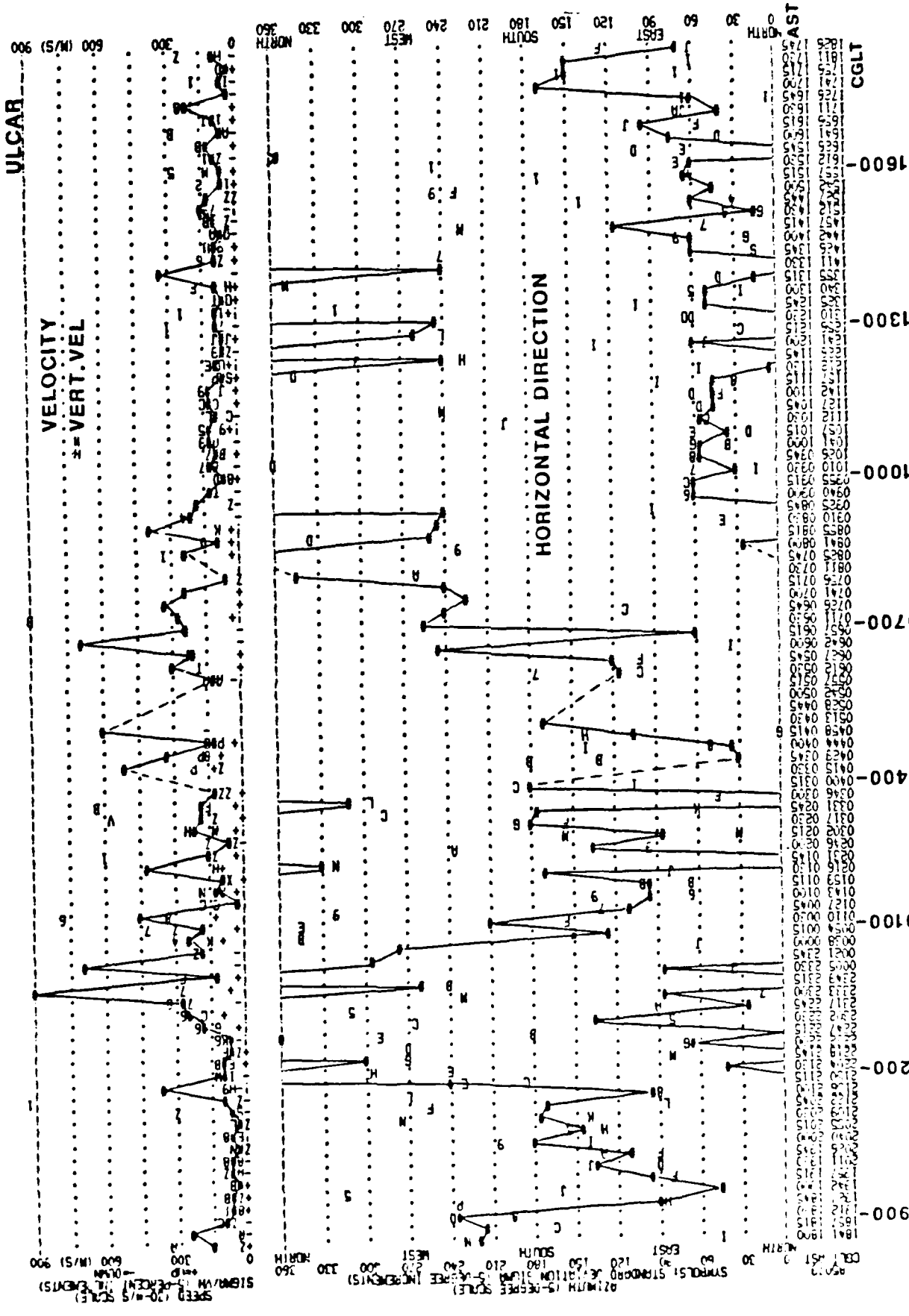

Figure 2.4 F-Region Drift, Goose Bay, Labrador, 20/21 March 1985, 1800 - 1745 AST

to the polar cap convection pattern would lead us to expect antisunward drift motion throughout the day and night. Repeated evidence of antisunward drift in our measurements at both locations establishes this flow as a regular feature in the polar cap F-region.

The January/February 1984 drift campaign at Thule is summarized in Figure 2.5, which shows the median velocities for four days (30/31 January, 31 January/01 February, 01/02 and 03/04 February). The dashed curve indicates the antisunward direction. The velocity curves for each day were systematically smoothed by comparing the three simultaneous measurements for consistency during each 15-minute period and rejecting the velocities whose horizontal directions varied by more than 30°. The medians of these smoothed curves are plotted in Figure 2.5. Note that the drift velocity magnitudes are in general considerably larger than those in Goose Bay: between 300 and 600 m/s and higher. Figure 2.6 shows the drift velocities in the F region over Qanaq from 29 to 31 July 1986. The format of this graph is similar to that of Figures 2.3 and 2.4, showing the 15-minute velocities for the simultaneous measurements (the DGS 256 makes <u>four</u> simultaneous drift measurements) with graph symbols which represent the standard deviation. The medians for each 15-minute period are joined by a solid line (a dashed line indicates a break in the time continuity of the velocities); the straight line approximates the antisunward direction. These drift measurements were made using the automated range selection described in Section 2.2. Although the graph symbols are difficult to read because two days are compressed onto one graph, one can still note the consistency among the four simultaneous measurements and the low standard deviations throughout most of this two-day period. During times of slow changes in the drift, the standard deviation rarely exceeds

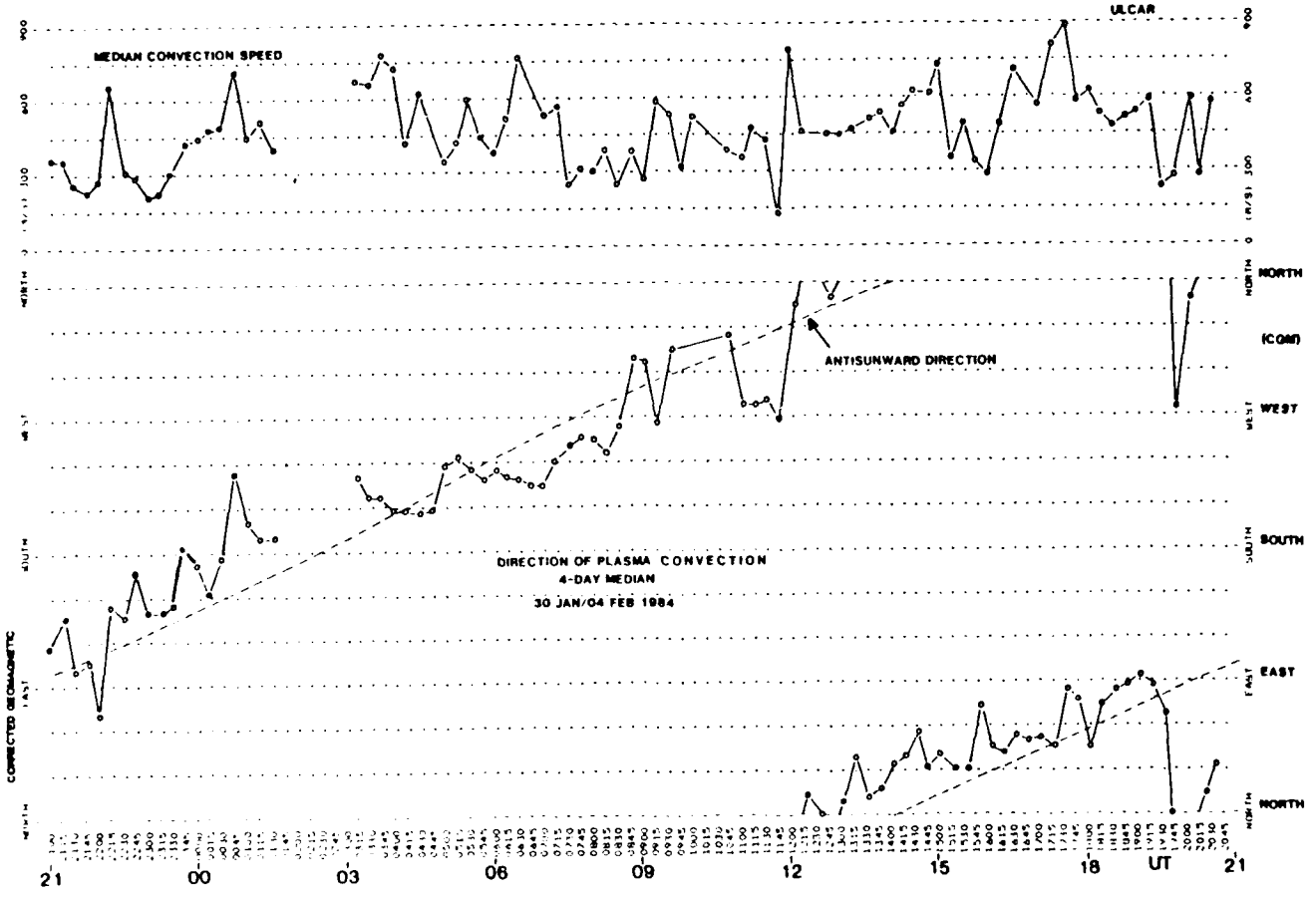

Figure 2.5 Direction of Plasma Convection, Thule, Greenland 4-Day Median, 30 January/04 February 1984

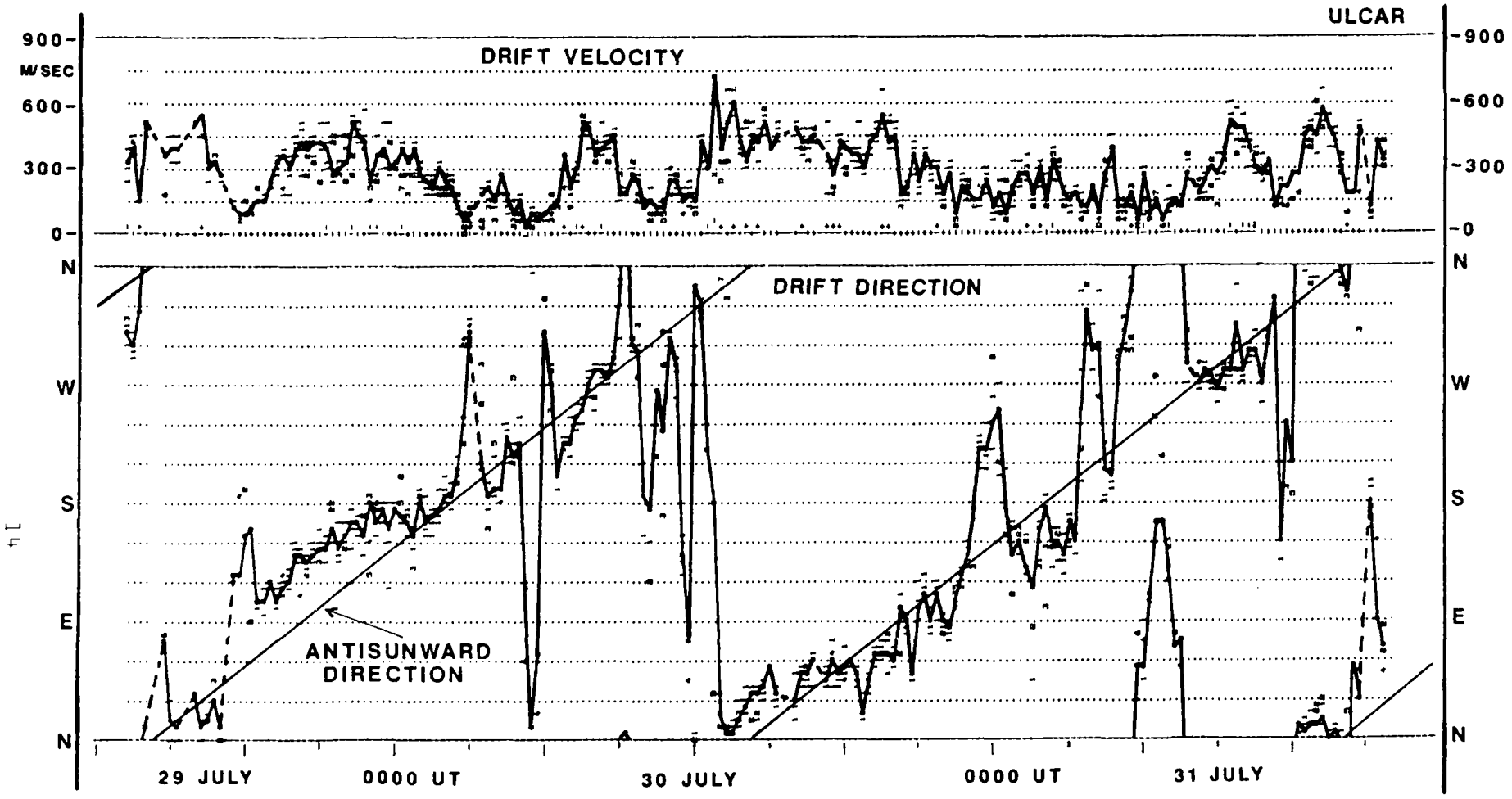

F-REGION DRIFT 29 TO 31 JULY 1986
DIGISONDE OBSERVATIONS AT QANAQ, GREENLAND

THE VELOCITY VARIES BETWEEN 100 AND 500 M/S. THE DIRECTION IS CLOSE TO ANTISUNWARD.

Figure 2.6

2, i.e. 10° in azimuth. At times of rapid changes, for example around 5:30 UT on 30 July (Figure 2.6), the standard deviation calculated over 15 minutes is larger. These rapid changes in drift direction are generally associated with a decrease in the magnitude of the velocity.

Since October 1986 three drift measurements at Qanaq are conducted each month on the three regular World Days, using the automatic drift mode.

2.1.3 Drift Observations at Argentia

Drift observations have been made with the DGS 256 in Argentia in February, April and October 1986. It is expected that the nighttime F region at Argentia, like that at Goose Bay, is coupled to the polar cap convection pattern during periods of moderate and high magnetic activity, and therefore would show evidence of a drift reversal from west to east around local magnetic midnight. Figure 2.7 shows the drift velocities at Argentia on 10/11 February 1986. On 10 and 11 February, ΣKp was 17+ and 26, respectively. Some predominance of westward drift is apparent during the first twelve hours, and later a relatively well defined southeastward drift indicates a drift reversal a few hours after midnight (CGLT). As indicated above, a reversal of drift direction is usually accompanied by low velocities and random horizontal directions. This is the situation during the first few hours as the drift reverses from eastward to westward, and again after 0300 CGLT as it returns to an eastward flow. The westward drift seems to prevail until 0300 CGLT; this is also observed on the following day (not shown here).

On 9/10 April 1986 (Figure 2.8), there is no clear pattern in the trend of the drift direction for most of the day. The dashed lines joining the medians indicate periods

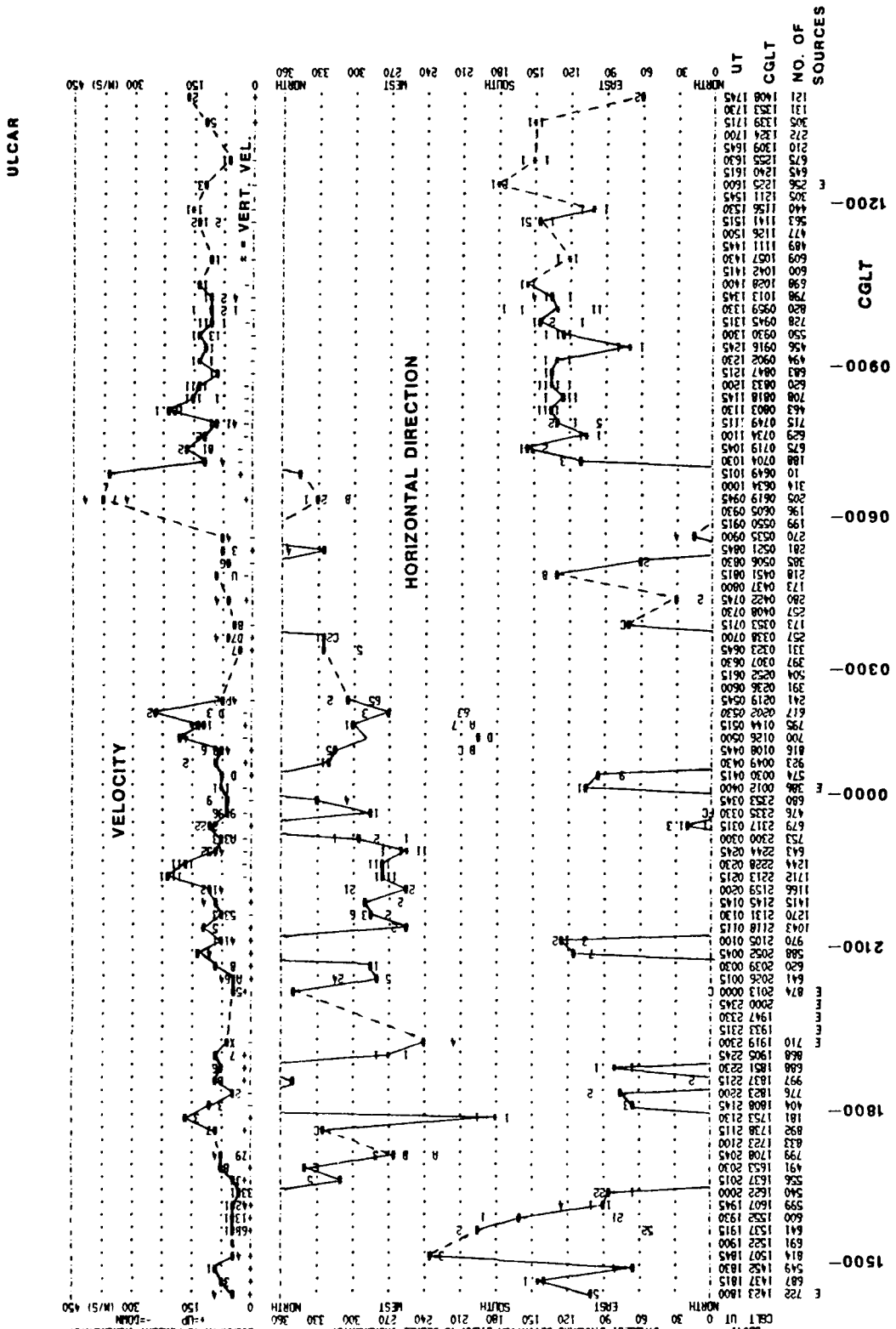

Figure 2.7 F-Region Drift, Argentia, Newfoundland, 10/11 February 1986, 1800 - 1745 UT

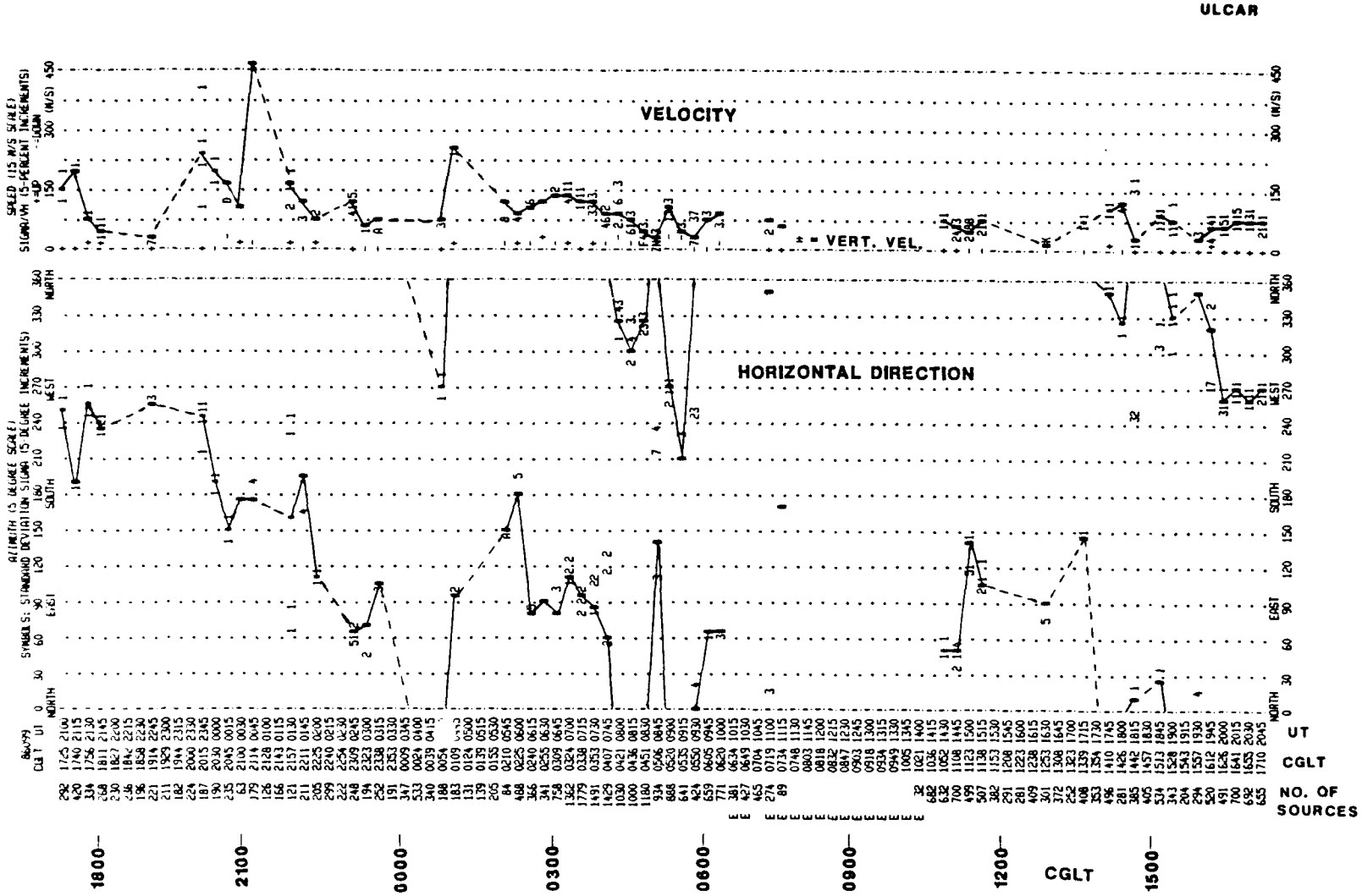

Figure 2.8 F-Region Drift, Argentia, Newfoundland, 9/10 April 1986, 2100 - 2045 UT

when no well defined drift velocities could be calculated. The number of sources (given below the CGLT) indicate that a significant number of sources were measured during most of these time periods. Like the drift measurements in Qanaq, these drift observations were also made using the automatic range selection mode. Since pairs of simultaneous measurements are made at essentially the same range (Section 2.2), the resulting velocities are automatically rejected by the drift analysis if the two velocities of a pair differ considerably. This situation occurred many times during the 24-hour period. The small Doppler spread during those periods led to large errors in the calculation of the drift. At about 1615 CGLT, the drift is consistently westward. This consistency continues for the next few hours (not shown), after which time the drift measurements were terminated.

2.2 Automating the Digisonde Doppler Drift Measurements

In the drift mode, the Digisonde 256 measures only at one selected range for each of the four (or 1, 2, or 8) sounding frequencies. To obtain useful data, the sounding frequencies must be carefully selected and the range must follow the range of the F-region (or E-region) echo, a process that required a trained operator continuously monitoring the ionospheric echoes on an oscilloscope. Now this process has been fully automated by implementing the autodrift routine in the Digisonde ARTIST computer.

2.2.1 Autodrift Concept

To operate in the autodrift mode, the Digisonde must be set up for the drift mode with four sounding frequencies. The autodrift routine inspects the scaled ionogram data and selects two sounding frequencies and their respec-

tive ranges (virtual heights). The sounding frequencies remain fixed until a new ionogram is obtained. Ranges and receiver gains are adjusted at the end of each drift measurement (called a case, generally 10, 20 or 40 sec long).

2.2.2 Frequency Selection

The current autodrift routine limits observations to the F region. The frequency interval foF2 - fminF is divided in two parts. In each subinterval, the frequency with the best signal-to-noise ratio is selected for the drift sounding. The signal and noise information is contained in the scaled ionogram data. Frequencies close to foF2 and fminF are avoided. As will be shown below, autodrift requires to set F1 = F2 and F3 = F4 (F1, F2, F3 and F4 are the drift sounding frequencies), so only two frequencies need be selected.

2.2.3 Range Selection

The ranges of the echoes at the selected frequencies are also available from the ionogram scaling algorithm. Ranges H1 and H2 (for the first frequency pair) are set apart by 10 km, and so are the ranges H3 and H4. For each pair, autodrift compares the spectral amplitudes at the end of each case (when the drift data are transferred from the Processor to the ARTIST) and corrects the range with the weaker amplitude by 20 km. This way, the two ranges for each pair will hover around the range of the echo following the height changes of the ionosphere.

2.2.4 Receiver Gain

When the frequencies and ranges are selected, the receiver gain is arbitrarily set to an average value (G = 2).

Adjustments are made in 6 dB increments at the end of each case until the peak spectral amplitude is 12 dB below the possible maximum.

2.2.5 Autodrift Coding

The autodrift program is coded in Fortran and resides in ARTIST as an independent program. The ARTIST operating function was converted to a multi-tasking mode so as to enable autodrift execution during ionogram scaling. This modular approach facilitates future program enhancements.

2.2.6 Autodrift Operation

To activate the automatic drift mode the P3 parameter (see p. 58 in the Revised Digisonde Manual) in the DRIFT program must be set to a value larger or equal to 8. As mentioned earlier, a four frequency drift program must be selected, for instance L = F, N = 6, T = 8 (see Table 5.11 in the Revised Digisonde 256 Manual). It is important for P3 $\geq$ 8 so that the ionogram data are transferred from the Processor to the ARTIST. It is advisable to start the drift measurements directly following the ionogram, so that the selected frequencies and initial heights are correct. This is achieved by setting the drift starting times in the AUTO arrays (see p. 100A in the Revised Manual) equal to the ionogram starting times.

2.2.7 Testing Autodrift

Autodrift was extensively tested at Argentia and Qanaq. The program tracks the F region echoes and produces good drift data. Occasionally, however, characters sent from ARTIST are missed by the Processor. The Processor firmware

requires updating to provide a faster and error free communication protocol between the ARTIST and the Processor.

Figure 2.9 is an example of a typical drift data printout from Qanaq when the Digisonde operated in the autodrift mode. The amplitudes (on the left side) and the phases (on the right) for 64 spectral lines are printed in one line. Four data lines comprise one drift case, followed by the time, in minutes and seconds, at which the case ended. The four data lines are the spectra for the four sounding frequencies as indicated at the beginning of each line; height range and receiver gain follow. While the sounding frequencies remain constant during the 50 seconds of observation displayed in Figure 2.9, the height ranges and gains vary. In this example, the Doppler spectrum covers the frequency range from -3.0 to +3.0 Hz. The Optifont is used to display the spectral amplitudes. The spectra for antenna one are shown here; this is indicated by OUTPUT switch P3 = A (Digisonde 256 Manual, p. 58).

2.2.8 Recommendations for Further Improvements

The autodrift program must be made more flexible to allow for selection of E, F1 and F2 layer measurements. A frequency scan mode should be implemented which changes the sounding frequencies from case to case, scanning the frequencies from fminF to foF2, thus probing the F region from the bottom to the peak.

Another area of improvement is to provide remote data outputs in the drift mode. Presently, the proper operation of the receiving antenna array and the validity of the real-time drift data can only be verified at the sounder site. In the future, autodrift should analyze the drift data and display the status of each antenna for remote diagnostic purposes.

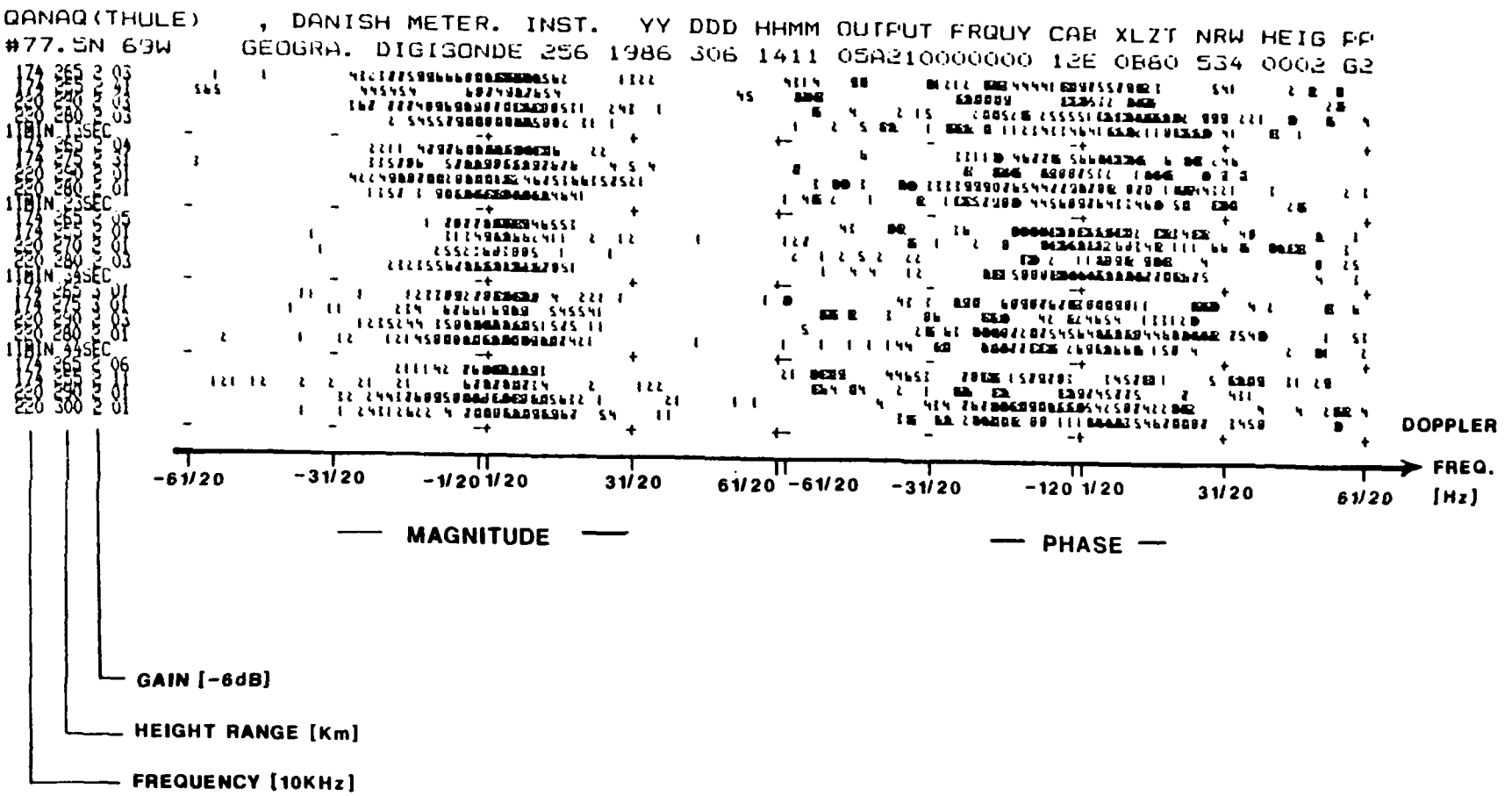

Figure 2.9 Example of On-Line Printout of Drift Doppler Spectra, Qanaq, Greenland, 2 November 1986, 1411 UT

Finally, a major enhancement in the Digisonde Doppler drift technique will be the development of real-time drift velocity evaluation. Currently, the raw drift data are stored on magnetic tape to be analyzed in a mainframe computer. However, implementing the drift velocity calculation into ARTIST requires major modifications because of the limited speed and memory available in the ARTIST computer.

2.3 Conclusions and Recommendations for Future Drift Observations

The drift results shown above are only a few examples of the drift observations that have been analyzed. Our results provide proof for a) the existence of the anti-sunward polar plasma convection pattern and b) the validity of the Digisonde Doppler drift technique using HF radio waves transmitted from ground stations for measuring this convection pattern.

A detailed analysis remains to be done which interprets the observed data in terms of available interplanetary magnetic field (IMF) data and K_p values. Now that the observations are completely automated and the computer processing techniques developed, systematic drift studies can be conducted. We recommend to make drift observations for two minutes every 15 minutes after each ionogram.

3.0 AN IMPROVED ARTIST

By "ARTIST" we mean today the microcomputer in the Digisonde 256 which postprocesses the ionogram and drift data and which provides the interface between the sounder and the on-site and remote terminals and peripheral equipments. In Section 3.1 we use the name ARTIST in its original meaning as an algorithm for the automatic real-time ionogram scaling and true height calculation.

By-and-large the automatic scaling routines in ARTIST performed very well at all stations: Goose Bay, Argentia, Qanaq, Richfield (Utah), Erie (Colorado), Wallops Island (Virginia) and Lowell (Massachusetts). Some of the weaknesses in the scaling routines have been removed during this contract period, others need to be worked on. In a large study, the profiles of some 1,000 autoscaled ionograms were compared with Dudeney's (1983) model profiles, and the results of the hmF2 comparison is discussed in a paper by McNamara et al, 1987. As part of this study, methods were developed for an efficient quality control of the automatically obtained profiles. These methods are described in Scientific Report No. 3 (McNamara, 1986).

3.1 Automatic Ionogram Scaling

The three-year contract period has seen a steady increase in the reliability with which ARTIST is able to automatically scale Digisonde ionograms. This progress is reported below. Comparisons between automatically and manually scaled data are also given. Previous comparisons have been described by Reinisch et al (1982).

The performance of the improved ARTIST algorithms was tested by comparing automatically with manually scaled foF2 values. Two groups of data were used: 188 high latitude ionograms (August 27-29, 1983) from Goose Bay, Labrador, and 316 mid-latitude ionograms (May 17-21, 1984) from Tullahoma, Tennessee. Figures 3.1 and 3.2 show the error distributions for the autoscaling results obtained for these stations. For Goose Bay, 100% of scaling found foF2 within 1 MHz error limit, with a corresponding figure of 98% for Tullahoma. Also, 97% of the mid-latitude scalings were accurate to 0.5 MHz, which is 2.2% better than the high latitude results. The superior scaling accuracy in mid-latitude is even more pronounced when a 0.3 MHz error limit is considered, namely 92% vs. 87%. The results are not that surprising since the ionosphere is less disturbed at mid-latitude. If the spread F ionograms are discarded in the Goose Bay data group (54 out of 134 ionograms), the statistics improve to 95.5% within 0.5 MHz error limit, and 88.5% within 0.3 MHz. The occurrence of spread F was rare in Tullahoma, so we did not consider the no-spread distribution.

Improvements in the ARTIST algorithms have been implemented as the need arose, as indicated by intensive studies of the results for a wide range of conditions. The improvements are described below.

(A) Redefine the Trace Center after the E-Trace is Extracted

Occasionally the scaled F-trace was found extended into the multiple echoes of the E-layer. This occurred because the trace center was misdetermined, which in turn created an erroneous baseline. The error is now avoided by searching the trace center again and, using the knowledge of the scaled E-trace height, discarding the multiple E-echoes.

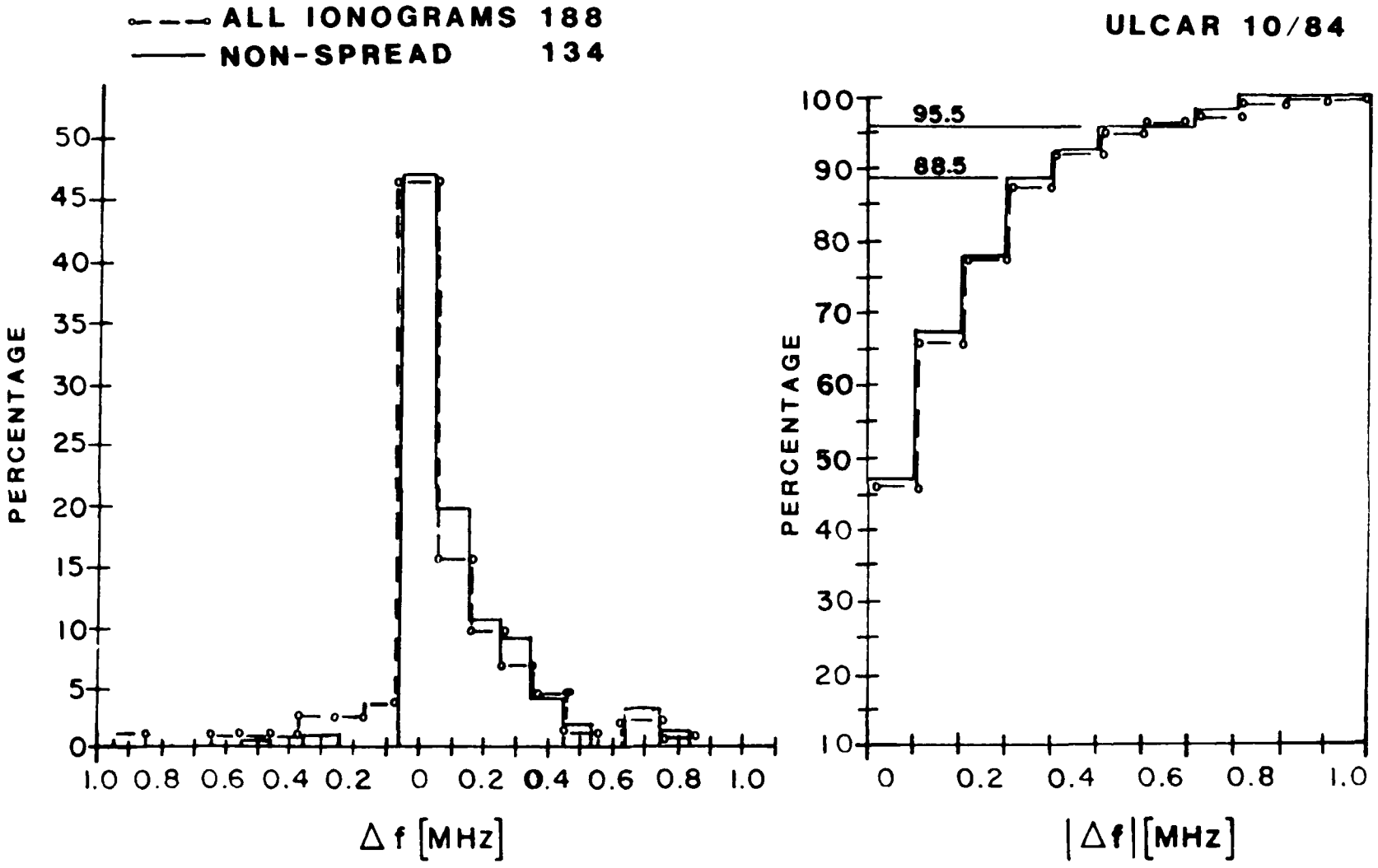

Figure 3.1

ERROR DISTRIBUTION OF FOF2 (MANUAL-AUTO FOF2)
AUG 27 8:29-29 8:14 AST GOOSE BAY, LABRADOR

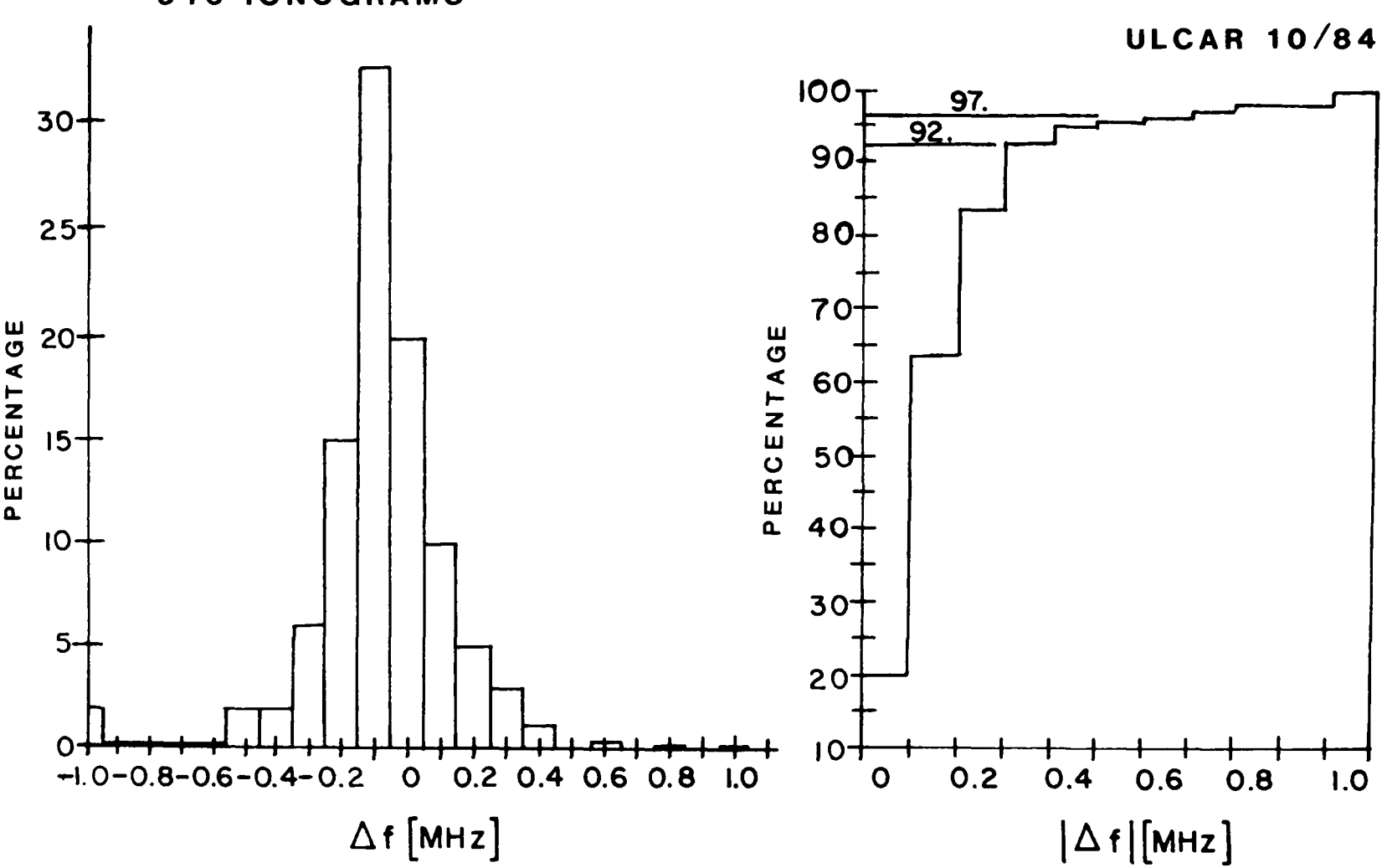

Figure 3.2

ERROR DISTRIBUTION OF FOF2 (MANUAL-AUTO FOF2)
MAY 17-21 1984 TULLAHOMA, TENN.

(B) Determine the Frequency Range for Hyperbolic Fitting

This addition is particularly important to ionograms where the F1 layer is present and the F2 trace is short. If we allow the hyperbolic fitting procedure to include the F1 trace, the F2 layer may be missed entirely. Range spread and dispersion near the F1 cusp can contribute significant amplitudes to the search hyperbolas, and foF1 is incorrectly identified as foF2. Now, before starting the fitting process, the ionogram is scanned for the possible foF1, and this is used to define the lower frequency bound for the fitting procedure.

(C) Lower F1 and F2 Traces Separately to the Leading Edge

The initially scaled trace follows the maximum echo amplitudes and is then lowered to the leading edge of the echo trace by the averaged height drop. The method works well for a one-layer F region, but in the case where the F1 layer is also present, a common drop for the entire F-trace is clearly inadequate. The program now determines separate height drops for the F1 and the F2 trace, generating results more in agreement with the manual scaling.

(D) Determine the Minimum Height of the F-Trace

In the prior program, the minimum height was defined as the lowest flat portion of the trace which varied by less than two height bins within a three bin frequency range. This strict condition may not be met, especially in the two-layer situation where the F2 trace is short and the slope is steep. A less restrictive requirement (six height bins variation) is now applied.

(E) Fine-Tune foE

Since the E- and F-traces are processed separately, it sometimes happened that scaled E-trace points (at or near foE) were located above the F-trace. The new program successively reduces foE to the next lower frequency until all E trace points are below the F trace. The new foE cusp is then checked to see if there are any O-echoes in the 4-bin range window. If an O-echo is not found foE is further reduced, and so on.

Occasionally ARTIST scaled the minimum frequency of the F-trace at a frequency lower than foE. This occurred most frequently in the presence of night E, when the E and F traces overlap in frequency. Since it is generally assumed the E trace is the result of slightly oblique echoes (although not indicated by the echo status) it was decided to let fminF set the value of foE to foE = fminF - 0.1 MHz. This leads to more systematic results, since fminF is determined very carefully. This new method will also lead to improved foE values in cases where foE is difficult to determine in the ionogram because of frequency spread on the E trace, as illustrated in Figure 3.3. It is clear that the prior ARTIST program determined too high an foE value of 3.4 MHz. The revised program (Figure 3.4) finds the correct foE value of 3.2 MHz. The new E trace is determined by applying the previously described "parabolic" fit keeping foE = fminF - 0.1 MHz fixed.

(F) Pulse Fitting at fminF and foF1

Generally the trace is composed of the smoothed baseline and the F2-hyperbola. The retardation at fminF and the cusp at foF1 were sometimes distorted in the smoothing process. The shapes of these two regions are important in

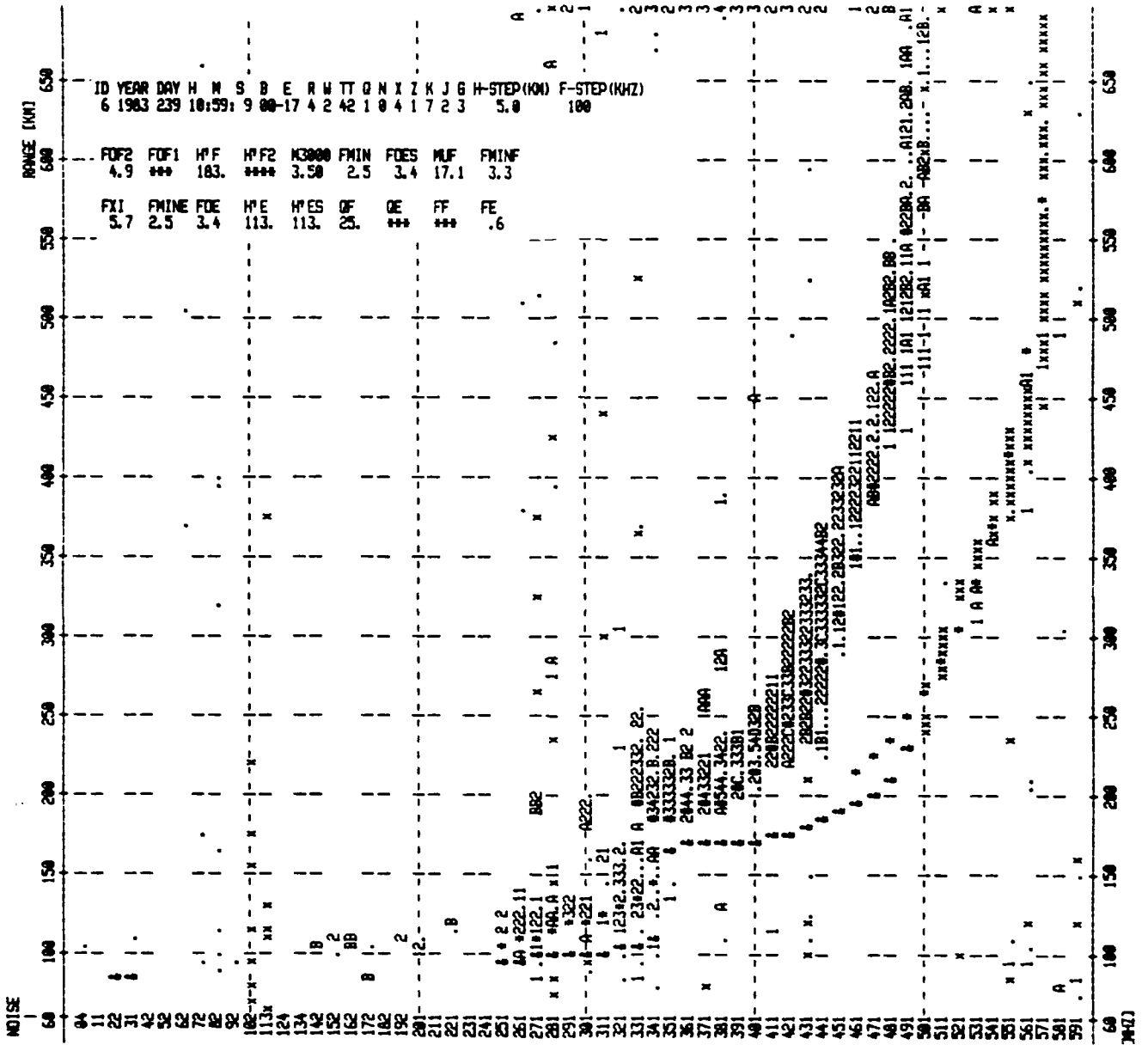

GOOSE BAY LABRADOR **27 AUGUST 1983 10:59 AST**

Figure 3.3 ARTIST Scaled Ionogram, Goose Bay, Labrador 27 August 1983, 1059 AST; Note foE has been Scaled Erroneously High

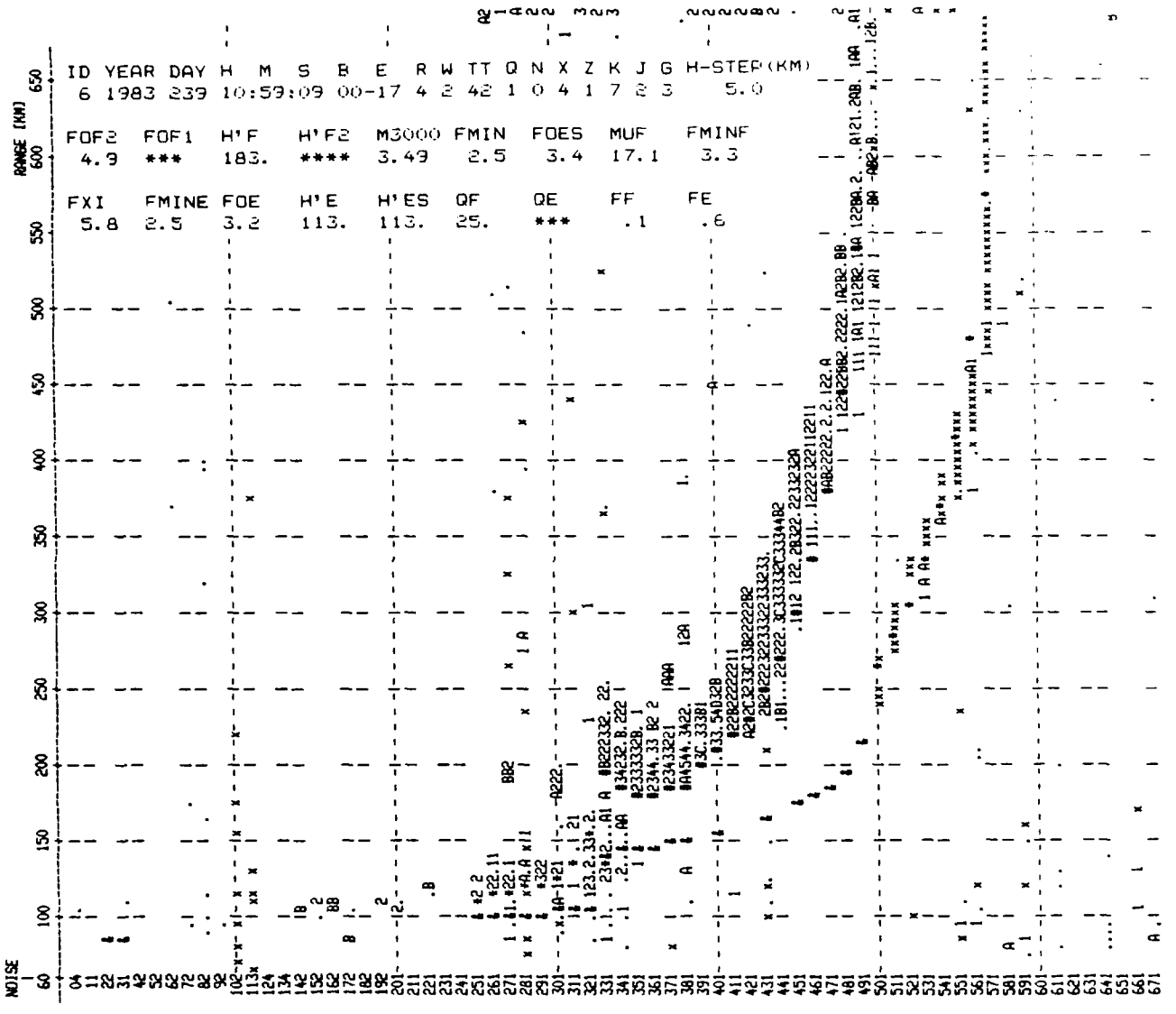

GOOSE BAY, LABRADOR **27 AUGUST 1983 10:59 AST**

Figure 3.4 Improved ARTIST Scaled Ionogram, Goose Bay, Labrador, 27 August 1983, 1059 AST; Note foE has been Scaled Properly

determining the transition region ionization in the inversion procedure. Therefore improved h'f values are determined, by applying a pulse fitting technique at each frequency in the neighborhood of fminF and foF1.

(G) Construct the Entire Es Trace

Previously only the top frequency of the Es layer was scaled. Now the entire Es layer is extracted by using the pulse fitting method.

(H) Improved foF2

When the O and X traces are clearly defined at the critical frequencies, they generally display a dispersion-caused range spread which contains a substantial amount of amplitudes. We know that the critical frequencies of the O and X traces are separated by one-half of the gyro-frequency. This fact is now used to eliminate the 100 or 200 kHz errors in foF2 introduced by the hyperbolic fitting. Summing the O and X amplitudes individually for each frequency, starting at the height of the baseline, generates two amplitude arrays O(f) and X(f). Searching for the maximum of O(f) + X(f + 1/2 fH) determines foF2 precisely, when the traces near the critical frequency are well developed. However, in the process of summing the amplitudes, caution must be exercised not to include multiple or oblique echoes and interference. Therefore the upper edge of the trace relative to the baseline is constructed. Starting from the baseline height, a 4-bin window is moved up the range in one bin steps until there is a drop of amplitude of 12 dB per bin, marking the upper limit. Unfortunately, the O and X traces do not always occur in pairs because of defocussing, absorption or interference, in which case this "double gate" improvement technique is not applied.

The "double gate" technique produces very accurate foF2 values in ionograms with well defined O and X traces. However, when there are mixed oblique and X echoes in the vicinity of the critical frequency, which occurs frequently in disturbed ionograms, the baseline may not be able to follow the echo trace up to foF2, and the method does not work well. Therefore, the baseline has to be checked before the gate method is applied.

A 4-bin window is placed on each baseline point and the majority tagging within the window is recorded to represent this point. Then the baseline tagging is smoothed, using three points at a time. In the smoothing process, "oblique" tags are adjusted when they are surrounded by O or X tags. Frequencies without baseline points are ignored. At this point, the baseline is examined to see if it delineates the O or the X traces. Starting from the high frequency end of the baseline, the first two consecutive O tags are determined. This is assumed to be the frequency where the X trace emerges from the O trace. We now correct or reconstruct the baseline by forcing it to increase monotonically with frequency and follow the O-trace. The height of a baseline point is compared with that of the previous frequency. If it is lower, it is made equal to the previous height. If it is X-tagged, it is replaced by the position of the next FLM (first local maxima) found at higher height. Again when no FLMs are found for five consecutive frequencies, the baseline end is assumed. Figures 3.5 and 3.6 show scaling examples of the current version of ARTIST.

(I) Second Try Baseline

In constructing the baseline, four first local maxima (FLM) are required to be in the trace center window in

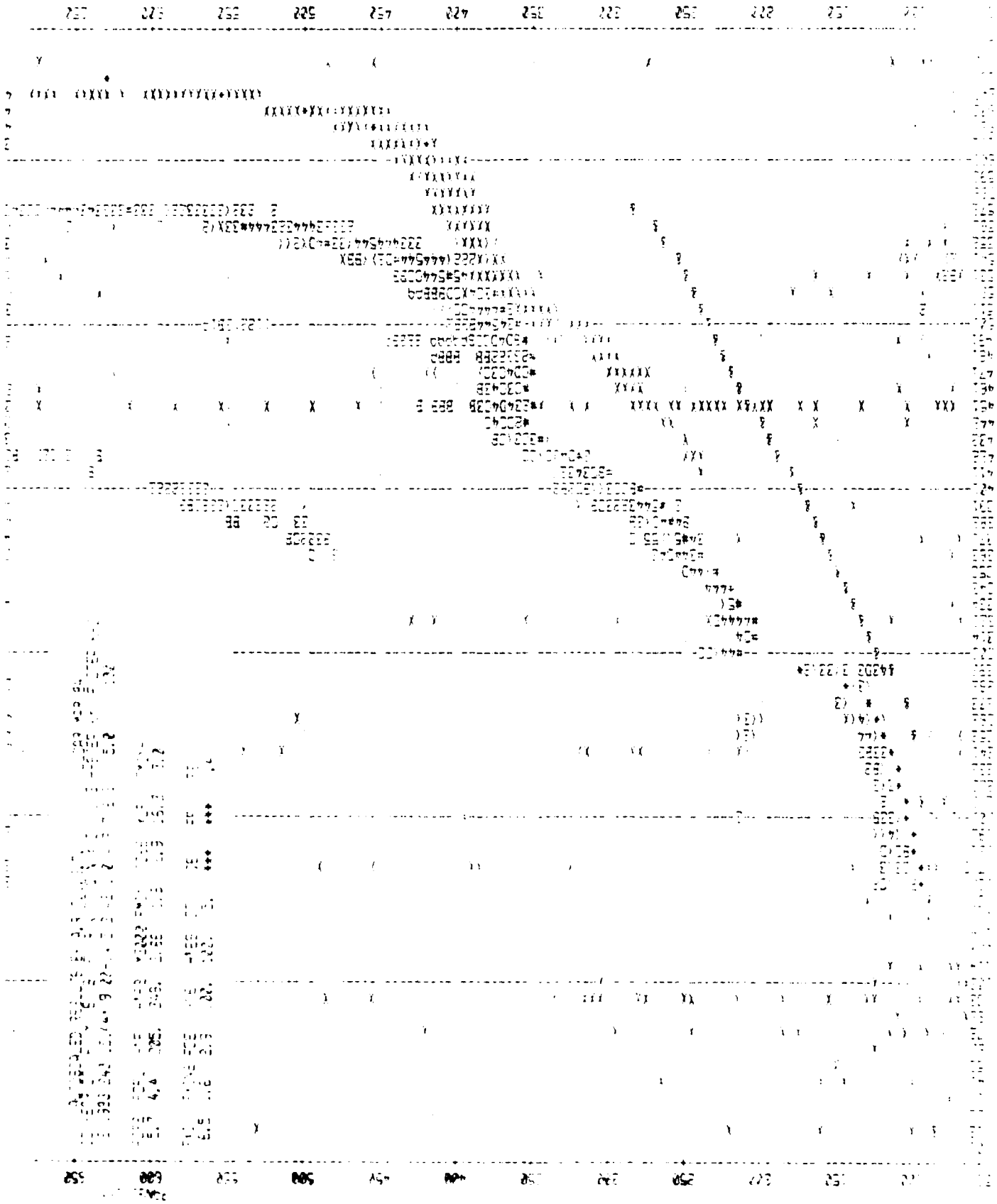

Figure 3.5 ARTIST Scaled Ionogram, Goose Bay, Labrador, 30 August 1983, 1544 AST

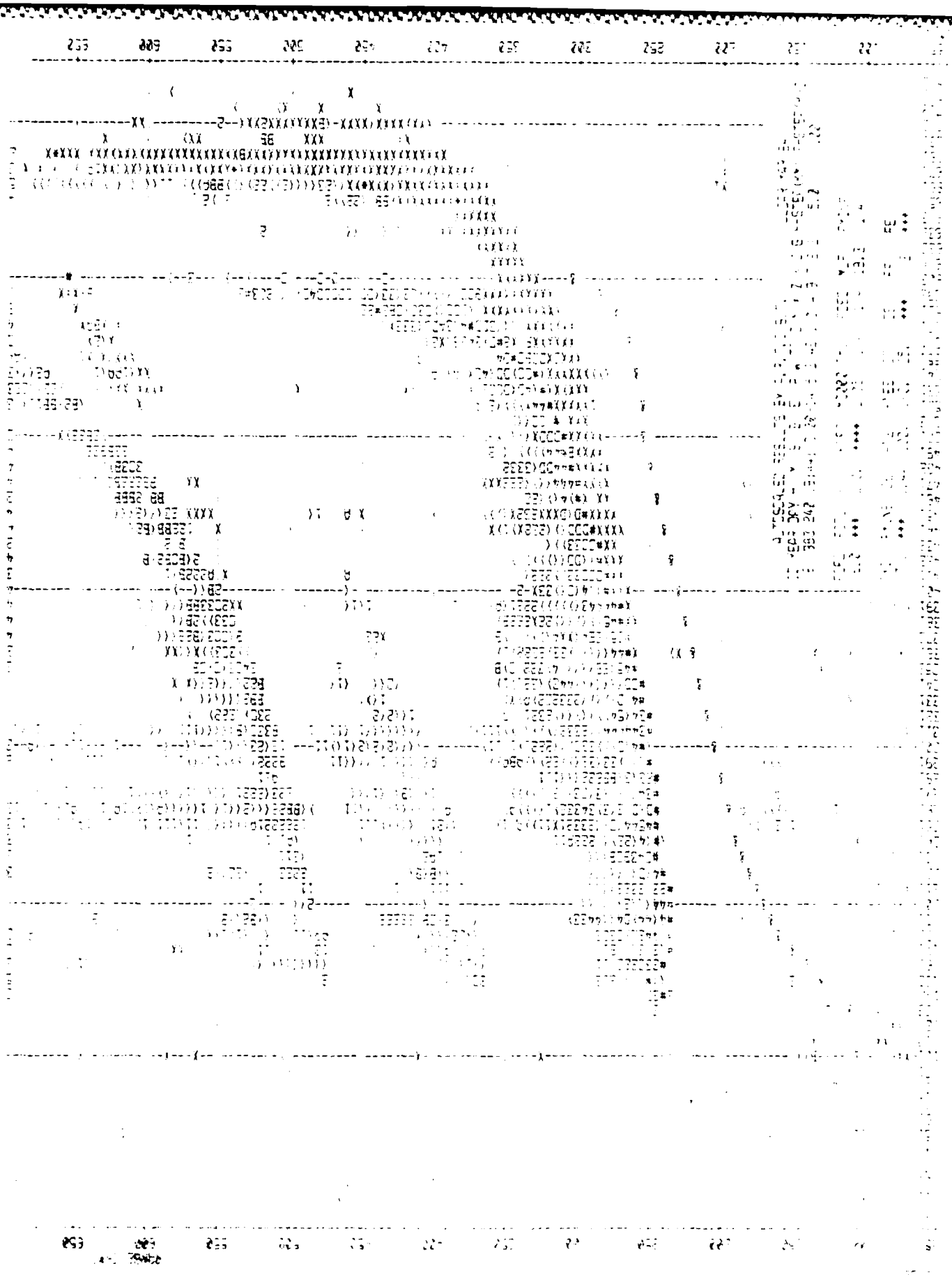

Figure 3.6 ARTIST Scaled Ionogram, Goose Bay, Labrador, 28 August 1983, 1944 AST

order to be qualified as such. For some night ionograms, the F trace is short and has a steep slope, and the above condition cannot be satisfied. Before declaring that no F-trace is found, the program now makes a different search for the center window. Starting at 300 km all O-echo amplitudes (after suppressing the stand alone pixels) are summed for each frequency and the frequency with the maximum sum is recorded. Then a 4-bin range window is slid along the height and the maximum is marked as the baseline point. The procedure is repeated on both sides of the frequency with the maximum sum determining the heights of the maximum amplitudes. When two consecutive frequencies of zero amplitude are encountered, the fminF or the high-frequency baseline end is assumed.

Figures 3.7, 3.8 and 3.9, 3.10 illustrate the differences in scaling before and after the improvement of March 1984. Not all the modifications discussed above were implemented at that time.

Further modifications to the ARTIST are proposed. These include:

1. Scaling the extraordinary trace separately, as an aid to the subsequent N(h) profile analysis. Preliminary studies indicate that difficulties will be encountered in the effort to ensure that the scaled O and X traces are consistent with each other, which they must be before they can give reliable results for the starting and valley problems. The difficulties are set partly by the fact that the X trace is relatively weak in the frequency ranges for which it is required for N(h) analysis. The quantization of the h' values into 5 km bins will also be a source of errors, since it is the differences $h'_O = h'_X$ which contain the required information.

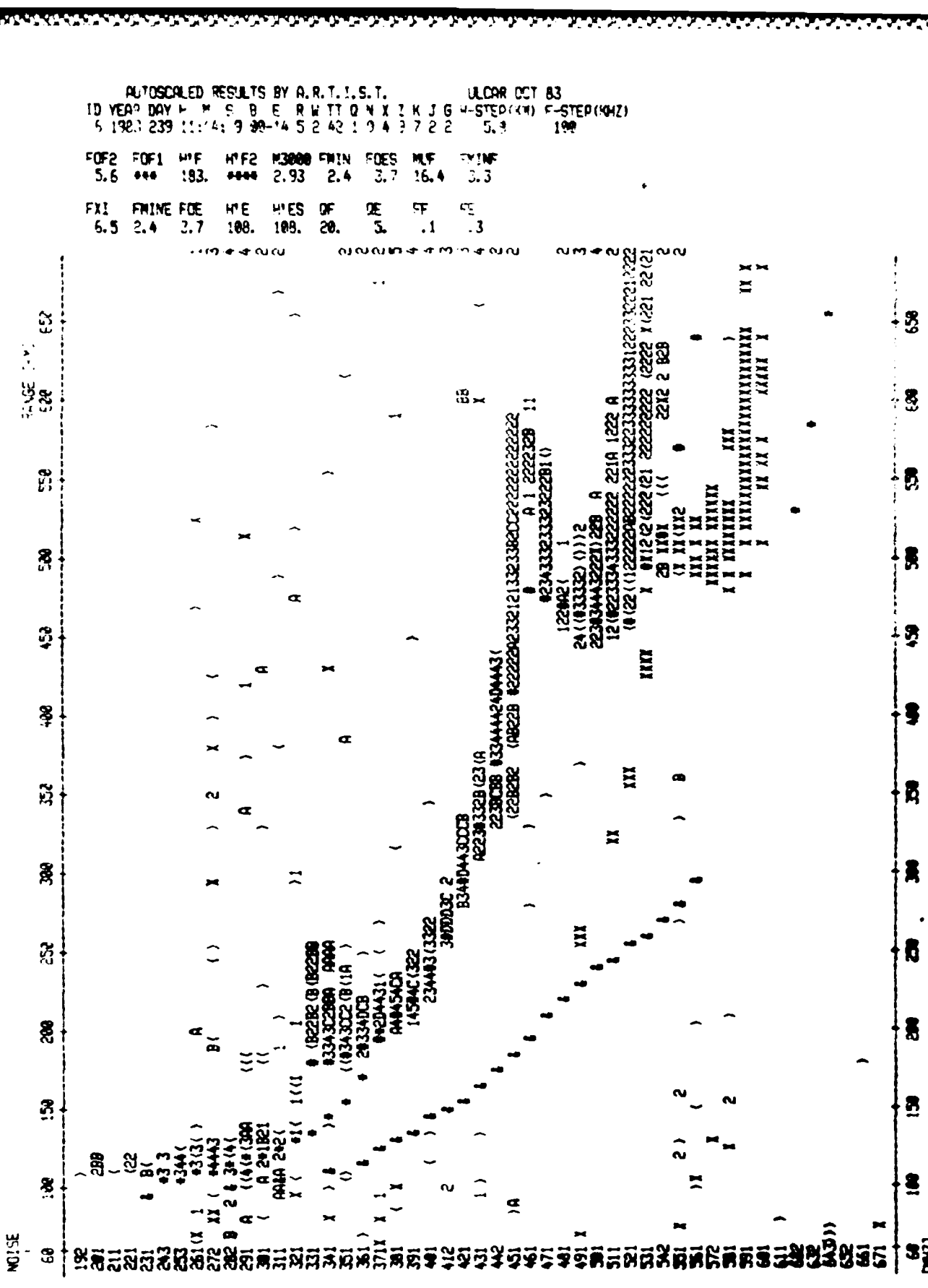

Figure 3.7 ARTIST Scaled Ionogram, Goose Bay, Labrador, 27 August 1983, 1144 AST; Note F-Region Values

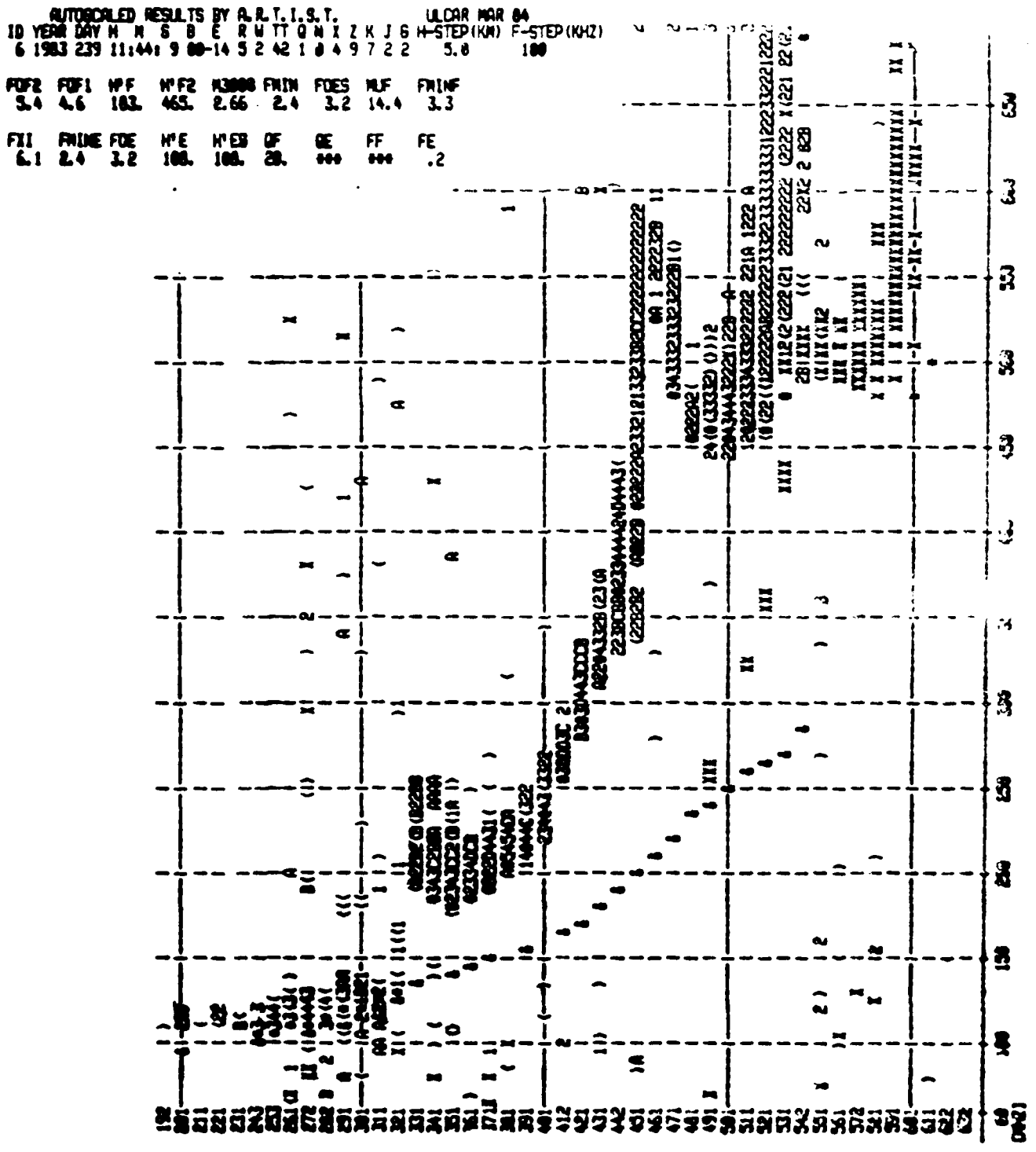

Figure 3.8 Improved ARTIST Scaled Ionogram, Goose Bay, Labrador, 27 August 1983, 1144 AST; Note Improved F-Region Values

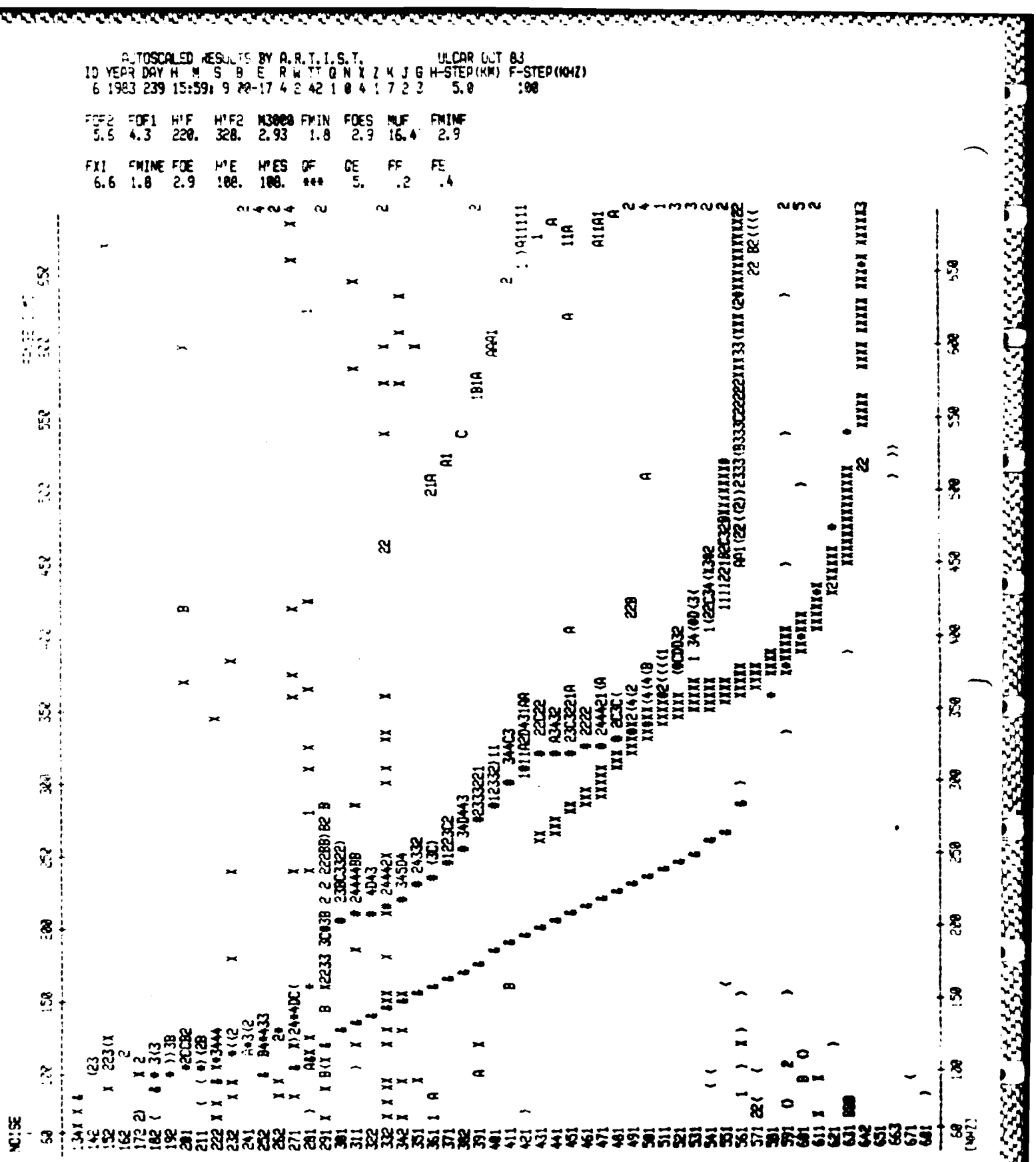

Figure 3.9 ARTIST Scaled Ionogram, Goose Bay, Labrador, 27 August 1983, 1559 AST; Note fminF and fxI Values

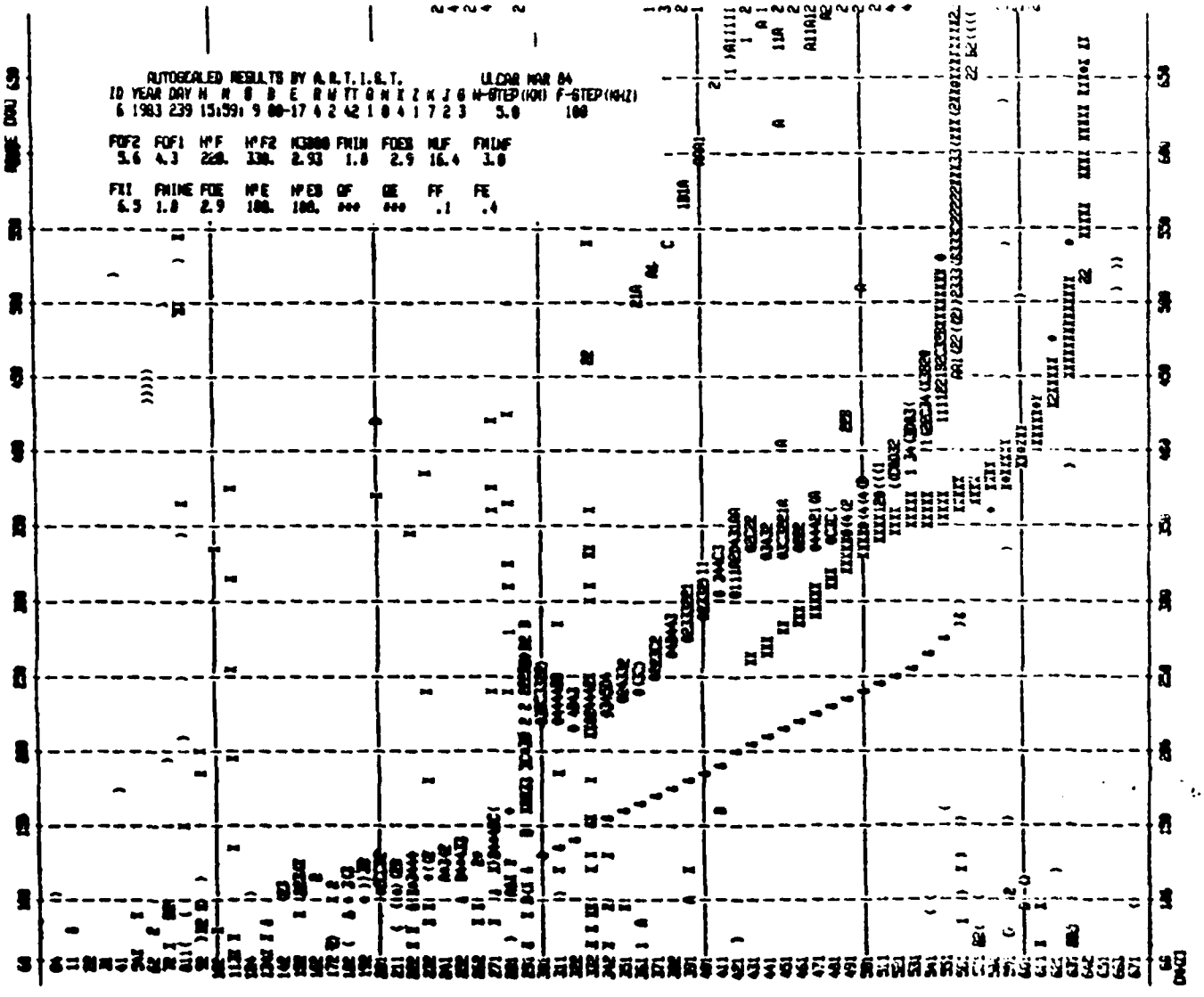

Figure 3.10 Improved ARTIST Scaled Ionogram, Goose Bay, Labrador, 27 August 1983, 1559 AST; Note Improved fminF and fxI Values

2. The present scaled trace tends to lie higher than a manually scaled trace where it starts to curl up towards foF2. It is intended to modify the fitted O-ray hyperbola to force it more towards the leading edge of the trace. This can be achieved by keeping the fitted values of ho and foF2, and increasing the parameter "a" of the hyperbola to optimize the fit to the O-ray amplitudes, but this time weighting the amplitudes to make the pixels near the leading edge more important. Various weighting schemes will need to be tested, such that the algorithm continues to follow the inner edge of the trace in the presence of strong frequency spread.

3. The technique for evaluating M(3000)F2 can be modified to make it consistent with the standard URSI method. The MUF slider can be represented to within 0.5% by the curve (Paul, 1982)

$$M = (67.654 - 0.0149\ h')/h' ** 0.5$$

The value of M(3000)F2 can be obtained by determining the maximum of the product $f \times M$, and then dividing by foF2. The scaled value of M(3000)F2 will be flagged as unreliable (because of difficulties encountered in automatically scaling the F2 cusp) when the maximum of $f \times M$ occurs at the last scaled frequency below foF2.

4. The value of the M factor for distances "D" other than 3000 km, or alternatively MUF(D), will be obtained using the procedures recommended by CCIR in reports 894, "Propagation prediction methods for high frequency broadcasting" and in the Supplement to Report 252, "Second CCIR computer-based interim method for estimating sky-wave field strength and transmission loss at frequencies between 2 and 30 MHz." These are minor changes introduced in the interests of standardization with the internationally agreed techniques.

5. The predicted value of foE will be calculated using the techniques described in the Supplement to CCIR Report 252, mainly in the interests of standardization, although some increase in accuracy over the present method is expected. The predicted value of foE will not be allowed to fall below 0.36 MHz at night, in agreement with a limited number of observations.

6. The scaled values of foF2, foE and M(3000)F2 will be used to calculate a reasonably accurate value of hmF2 using the Dudeney (1983) model. This model makes allowance for the retardation due to underlying model layers, and reduces to the well known Shimazaki (1955) result at night. The model has been found to be sufficiently accurate to flag erroneous automatic scalings.

3.2 ARTIST Tape Output

The ARTIST tape output has been standardized and can be understood in terms of the control characters written. The tape recording formats for drift data and P1 = 1 ionogram data were described in detail in the Digisonde 256 Revised General Description. Here we describe the format for the ARTIST results.

After processing an ionogram, the results are written onto a 9-track magnetic tape of density 1600 bytes per inch (BPI). The results for each ionogram are recorded in a 4K byte block. Each byte is packed with two characters in binary coded decimal (BCD) format except the preface, the block type character and the control character, which have only one binary character per byte.

The first byte of the block is the block type (hex 0F for ARTIST results). The next two bytes are the total number of bytes in the block including the end code charac-

ters. The results contain information for the whole ionogram for archiving purposes. They include the preface, scaled parameters, trace heights, amplitudes and Dopplers, and the electron density profile coefficients. The information is grouped in classes. Each class is given a code for identification. Table 3.1 lists the code numbers and the corresponding classes. The classes are of various lengths, in terms of the number of bytes. The length of certain classes will change from ionogram to ionogram because of the variation in trace length. However, the length of each datum within a class is fixed. For example, one byte is used for each preface character, two bytes are reserved for each ionospheric parameter so a value of 12.5 will be stored as 01H 25H. Each class is headed by a group of four bytes. The first two bytes are control characters (CCH) which serve as a separator between classes followed by a byte for class code, and the last byte defines the data length. At the end of the last output class, two bytes of end code (077H) are appended. Figure 3.11 shows the actual storage of one ionogram block.

Class code 00, assigned to the preface, uses one byte for each character. Class code 01, assigned to the scaled ionospheric parameters, uses two bytes for each value. Tables 3.2 and 3.3 list the preface and the scaled parameters, respectively. Class codes 02 to 04 are reserved for the F-trace information. Class code 02 contains the h'(f) values in km starting at the minimum frequency of the layer, incrementing in 100 kHz steps to the critical frequency. Two bytes are used for each trace point. If an echo is not found for a particular frequency, 9999 is filled in. Class code 03 contains the amplitude of the maximum trace point, the data length is one byte. The amplitudes range from 0 to 31. The magnitude in decibels can be calculated by checking the value of Z in the preface; for Z small or equal to 8, the unit

Class Code	No. of Bytes for Each Data	Contents	Unit
00	1	Preface 100 bytes are reserved, only 57 bytes are used.	
01	2	23 ionospheric parameters	
02	2	leading edge of F-trace	km
03	1	amplitudes of maximum F-trace	*0-31 levels
04	1/2	Doppler number of maximum F-trace	
05	2	leading edge of E-trace	km
06	1	amplitudes of maximum E-trace	*0-31 levels
07	1/2	Doppler number of maximum E-trace	
11	1	median amplitudes of F-trace at the cusp and each MHz	dB
12	1	median amplitudes of E-trace at the cusp and each MHz	dB
13	1	median amplitudes of Es-trace at the cusp and each MHz	dB
14	3	E-region profile coefficients	
15	3	F2-region profile coefficients + average error + slab thickness + void	km
16	3	Monotonic solution, one set of coefficients for E and F regions	
17	1	20 flags	
18	3	F1-region profile coefficients	
19	3	the start frequency for true height analysis of E, F2, F1 layers	
20	2	station characteristics	
40	1	AWS station ID in ASCII	
77	1	end of ionogram indicator	
0CCH	1	control character used as class separator	

Table 3.1 Definition of Class Code of Block Type 15

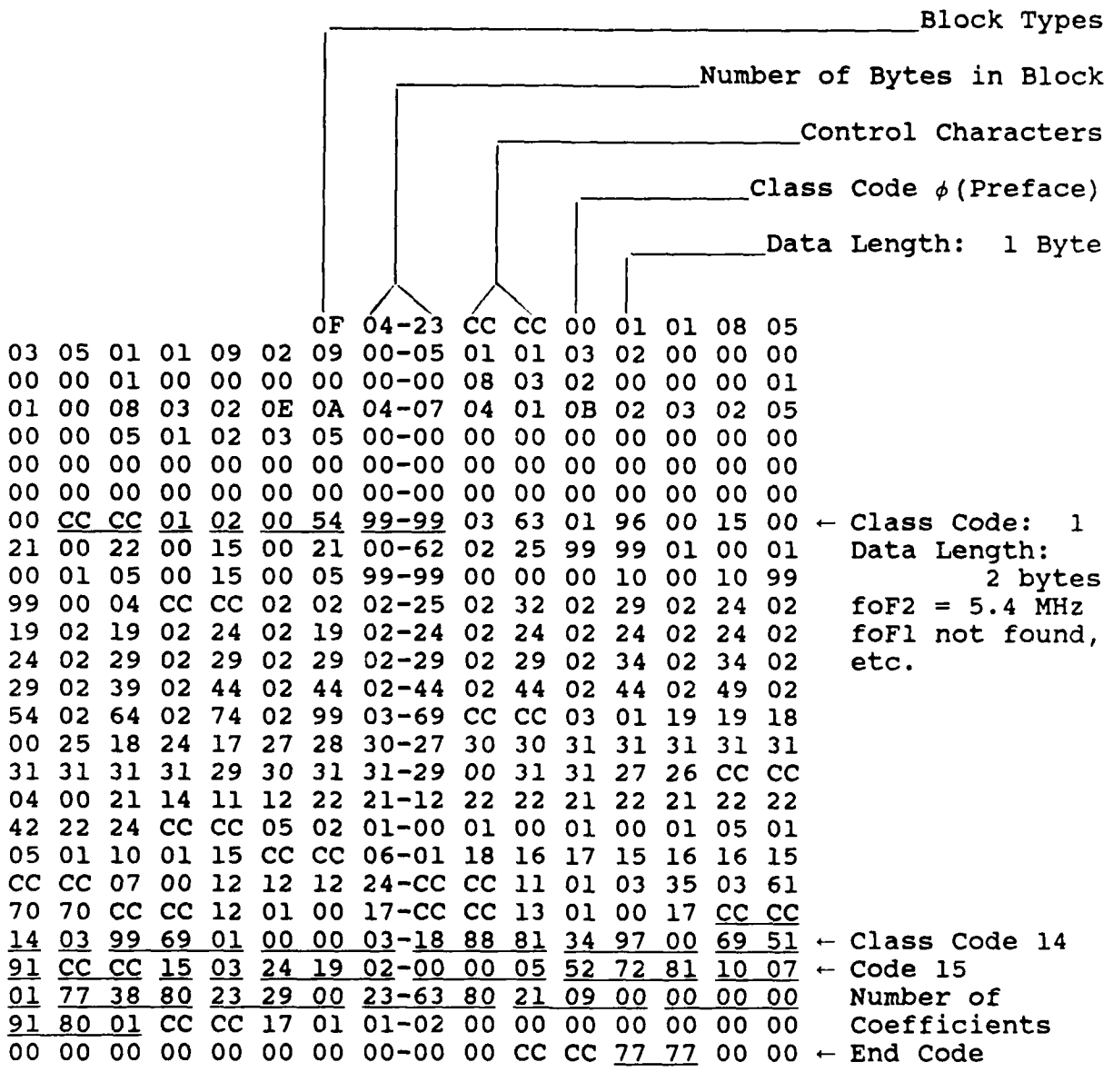

Contents of Class Code 14 (E-region)
Data Length: 3 bytes
Z(foE) = 99.69 km
Three are three polynomial coefficients: -18.88, 3.497, 0.6951

Class Code 15 (F-region)
Data Length: 3 bytes
Z(foF2) = 241.9 km
There are five coefficients: -52.72, 10.07, -7.738, 2.329,
-2.363, 2.109
Slab Thickness = ϕ km
Void = 91.8 km

Figure 3.11 Magnetic Tape Storage Format for Ionogram Data

PREFACE POSITION	SYMBOL	FUNCTION
0		Raw data record type, either 9 or 12
Date and Time		
1 - 2	Y = YY	Year
3 - 5	D = DD	Day
6 - 7	H = HH	Hour
8 - 9	M = MM	Minute
10 - 11	S = SS	Second
General Control Parameters		
12	S	Program Set
13	P	Program Type
14 - 19	J	Journal (internal controls)
Nominal Frequency		
20 - 25	F = FFFFFF	Frequency (100 Hz)
Output Controls		
26	P1	Tape Write Control
27	P2	Printer Control
28	P3	Maximum Method Options
29	P4	Printer Cleaning Threshold
30	P5	Printer Gain Level
31	P6	For Future Use
32	P7	For Future Use
Frequency Choice		
33 - 34	S = SS	Start Frequency (MHz)
35	Q	Frequency Increment
36 - 37	U = UU	End Frequency (MHz)
Test Output		
38	C	Trigger
39	A	Channel A: Digital
40	B	Channel B: D/A

Table 3.2 Tape Recorded Preface

PREFACE CHARACTER	SYMBOL	FUNCTION
Station Identification		
41 - 43	V	Station No. from INCPU Personality
Operating Parameters		
44	X	Phase Code
45	L	Antenna Azimuth
46	Z	Antenna Scan
47	T	Antenna Option and Doppler Spacing
48	N	Number of Samples
49	R	Repetition Rate
50	W	Pulse Width and Code
51	K	Time Control
52	I*	Frequency Correction (from CORE)
53	G*	Gain Correction (from CORE)
54	H	Range Increments
55	E	Range Start
56	I	Frequency Search
57	G	Nominal Gain

Table 3.2 Tape Recorded Preface (Continued)

Order	Scaled Parameter	Description	Unit
1	foF2	F2 layer critical frequency	100 kHz
2	foF1	F1 layer critical frequency	100 kHz
3	M(D)	MUF(D)/foF2	
4	MUF	Maximum usable frequency for distance D (selectable)	100 kHz
5	fmin	Minimum frequency for E or F echoes	100 kHz
6	foEs	Es layer critical frequency	100 kHz
7	fminF	Minimum frequency of F-trace	100 kHz
8	fminE	Minimum frequency of E-trace	100 kHz
9	foE	E layer critical frequency	100 kHz
10	fxI	Maximum frequency of F-trace	100 kHz
11	h'F	Minimum virtual height of F1 trace	km
12	h'F2	Minimum virtual height of F2 trace	km
13	h'E	Minimum virtual height of E trace	km
14	h'Es	Minimum virtual height of Es layer	km
15	HOM	Maximum trace height of E layer using parabolic model	km
16	Ym	Half thickness of E layer	km
17	QF	Average range spread of F-trace	km
18	QE	Average range spread of E-trace	km
19	Down F2	The lowering of maximum F-trace to the leading edge	km
20	Down E	Lowering of E-trace	km
21	Down Es	Lowering of Es-trace	km
22	FF	Frequency spread between fxF2 and fxI	100 kHz
23	FE	As FF but considered beyond foE	100 kHz
24	D	Selected MUF distance	km
25	f_v	Equivalent vertical frequency for MUF	100 kHz
26	h	Virtual height at fv	km

Table 3.3 Scaled Parameter List Recorded on Tape

amplitude is 2 dB, for Z greater than 8, the unit is 3 dB. Class 4 records the Doppler number which has a data length of half a byte. Ionograms that measure the O and X polarization have a maximum of eight Doppler lines. In this case, the numbers 0 to 7 are used to represent the Doppler lines where 0 always stands for the most negative and 7 denotes the most positive Doppler. Similar format characteristics of the E-trace are stored for Classes 5 through 7. Classes 8, 9, 10 are not used at the moment. Classes 11 through 13 contain the median amplitudes of the F, E and Es traces, respectively, occupying one byte each. The median amplitudes are presented for each MHz and are normalized to the reflection height of 100 km. Special consideration is given to the cusp region where the median amplitude is selected among the last five frequencies of the trace. The first data byte stores the total number of amplitudes of the trace at 1 MHz intervals. For example, if the trace runs between 2 to 5 MHz, excluding the cusp frequencies, the number 4 will be stored in that byte; the second byte is the average cusp amplitude, and the third byte is the start frequency in MHz (in this case 2) followed by the amplitudes at 2, 3, 4, 5 MHz.

Classes 14 and 15 contain the profile coefficients of the E and F traces, respectively. Each coefficient takes up three bytes, i.e. 6 digits. The format is the same as in the AWS message: AAAAPN where AAAA are the four most significant digits of the coefficient which represents A·AAA, P is the sign indicator for both AAAA and power N. The coding for P is as follows:

7 = AAAA and N negative
8 = AAAA negative, N positive
9 = AAAA positive, N negative
0 = AAAA and N positive
N = power of 10 with which AAAA is multiplied.

For example, a coefficient of -29.23 will be stored as 29H 23H 81H. The recording order is listed as follows:

Byte	
1 - 3	the true height of the layer peak in km
4 - 6	the number of terms of coefficients (M)
7 - 9	first coefficient
10 - 12	second coefficient
.	
.	
.	Mth coefficient
n - n + 2	Average Absolute Error per point in km between calculated and scaled virtual height
n+3 - n+5	slab thickness in km } only in Class 15
n+6 - n+8	void in km } only in Class 15

Class 16 is used for the monotonic solution and has the same format as Class 14. Class 17 contains a set of flags with data lengths of one byte each. Table 3.4 lists the contents of the flags.

Code 18 is used for the profile coefficients of the F1 trace and has the same format as Class 14. Class 19 contains the start frequencies used for the E, F1, F2 layers for true height analysis. Each frequency takes up three bytes, i.e. 6 digits, specifying the frequency in units of 100 Hz. If a particular trace is not found, the corresponding start frequency is set to 99H 99H 00H. Code 20 is used for the station coordinates; each datum consists of two bytes. The list is shown in Table 3.5. The minus sign for the latitude is indicated by a 9 in the most significant digit. Code 40 records the AWS station identification in ASCII characters. For example, the station ID for Argentia, Newfoundland, is stored as 'HICN6 CYAR 71807'. In order to read back the above new codes from tape, corresponding adjustments have been added to the program AROUTPUT.

Flag Order	Content	Description
1	0	E-trace is not found
	1	Scaled E-trace
	2	Predicted foE is used
2	0	No profile, since no F trace found
	1	E profile only, F trace too short
	2	Separate set of coefficients for E and F
	3	Monotonic solution
	9 - 16	Profile error codes, no profile solution
	9	Frequency range error
	10	Large gap between E and F traces
	12	F2-trace is too short
	13	F1-trace is too short
	14	Gap near E-trace critical frequency
	15	Gap near F2-trace critical frequency
	16	Gap near F1-trace critical frequency
3	Number of roots	If roots are found in F profile
4	1	foF1 is scaled
5	0 - 9	Qualifying number, refer to AWS IONOS message specification
•	Not used	
•	Not used	
•	Not used	
20	-	Internal use in ARTIST execution

Table 3.4 Contents of Class Code 17 of ARTIST Result

Sequence #	Description	Unit
1	Gyrofrequency	1 kHz
2	Dip Angle (0 to 90.0°)	0.1 degree
3	Geographic Latitude (0 to ±90.0°)	0.1 degree
4	East Geographic Longitude (0 to 359.9°)	0.1 degree

Table 3.5 Tape Format for Station Coordinates

A simplified profile output for routine printout has been developed to conserve paper and is shown in Figure 3.12. The first line prints the slab thickness (W) in kilometers, the next three lines are the E, F1, F2 coefficients. There are nine fields for each layer. The first field is the start frequency in MHz for true height calculation, the second field is the peak height at critical frequency followed by five coefficients in km units. Only three coefficients, however, are used for the E-layer, the two unused fields are left blank. The eighth field displays the average absolute deviation in km of the calculated and autoscaled trace. The last field is reserved for the number of roots found in the profile solution. When the parabolic model is used for the E-trace, the third field is the half thickness of the layer. If a particular trace is not scaled all fields are blank filled.

3.3 ARTIST Utility Programs

Utility programs have been developed and added to ARTIST which enhance the efficiencies of ARTIST. These programs, if required, are usually run before the on-line automatic ARTIST operation. Their functions are briefly explained in a "Manual Operation List" (Figure 3.13) which is displayed on the screen when the ARTIST is reset. The following are more detailed descriptions of each option program.

1. No user input is necessary to proceed with normal on-line automatic ARTIST operation.

2. UPDATEC will transfer the new software on the floppy disk onto the Hard Disk. C:.

3. DATE and TIME will act directly on the battery powered clock in the ARTIST. Incidentally, the date and time from the ARTIST battery powered clock are transferred to

```
+------------------------------------------------------------------+
+        T.O.A.D. - RICHFIELD, UTAH    LAT 39N   LONG 112W         +
+                                      Dip 71.7  fH 1.4 MHz        +
+      DIGISONDE 256 - VS.02.A       UNIVERSITY OF LOWELL, USA     +
+------------------------------------------------------------------+

STATION YEAR DAY H  M     OUT OPT B  E  Q CAB XLZT NRW HEIG PROGRAM
  891   1984 285 16:59 UT 1484300 01- 9 1 12E 44B2 534 1204   A1

FOF2  FOF1  H'F   H'F2  M3000 FMIN  FOES  MUF   FMINF
 6.8  4.1   208.  270.  3.20   1.9   3.2  21.8   3.0

FXI   FMINE FOE   H'E   H'ES  QF    QE    FF    FE
 7.7  1.9   2.8   105.  110.  5.    ***    .2    .6

AUTOSCALED TRACES [KM]:
-----------------------
 3.  218.  208.  211.  211.  206.  216.  226.  236.  246.  251.
 4.  265.  273.  280.  273.  275.  275.  275.  270.  270.  270.
 5.  270.  275.  275.  275.  280.  280.  285.  290.  295.  300.
 6.  305.  310.  315.  325.  330.  345.  365.  410.  530.
 1. ***** ***** ***** ***** ***** ***** ***** ***** *****  100.
 2.  105.  105.  105.  110.  110.  115.  120.  130.  150.

NORMALIZED AMPLITUDE AS AT REFLECTION HEIGHT 100KM IN [DB]
       TOPF    2.    3.    4.    5.    6.
 F      29.    0.   51.   68.   69.   66.
 E      25.   43.
ES      18.


PROFILE - ULCAR
---------------
   W =    .0  KM
   FSTART PEAK HT   AO       A1       A2       A3       A4      DEV   ROOTS
    [MHZ]  [KM]     [KM]     [KM]     [KM]     [KM]     [KM]  [KM]/PT
E    .199 105.879 -24.457   6.666  -3.093                        1.1    -
F1  2.899 166.233 -47.419  -9.093  -2.099   -.018  -1.735  11.9    -
F2  4.199 245.895 -69.529  -6.622  -2.657   -.137   -.721   5.3    -
```

Figure 3.13 Simplified Printer Output for ARTIST Scaled Ionospheric Data, Richfield, Utah, 12 October 1984, 1659 UT

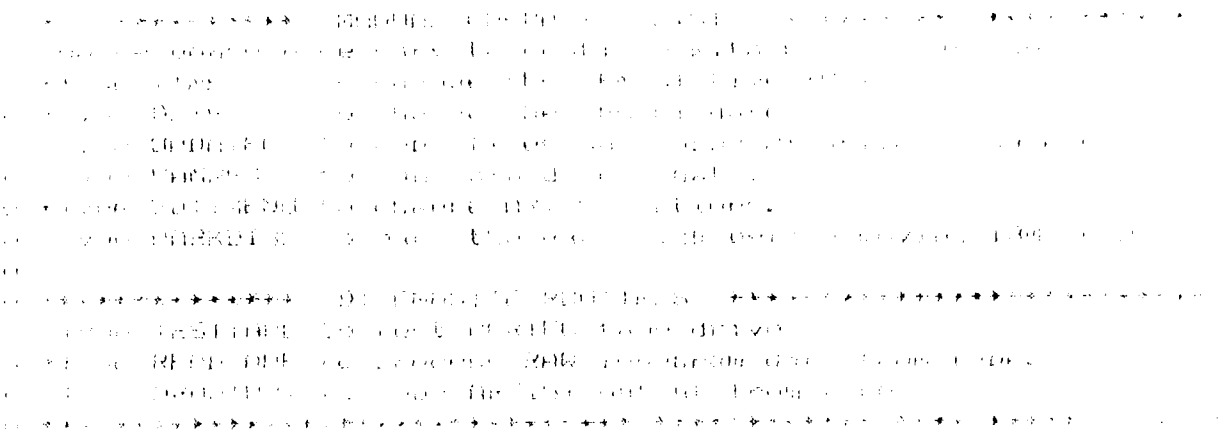

Figure 3.13 APTIST Utility Program, Manual Operation List

the Processor clock when resetting the ARTIST, and at seventeen minutes after each hour if there is a difference between the ARTIST clock and the Processor clock of more than two seconds; so it is important to have the ARTIST clock set accurate to the second.

4. The PARKDISK command will park the head on the hard disk drive before one moves the computer. It performs the same function as the "prepare for moving" option on the IBM setup disk.

5. There are some test routines accessed by the TESTAR command. One of the Test routines, TESTTAPE, is particularly convenient for exercising the Tape subsystem.

6. EDITMENU will allow the editing of either the on-line ARTIST menu or the Tape Playback menu.

4.0 N(h) PROFILE CALCULATIONS

4.1 Review of ULCAR's True Height Algorithm

4.1.1 Principle Approach

The calculation of the true height profile from the virtual height traces can be separated into three basic parts: the estimation of a starting height, the calculation of a valley between the E and F layers of the ionosphere, and the true height inversion for the idividual ionospheric layers. ULCAR's treatment of the starting height and valley parts of the calculation have changed throughout the contract period and represent some of the improvements made to the N(h) profile algorithm. These are discussed below. The method developed at ULCAR to solve for the true height profile for a particular ionospheric layer is as follows. The profile (z. vs. f) is expressed as

$$z = z_m + g^{1/2} \sum_{i=0}^{I} A_i \, T_i^*(g) \qquad (1)$$

where the A_i's are the coefficients of the polynomials (z_m refers to the peak height of the respective layer and can be found by: z_m = start height - $\sum A_i$), the T_i^*'s are shifted Chebyshev polynomials (Snyder, 1966), and g is the function

$$g = \frac{\ell n \; f/f_{end}}{\ell n \; f_{start}/f_{end}} \; . \qquad (2)$$

Here f_{start} and f_{end} refer to the start and end frequencies for the respective layer and f is the frequency being con-

sidered. These polynomials are particularly well suited for handling the "wiggles" often observed in autoscaled traces, and with the factor g the expansion can accurately follow the peak of the layer at the critical frequency . The true height is obtained from the values of the coefficients A_i, which must be determined. Equation 1 is integrated to give the virtual heights of the layer in terms of the coefficients (Huang and Reinisch, 1982). This expression for the virtual heights is least-squares fitted to the autoscaled (measured) trace after the effects of underlying ionization have been removed from the trace. This yields the coefficients of the polynomials and, hence, the true height of the ionospheric layer. The average deviation of the calculated virtual heights from the measured trace serves as quality indicator. Another advantageous feature of this approach is that the true height is contained in a relatively small number of coefficients. The algorithm uses three terms (I = 2) for the E layer, five terms (I = 4 ...) for the F1-layer when present, and five terms (I = 4) for the F2-layer. In addition to the polynomial coefficients, the top height of each layer is calculated which is necessary to compute the true height.

The ULCAR approach was developed to work in real time on the ARTIST system and is optimal for data storage and subsequent recalculation of true heights (see eq. 1).

4.1.2 Shortfalls in the ULCAR N(h) Analysis Method

There were several shortfalls in the early versions of the ULCAR profile inversion algorithm:

1. Treatment of the valley between the E and F layers
2. E-layer profile

3. Starting height of the F layer at night

4. Starting height of the E layer

5. Presence of F1 layer

4.1.3 Steps to an Improved Algorithm

The initial model for the valley was that of Reinisch and Huang (1983). It was discovered that this model did not mesh well with the discrete autoscaled traces. To avoid the possibility of incorrect valleys, this model was removed and a monotonic (no valley) solution adopted while the valley problem was investigated. A model transition region between the E and F layers was developed. It was based on a slab of ionization above the E region with f_c = foE and a void V above the slab (see Figure 4.1). This model worked for most ionospheric conditions. For a certain class of ionograms, however, where the beginning of the F layer rises quickly, the calculations result in too large values for the thickness V, producing F profiles that are too high. The void part in the model was removed, therefore, and only the slab retained. The slab gives an estimate of the ionization content of the E-F transition region. Since it overestimates the ionization when a valley exists, the F layer profile will lie somewhere between the monotonic and actual solutions.

In the original program the E layer profiles were taken as parabolic in shape and the parameters describing the layer, foE, Y_E, and H_E came from autoscaling the E region of the ionogram. The time constraint of a real time system did not allow inverting more than the F layer and the memory space of the computer did not allow additional programming. With the removal of the subroutine for the Reinisch-Huang valley model and improvement in the computer's speed and memory space, the E layer solution was improved. A three term

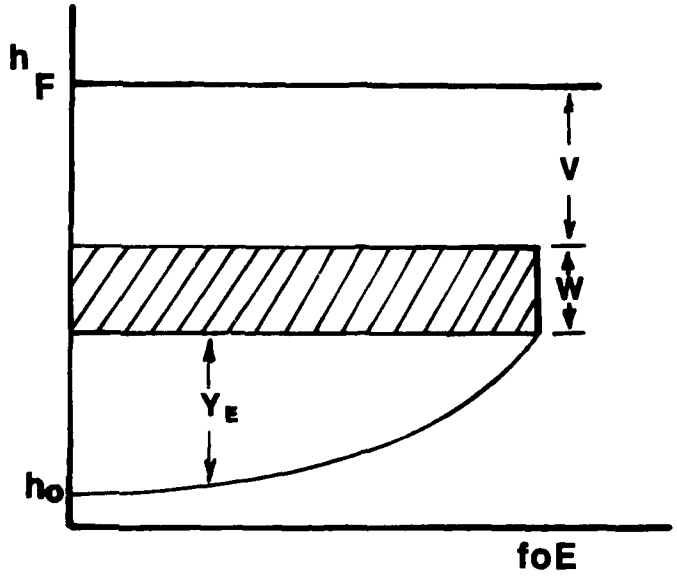

Figure 4.1 ARTIST Transition Region Model
(Old Program)

(Chevyshev) fit of the true height (I = 2 in equation (1)), including the effects of the magnetic field, is used and the resulting virtual height expression is least-squares fitted to the scaled virtual height trace. With this approach, the E region profile is computed using the data, rather than being assumed. In order to make these changes, the algorithm was rewritten in structured FORTRAN 77. The rewritten algorithm requires less memory and reduces computation time by a factor of three. Since the E region is better characterized, the estimate of the E region contribution to the virtual heights in the F region is improved as well.

For nighttime ionograms (no E region), the F region starting height was determined by extrapolation of the first three points of the trace. Because of the inaccuracies of autoscaling at the beginning of the F trace, the starting heights, and hence, to a lesser degree, peak heights of the layer, fluctuated from ionogram to ionogram. This was improved by the use of a better model which considers a parabolic F region given by

$$f^2 = f_c^2 \left\{ 1 - \left(\frac{h - h_m}{y_m} \right)^2 \right\}, \tag{3}$$

where h_m is the peak height of the layer, y_m is the semi-thickness and f_c is the critical frequency (foF2 here). Assuming zero magnetic field, this is integrated to give the virtual height as

$$h' = h_o + \frac{f}{f_c} y_m \ln \frac{f_c + f}{f_c - f} . \tag{4}$$

where $h_o = h_m - y_m$ (the bottom height of the layer). Equation (4) is least-squares fitted to the observed virtual

height vs. frequency data to give the parameters y_m and h_o. The correlation of the least-squares fit is used to determine how well the model applies; when the correlation is above 0.9 the starting height is given by h_o. When the correlation is less than 0.9 we use the old h'(f) technique of extrapolating the first three F trace points toward f = 0. With this model we also add several starting points to the scaled trace which usually starts above 1 MHz. Points at 0.2 MHz and halfway to fminF are added with the virtual heights given by equation (4). The addition of these points results in a smoothly varying monotonic trace compared with the non-monotonic results from the previous method (see Figure 4.2) as well as smooth variations of nighttime profiles with time.

The starting height for the E layer was fixed at 85 km (for Goose Bay Ionosperic Observatory) with no variation for time of day or season. This was improved by calculating a starting height for the E layer by the same method used for the nighttime F region starting heights (equations (3) and (4), with f_c = foE). The virtual height expression is least squares fitted to the scaled E region trace. This method provides a starting height value that is obtained from the data.

The single polynomial fit of the F1 and F2 layers was also changed. A single polynomial expression can not properly describe the peak region of the F1 layer (Figure 4.3) and does not satisfy the mathematical conditions specified in the development of the method (Gamache et al, 1985). The single polynomial fit discards the cusp points near foF1. The results of the single polynomial for both layers was compared with a fit of each layer separately for an ionogram taken at Goose Bay, Labrador on August 27, 1983 at 8:24 LT. Figure 4.3 illustrates the inadequacy of the single polynomial description incapable of reproducing the cusp at

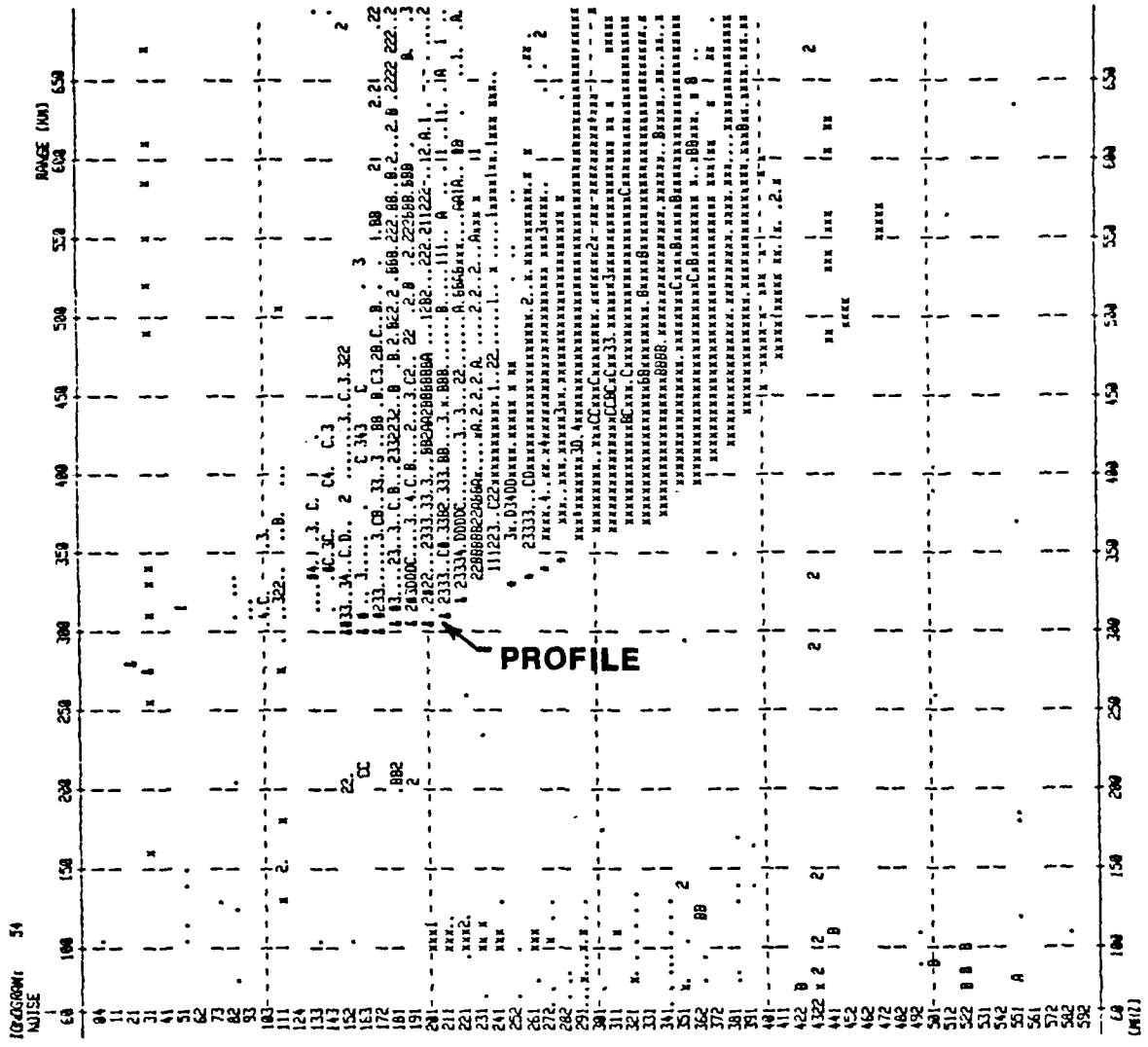

Figure 4.2 ARTIST True Height Profile (Old Program), Goose Bay, Labrador, 27 August 1983, 2144 AST; Note Unrealistic E-Region Profile

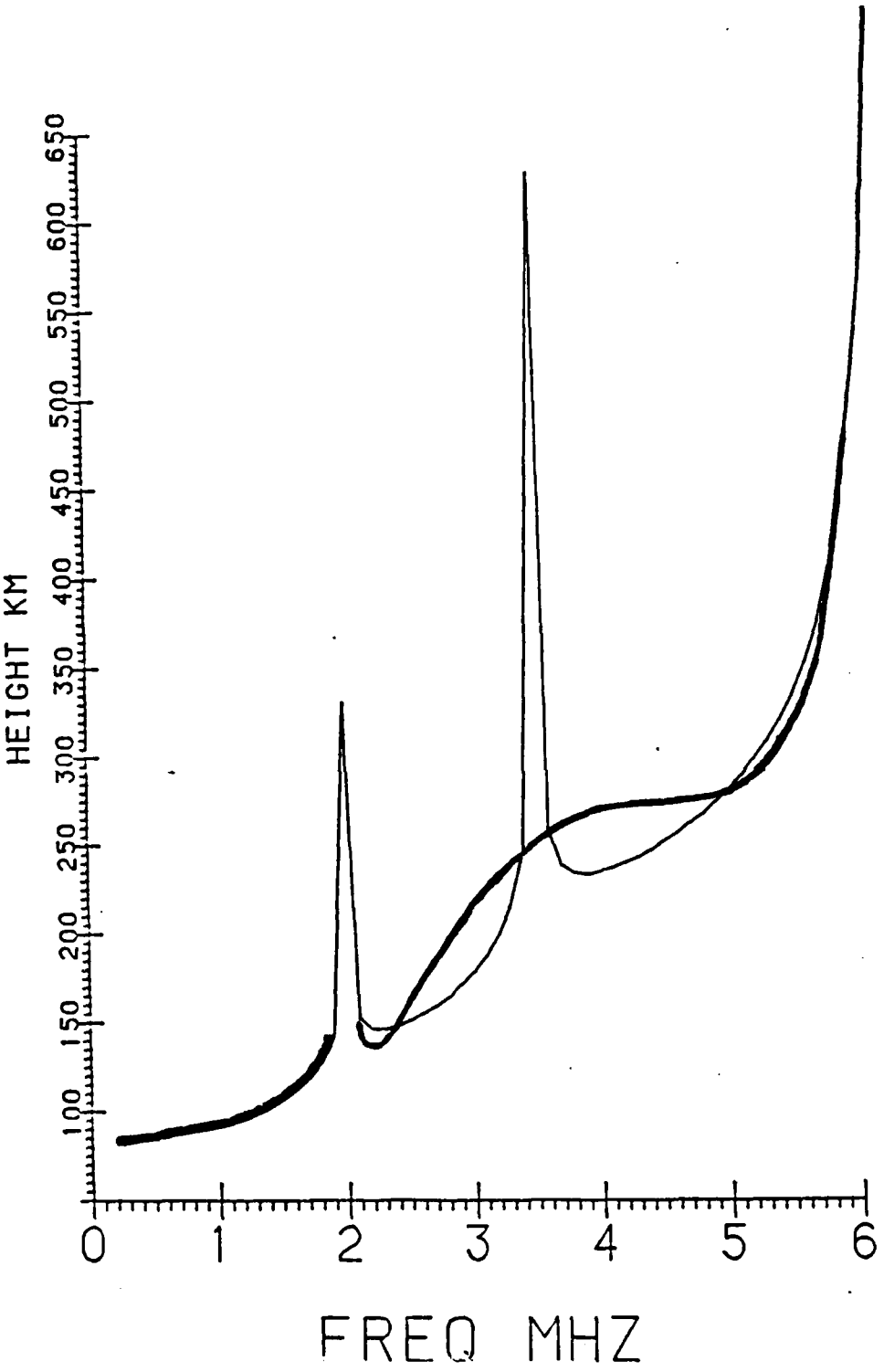

Figure 4.3 Recalculated Virtual Height Profile from the One-Layer Method Compared to the Measured Virtual Height Profile

foF1 = 3.5 MHz. The two polynomial description (Figure 4.4) on the other hand results in recalculated h' traces with very small absolute errors per point, namely 0.17 km/point for the F1 trace, and 0.48 km/point for the F2 trace (compared to 26.6 km/point for the single polynomial fit). The program was modified to treat each layer separately resulting in improved profiles when the F1 layer is present.

The final changes made to improve the algorithm deal with imposing physical constraints on the solutions and better adjusting the boundary conditions used in the inversion. In regards to the boundary conditions, the formalism fits from some start frequency to the final frequency (the critical frequency f_c). A problem occurs in the method at the final frequency, division by zero. In the previous algorithm, the final scaled point was eliminated giving results up to one point before f_c. The final point is now moved to f(critical) + 0.01 so that the last scaled point of the layer is used in the determination of the profile. The physical constraints on the profiles eliminate cases where the layer profile is non-monotonic, or one layer has a point lower than the peak height of the layer below it (or starting height when it is the E region). Traces are checked for unreasonable situations that would cause execution to stop and when encountered the inversion is stopped and control returned to the scaling program.

4.2 Current Status of the ULCAR N(h) Profile Program

4.2.1 Summary of Characteristics

ULCAR's N(h) algorithm uses the ordinary virtual height trace. The extraordinary virtual height trace is not currently available from autoscaling. The method uses a sum of shifted Chevyshev polynomials to represent the true height

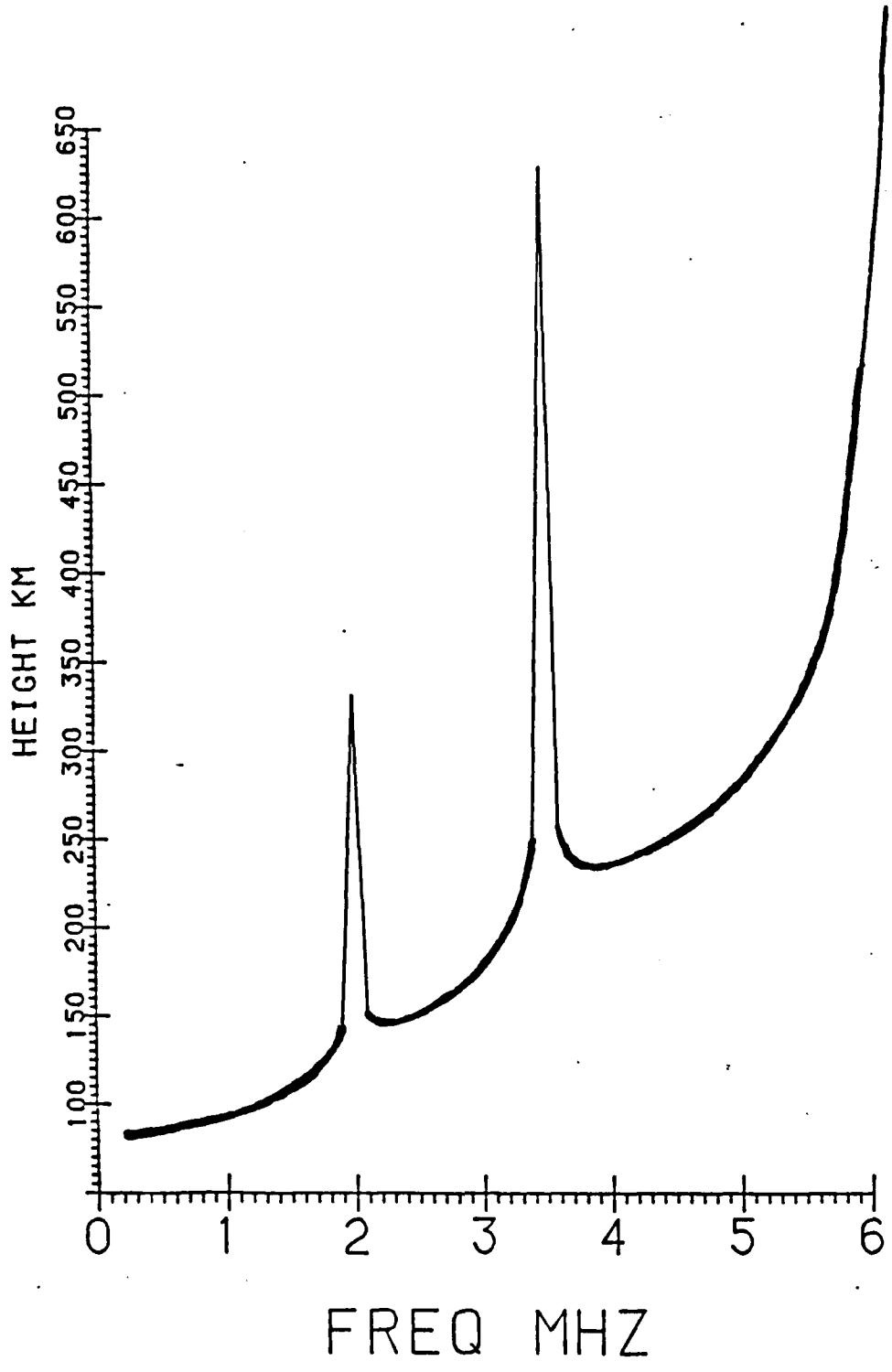

Figure 4.4 Recalculated Virtual Height Profile from the Two-Layer Method Compared to the Measured Virtual Height Profile

for each ionospheric layer (equation 1). The coefficients of the polynomial (3,5, and 5 for the E, F1, and F2 traces) are determined by least squares fitting the reduced virtual height trace (measured O-trace) to a virtual height expression developed from the polynomial fit to the true height. The reduced virtual height of each ionospheric layer has the impact of underlying ionization removed.

The starting height is determined from the data, thus diurnal variation and magnetically disturbed times are not overlooked. In this method we assume a parabolic profile (equation (3)), zero magnetic field and integrate the true height to obtain an analytical expression for the virtual heights (equation (4)). The parameters describing the layer are obtained by least squares fitting equation (4) to the observed virtual height trace. The correlation coefficient of the least squares is used to test the applicability of the model. If the fit is bad (correlation not near one) the routine resorts to the old models, otherwise the starting height is given by the parameter, h_o. For daytime ionograms, when the E ionization is present, the procedure uses the scaled E region trace to determine the starting height for the E layer profile. At night, when no E trace exists, the F layer trace is used and the starting height of the F region at 0.2 MHz is obtained. Because the trace usually starts above 1.0 MHz at night we also use the model (equation (4)) to add several virtual height points to the data. Without these points the profile may have unphysical characteristics, e.g. the true height decreases with increasing electron density. In practice it appears that this model of the starting height works well for both day and night conditions.

A slab of ionization with a plasma frequency equal to foE is used to model the ionization content of the E-F transition region and is determined by a least squares fit of

the expression for the virtual height. The ULCAR program accounts for the ionization content of the transition region This again allows the data to determine the parameters. The slab model tends to overestimate the ionization content, hence the widths are always smaller than the actual widths. This ensures that the ULCAR solutions are bounded by the monotonic solution and reality. Until the ARTIST system can handle the extraordinary trace in addition to the ordinary trace, the valley cannot be better described.

Physical constraints are applied to the trace throughout the procedure and to the resulting profiles from each layer. This helps ensure that the computer calculations will not terminate (abort) and also provides a consistent profile (a discussion of the physical properties of true height profiles can be found in Titheridge, 1985) from the start frequency to the final frequency of the data. When conditions are encountered that do not meet the constraints, attempts are made to adjust the data; if these adjustments do not correct the data, the profile calculation is stopped and control returned to the calling program. This is extremely important for real time systems. Some examples of these constraints are: when gaps in the data between layers are detected, the data are extrapolated to eliminate the gap since the presence of the gap often yields unphysical results and in many cases causes the computer program to abort. When the starting height of a layer is lower than the peak height of the underlying layer, the height of the upper layer is adjusted upward to eliminate this condition. When there is a data point missing just before the critical frequency, the calculation would abort; this condition is checked and when encountered a point is added by interpolation.

4.2.2 Program Implementation in ARTIST.

The ULCAR N(h) analysis program has been running as part of the ARTIST system from the spring of 1986 to the present. The program is documented and is written to conform to military standards of programming (MIL-STD-483). Thousands of ionograms under a diverse range of conditions (day, night, spread, magnetically disturbed,...) have been inverted to produce the true height profiles in real time. These data have been collected at several different geographic locations. An in-house version of the program, which differs only by the input and output of data, has also been run on scaled traces to produce true heights for ionograms taken at Erie, Colorado and Richfield, Utah. In all cases the inversion algorithm ran uninterrupted producing physically reasonable true heights. A time sequence of the profiles was produced to study the sunrise transition period at Goose Bay, Labrador (Figure 4.5). In Figures 4.6 to 4.9, profile inversion results from ionograms taken at Argentia, Newfoundland are shown (superimposed on the ionograms) to illustrate some of the possible situations that occur and are handled by the algorithm. Figure 4.6 shows a daytime ionogram (E, F1, F2 layers), the autoscaled trace is marked by *'s for the E region and by #'s for the F1 and F2 regions. The calculated profile is plotted with 5 km resolution by the "&" symbols. The same symbols are used in all figures. Figure 4.7 shows an ionogram with only an F2 trace. A model E-layer with foE = 0.8 MHz was used in calculating the F profile. Since no retardation is seen at the low frequency end of the F trace (because of the large gap between foE and fminF) a monotonic profile is assumed by the algorithm, producing F layer heights that are too low. The program needs further refinement to properly treat this situation. (An E layer model is used when the autoscaling does not find an E trace because of

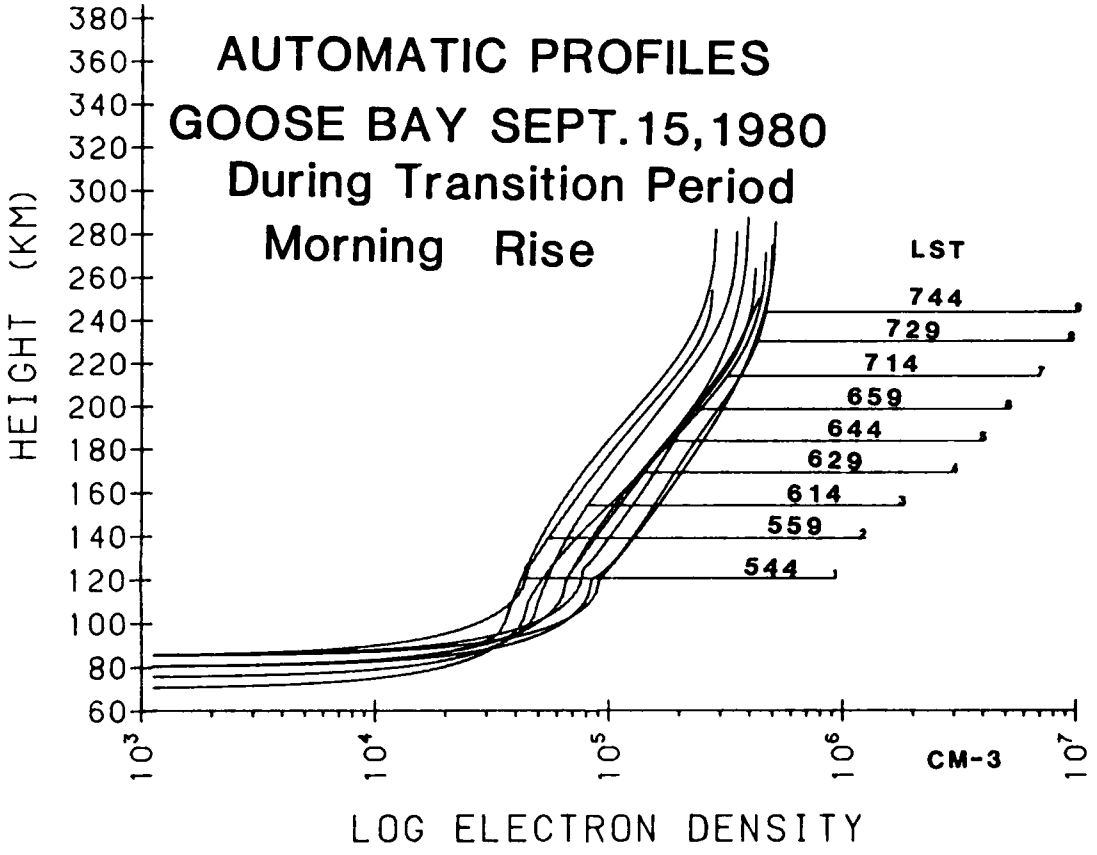

Figure 4.5 True Height Profile Through the Sunrise Transition, Goose Bay, Labrador, 15 September 1980, 0544 - 0744 AST

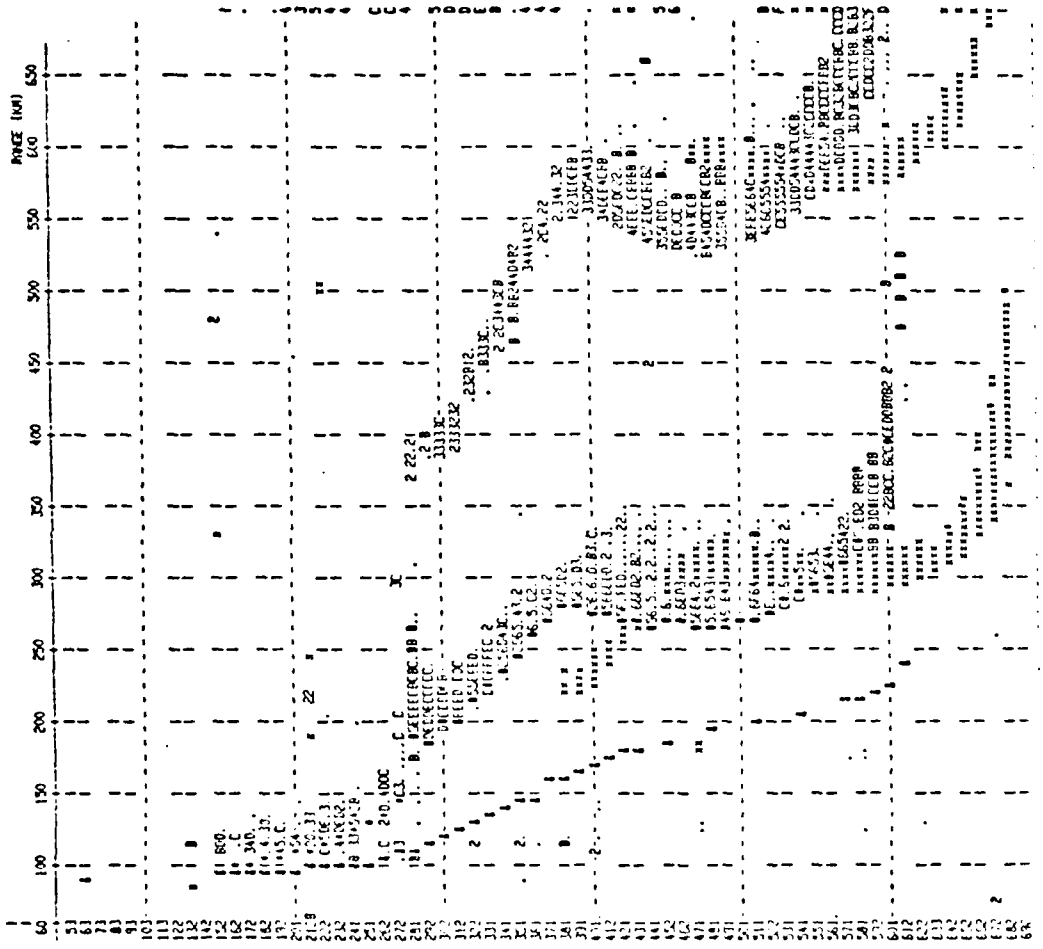

Figure 4.6 ARTIST Scaled Daytime Ionogram, Argentia, Newfoundland

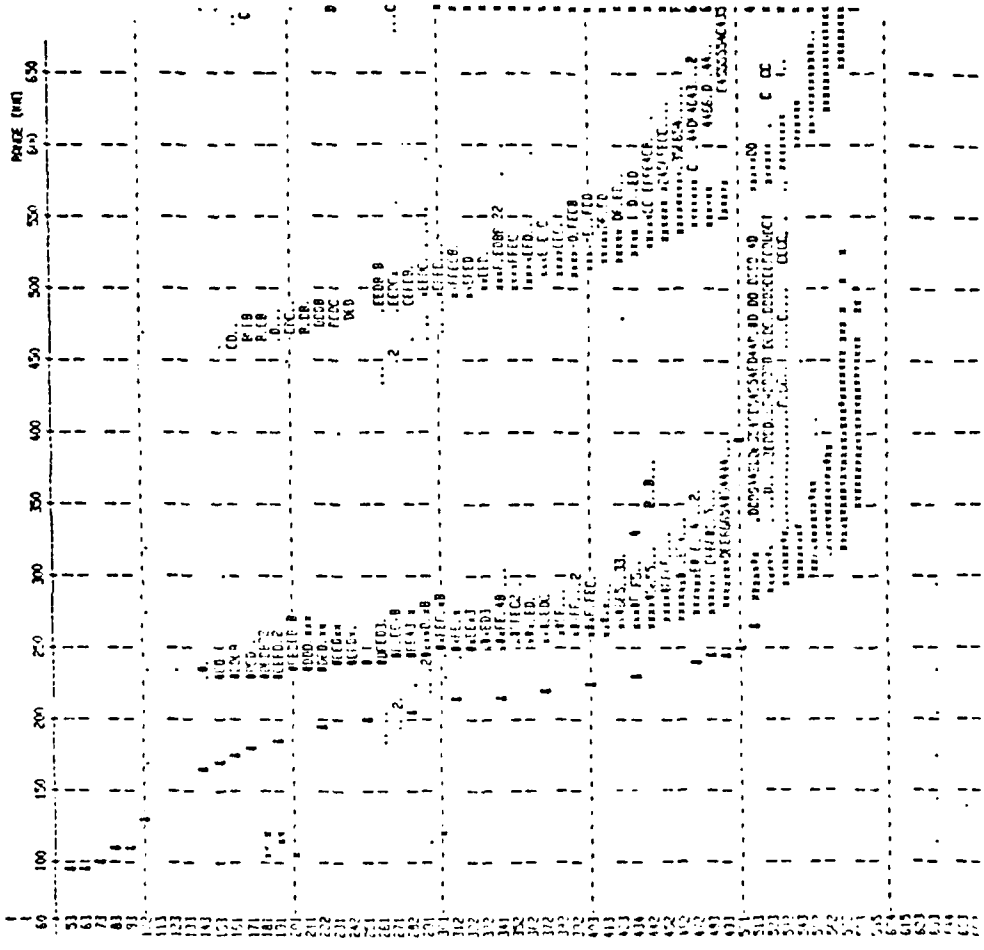

Figure 4.7 ARTIST Scaled Ionogram with High fmin, Argentia, Newfoundland

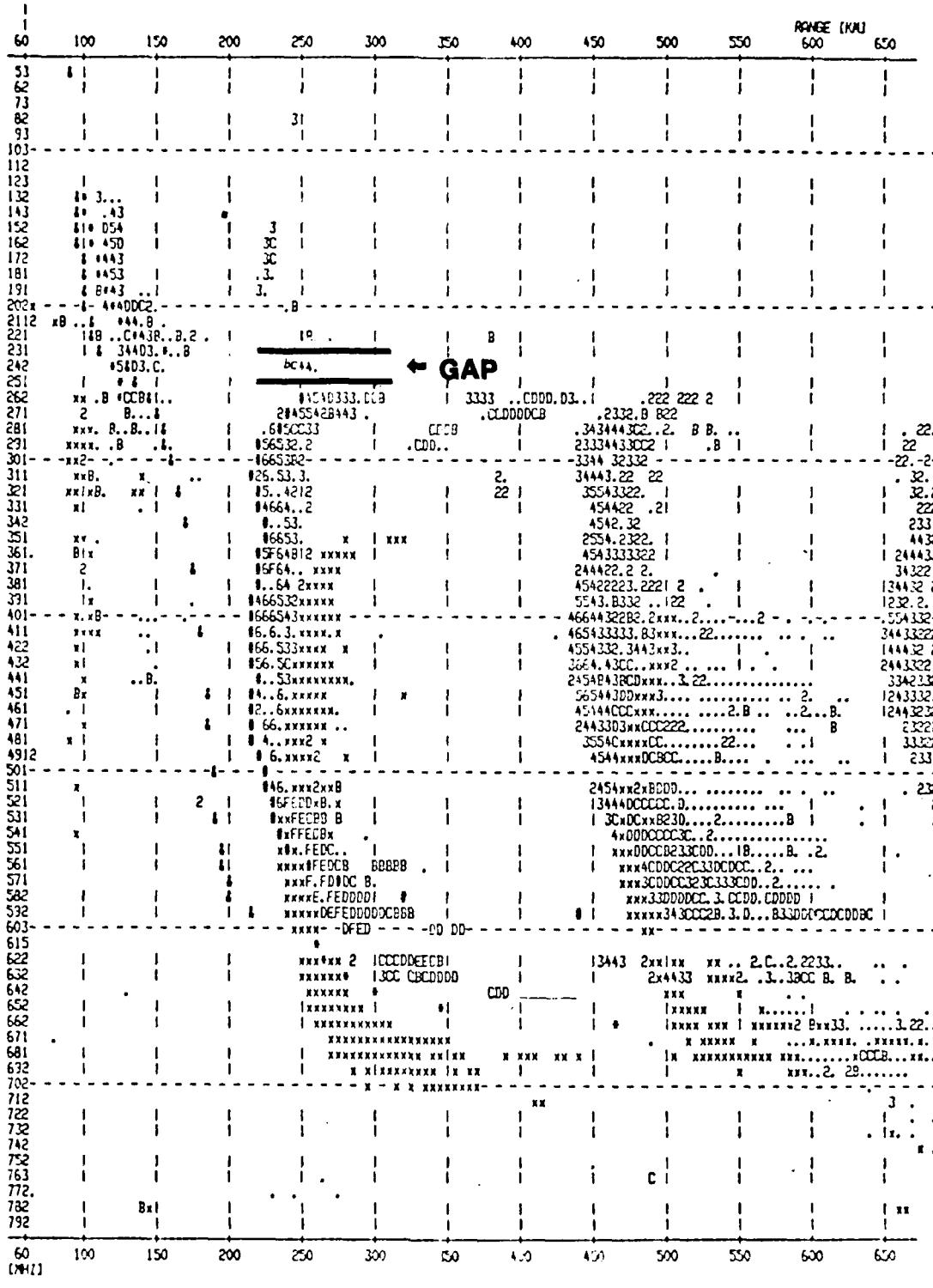

Figure 4.8 ARTIST Scaled Ionogram with Gap Between foE and fminF, Argentia, Newfoundland, 26 October 1986, 1159 AST

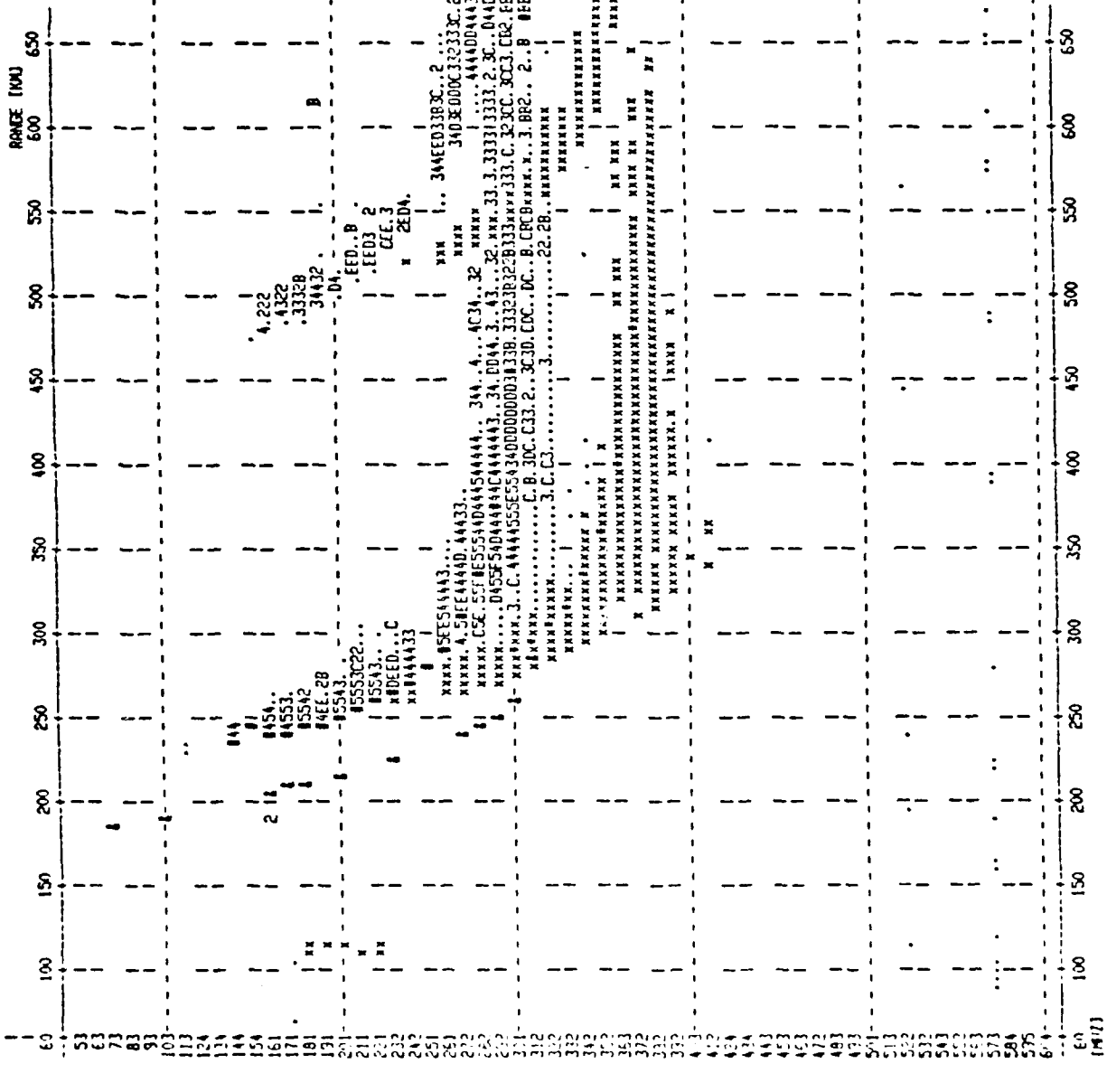

Figure 4.9 ARTIST Scaled Nighttime Ionogram with Realistic Low Frequency True Height Profile, Argentia, Newfoundland, 3 November 1986, 2359 AST

blanketing, absorption or system limitations at the low frequency end.) Figure 4.8 illustrates the filling of a small gap between foE and fminF to produce the profile in the figure. Figure 4.9 is a typical example of a nighttime ionogram and can be compared with the results in Figure 4.2. Note the current algorithm results in a physically acceptable profile compared with the old method that shows the true height decreasing with increasing frequency for the first few points (Figure 4.2).

4.3 POLAN N(h) Profile Program

We are considering the addition of the N(h) analysis program POLAN, developed by Titheridge (1978, 1985), to the ARTIST software. The principle advantage of the POLAN program is that it considers both the ordinary and extraordinary traces. This allows greater accuracy in the determination of the starting heights and of the valley parameters. POLAN was devised to be a stand alone program, i.e. a calling program sets up an array of input data and calls POLAN, on the return the array contains the true height. In order to run this as an option in ARTIST a series of subroutines had to be written to set up the data as input for POLAN in the ARTIST environment. To test this, a program was written to read an input array and store the data as if it came from ARTIST autoscaling, the routines then read the "autoscaled" data and go through the process of setting up the POLAN input array (virtual height data). There are a number of modes of operation of the POLAN program. For automatic real time processing we selected the single-polynomial-per-layer method; a model valley is placed between the E and F layers when only ordinary trace data are available; and the start height in daytime is given by the model of McNamara (1979). Station dependent parameters are the electron gyro-

frequency at the ground in MHz and the geomagnetic dip angle in degrees.

With the selection of the single polynomial/layer in POLAN the true height is given

$$h - HA = \sum_{j=1}^{NT} q_j (FN-FA)^j \qquad (5)$$

where HA and FA are the starting height and frequency of the layer, FN is the frequency under consideration, h is the true height that is being calculated, the q_j are the polynomial coefficients to be determined, and NT is the number of terms in the sum. The peak of the layer is described by a Chapman profile which is smoothly attached to the polynomial function given in equation (5).

The length h in equation (5) is related to the reduced virtual heights (underlying ionization removed) by

$$h''(i) - HA = \sum_{j=1}^{NT} jq_j \int_{FA}^{FR} \mu'(F_i,FN)\cdot(FN-FA)^{j-1}\, dFN \qquad (6)$$

where μ' is the group refractive index, and FR the plasma frequency at reflection. The integral is evaluated at each input point i and the coefficients q_j evaluated by least-squares. The methods of analysis are fully described by Titheridge (1985).

There are several reasons to consider adding a POLAN option to ARTIST, the most compelling is that POLAN contains code which considers the X-trace in the solution of the electron density profile. As stated above the X-trace improves the calculation of the valley parameters and of the starting heights. The program POLAN was found to be one of

the best two methods studied by an URSI Working Group set up to compare available methods (McNamara, 1979). (The ULCAR method was not part of the test.).

There are, however, some problems expected with dovetailing POLAN for real time ARTIST operation. The POLAN program was not written to operate as part of a real time system. It requires manually scaled traces as input, with no unrealistic features. This is not the case with autoscaled traces. While most of the ionograms can be autoscaled without problems, there are ionograms where gaps or oscillations occur. Here a human scaler simply corrects the data by eye. For real time processing this must be done by algorithms and a large part of the ULCAR profile method is devoted to this task. Similar routines must be written to operate on the autoscaled traces before they are inverted by POLAN.

The trace manipulation programs were written and tested on several thousand ionograms from Argentia, Newfoundland; Goose Bay, Labrador; Erie, Colorado; and Lowell, Massachusetts without aborting. The program POLAN has also been tested on some data from Erie, Colorado, and manually scaled ionograms from the WARF installation in California and the AFGL Airborne Ionospheric Observatory. The calculations were done using the selected mode of POLAN (mode = 5, start height from McNamara's model). The results displayed several problems with the POLAN solutions. In several runs the program aborted. These cases were corrected by manually smoothing the trace, adding points and adjusting the starting frequencies. Some results showed true heights that were nonphysical, i.e. decreasing height with increasing frequency. The causes of this were traced to the virtual height data starting at $\approx$1.5 MHz and greater and to erroneous virtual heights at the start of the F-trace. Once again the method to correct the data was to manually change the autoscaled traces.

At this time the POLAN program is not ready to be used in real time. Error checks for taking the square root of negative numbers, dividing by zero, and exceeding array bounds will have to be added and the data base must be conditioned so that execution does not terminate.

5.0 OBSERVATIONS AT GOOSE BAY, LABRADOR

AFGL's Goose Bay Ionospheric Observatory is operated by the Canadian Marconi Ltd. ULCAR has provided service and consultation to assure collection of uninterrupted, high-quality ionospheric data. Indeed, for the three year period 1983 to 1985 98% of the hourly ionograms were successfully recorded. Less than one quarter of the missed hourly ionograms were due to Digisonde equipment failures. Preventive maintenance, special experiments, and power outages accounted for more than three quarters of the missed hourly ionograms. The hourly ionograms were manually scaled and the data submitted to the World Data Center in Boulder, CO. The autoscalings from the Goose Bay ARTIST were continuously reviewed and compared with manual scaling in an effort to improve the scaling algorithms (see Section 3.0).

5.1 Hourly Ionogram Data

Hourly Goose Bay ionograms were scaled and tabulated for the following periods:

1983 -- complete

1984 -- January through April; September through November

1985 -- August

These ionospheric data were scaled and tabulated consistent with the URSI definitions and guidelines. In the past, the scaled ionogram data were stored on punched cards. The complete scaled ionospheric data base for Goose Bay was placed on magnetic tape and archived at the University of Lowell Center for Atmospheric Research. The archived data are available upon request in hard copy and magnetic tape format. The hourly Goose Bay data on magnetic tape include:

1975 through 1983 -- complete
1984 and 1985 -- as noted above.

5.2 Review of ARTIST Performance

In an effort to detect systematic errors or inconsistencies in the autoscaling process we developed a program that reads the autoscaled h'(f) data from tape and plots them in a compact way. Figure 5.1 shows 48 hours of observation for August 27 to 29, 1983. This compact presentation clearly shows the arrival of the mid-latitude trough at 21 AST on 27 August, when foF2 falls to 2.3 MHz. The occasional overlapping of the E and F traces is caused, at night, by auroral E layer traces extending beyond fminF. The overlapping during daytime is simply the result of improper autoscaling. Corrective measures were implemented in the program as described in Section 3.0.

5.3 AFGL's Coordinated Ionospheric Campaign

Special efforts were made for the AFGL coordinated ionospheric campaign to compare ionospheric observations from three stations, Lowell, Goose Bay, and Arecibo, for September and October 1984. The hourly ionograms for 16 days were scaled: days 261-268 (September 1984) and days 278-285 (October 1984). Plots of range and frequency spread versus time were made for each day. In the range spread plots three levels were considered: light spread 8-14 bins (bin spacing is 5 km), medium spread 15-26 bins, and heavy spread > 26 bins. For the frequency spread the steps were: light spread 200-500 kHz, trace 2-3 pulse widths; medium spread O-X connected, trace 4-6 pulse widths, and heavy spread > 6 pulse widths. The 16 daily plots containing the analysis were delivered to AFGL; an example of the frequency plots is given

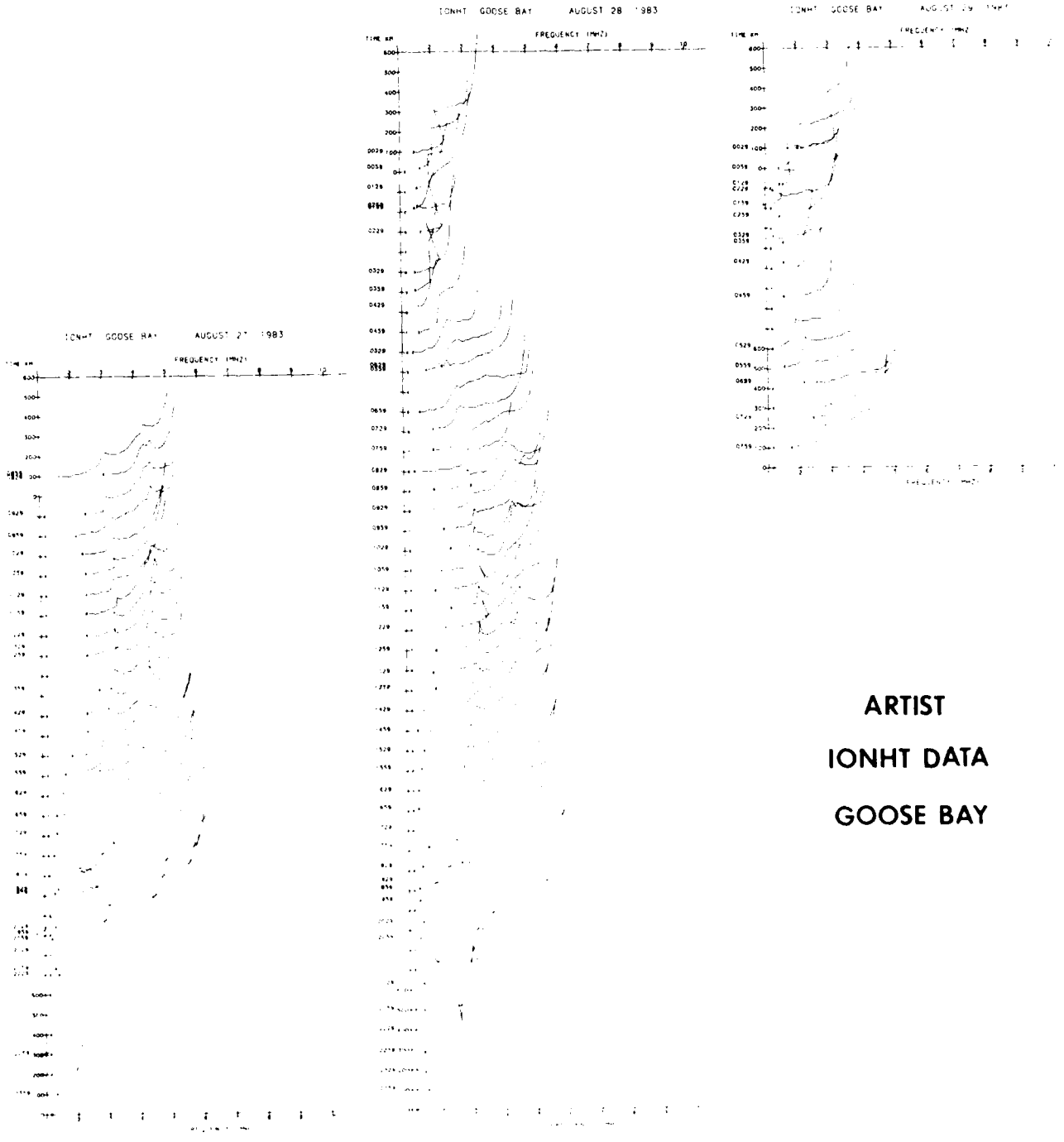

Figure 5.1 ARTIST Scaled I.F Data for [illegible]
Goose Bay, Labrador, [illegible]

in Figure 5.2. Drift measurements at Goose Bay are discussed in Section 2.1.1 of this report, and by Reinisch et al (1987).

5.4 Backscatter Observations

Backscatter ionograms from Goose Bay were analyzed to detect the arrival of the mid-latitude trough. In general, the trough is announced by the backscatter echoes two to three hours before it reaches Goose Bay. The average velocity of the approaching trough wall during the first half-hour after detection correlated well with the time of arrival of the trough.

To better understand the temporal variability of the Goose Bay ionograms we studied the now available microfiche prints (Section 13.0) of the ionospheric characteristics. The signature of a well developed trough is illustrated in Figure 5.3. This schematic shows the typical features seen on the frequency and range characteristics generated from the vertical and backscatter ionograms. On the frequency characteristic, or f-plot, for the vertical ionograms the trough clearly shows as a minimum in foF2 which is followed by the onset of aurora E or Es. The height characteristics show an increase in height and define an apparent width of the trough. Since the velocity of the equatorward trough motion varies from day to day, this time-width is only a coarse indication for the latitudinal width of the trough.

The height characteristics for the backscatter ionograms show two close echo traces of similar slope when the trough is approaching. We interpret these traces as [illegible] echoes from the equatorward (EW) and poleward (PW) [illegible] the trough. Since the background electron density [illegible] is not normally enhanced the reflection must occur [illegible]

AD-A192 270 HIGH LATITUDE IONOSPHERIC RADIO STUDIES(U) LOWELL UNIV 2/2
MA CEOTER FOR ATMOSPHERIC RESEARCH B W REINISCH ET AL.
JAN 88 ULRF-439/CAR AFGL-TR-87-0056 F19628-83-C-0092
UNCLASSIFIED FFG 4/1 NL

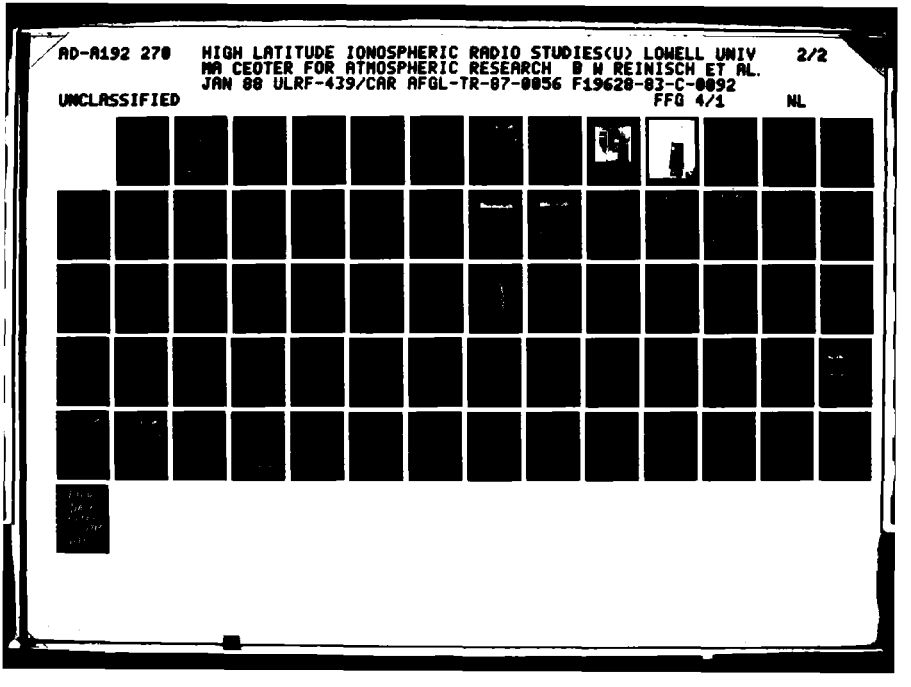

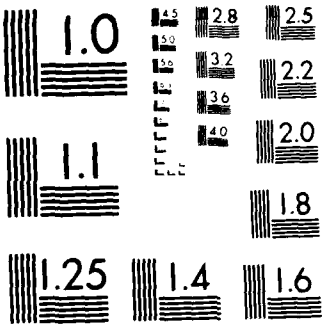

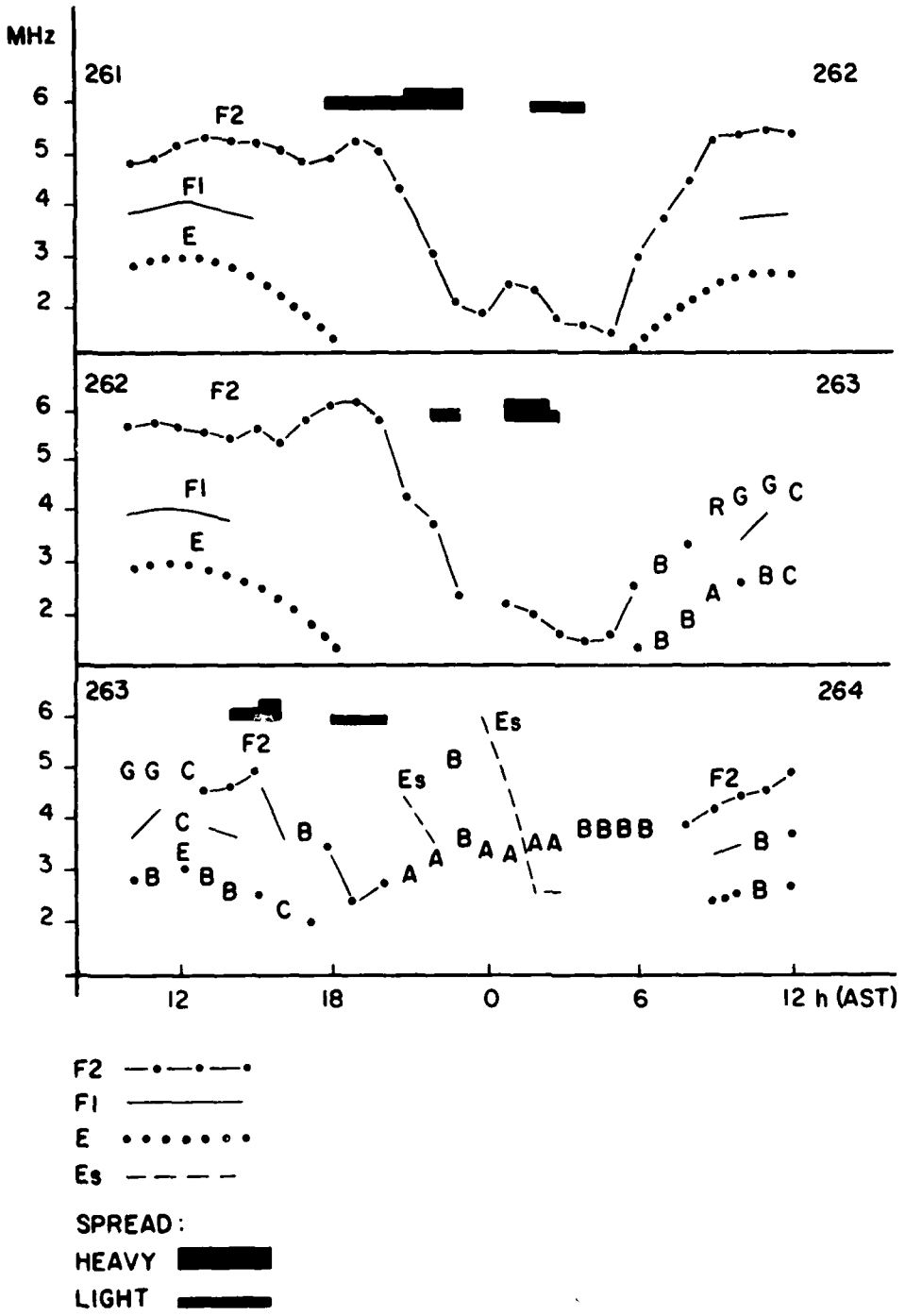

Figure 5.2 Critical Frequencies and Frequency Spread, Goose Bay, Labrador, 17/20 September 1984

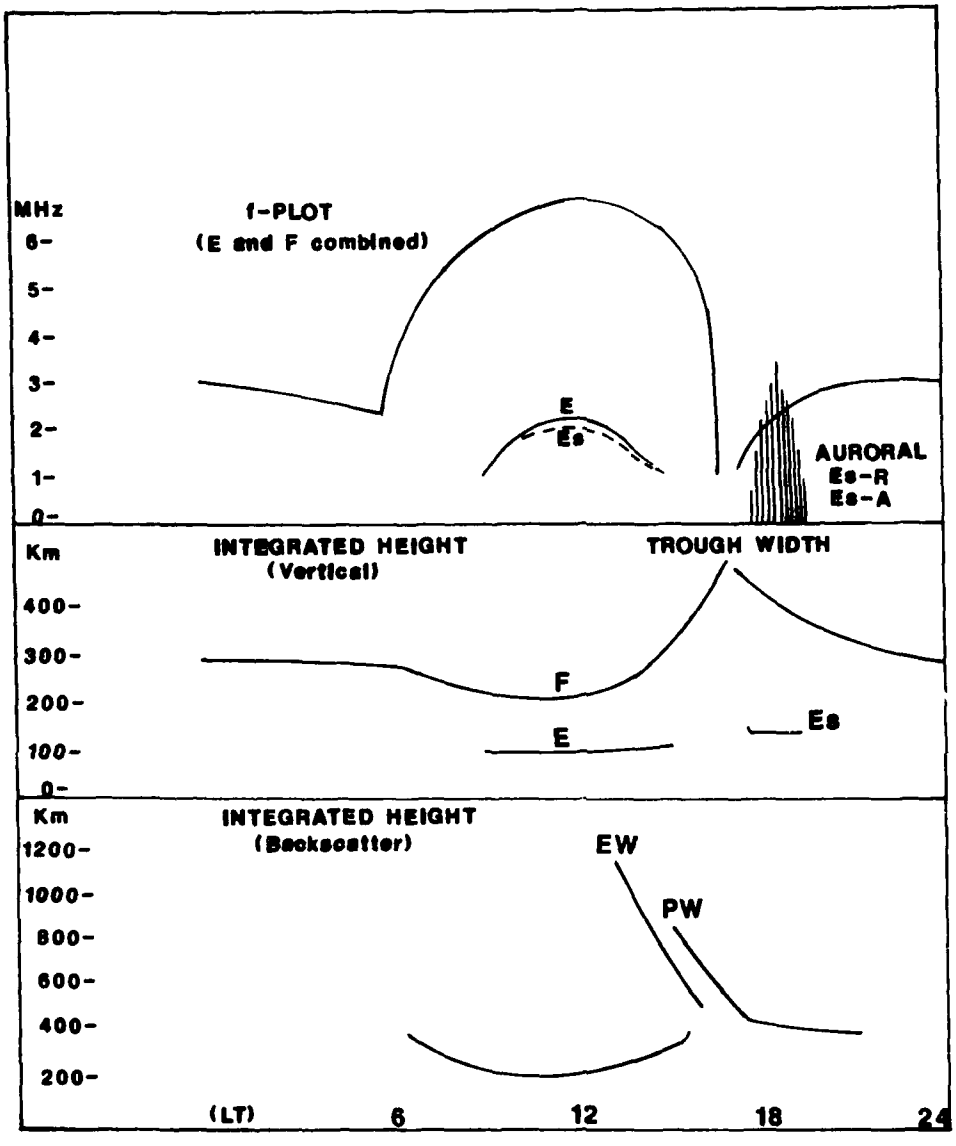

Figure 5.3 Schematic of Ionospheric Characteristics of a Well Developed Main F-Layer Trough

larities, associated with the steep horizontal gradient. Figure 5.4 is a schematic sketch of the trough, identifying the parameters that have been scaled.

Since microfiche characteristics were available for January 1984 we started analyzing these data in terms of the trough signature. Four specific times were scaled from the characteristics as shown in Figure 5.4.

1. Start and end of EW trace in oblique height characteristic.
2. Start and end of trough in vertical characteristics.
3. Start and end of PW trace on oblique height characteristics.
4. Start of aurora Es occurrence in E-region f-plot.

Frequently it is necessary to consult the individual ionograms to help interpret the characteristics. In Figure 5.5, we plotted the time of the first oblique detection of the equatorward trough wall versus time of arrival for the center of the trough at Goose Bay. For magnetically quiet days a three to four hours advance notice is provided by the oblique sounding. This reduces to one to two hours for magnetically active days (identified by stars in Figure 5.5). There are, however, a number of days (marked by x) that do not follow the general distribution.

The characteristics for January 1, 2 and 3, 1984 are shown in Figure 5.6. Overlay traces have been added to emphasize certain features.

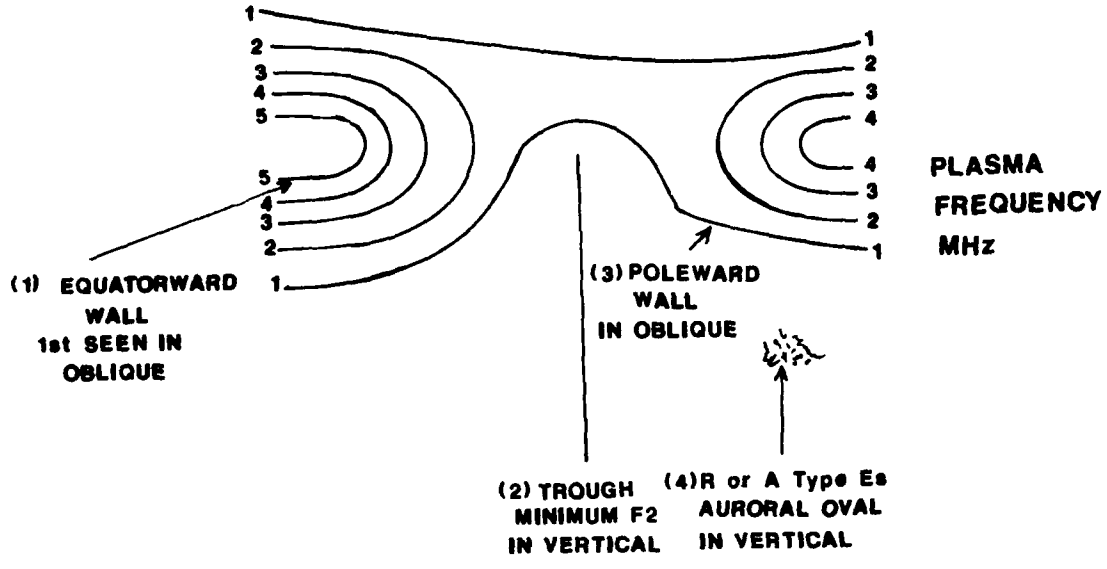

	(1)		(2)		(3)		(4)		COMMENT
IONOGRAM									
CHARACTERISTIC	START	END	START	END	START	END		TYPE	

Figure 5.4 Schematic of Meridianal Ionospheric Features and Associated Parameter Scaling Form

	DAY ACTIVITY	TIME 1st TRACE	ARRIVAL G.B.		DAY ACTIVITY	TIME 1st TRACE	ARRIVAL G.B.	
	1M	8	19:59		16Q			
JAN	2M	18:54	20:59	C	17Q	C	23:59	
84	3A	14:54	17:29	✓	18M	14:39	18:44	✓
	4A	13:24	16:59	✓	19S	17:09	19:14	*
	5A	14:39	18:29	✓	20Q	19:39	20:59	
	6Q	-	21:59		21Q	17:54	19:59	X
	7Q	18:14	22:59	✓	22Q	15:39	20:44	
	8Q	19:24	20:59		23Q	15:39	20:44	
	9Q	18:24	21:59	✓	24Q	17:39	23:59	
	10M	13:24	17:59		25M	15:39	18:44	✓
	11M	15:24	18:59	✓	26M	C	C	
	12Q	-	-		27M	-	18:59	
	13M	17:54	19:59	X	28M	15:24	18:29	✓
	14Q	17:14	20:29	✓	29S	17:54	19:09	*
	15Q	18:14	23:59		30S	17:24	18:14	*

● MAIN SEQUENCE
NO DOT, NO DATA 1st TRACE

* STORM

X ANOMALOUS

O NO TROUGH G.B.

✓ USE IN LINEAR REGRESSION

ACTIVITY

Q = quiet
M = medium
A = anomalous
S = storm

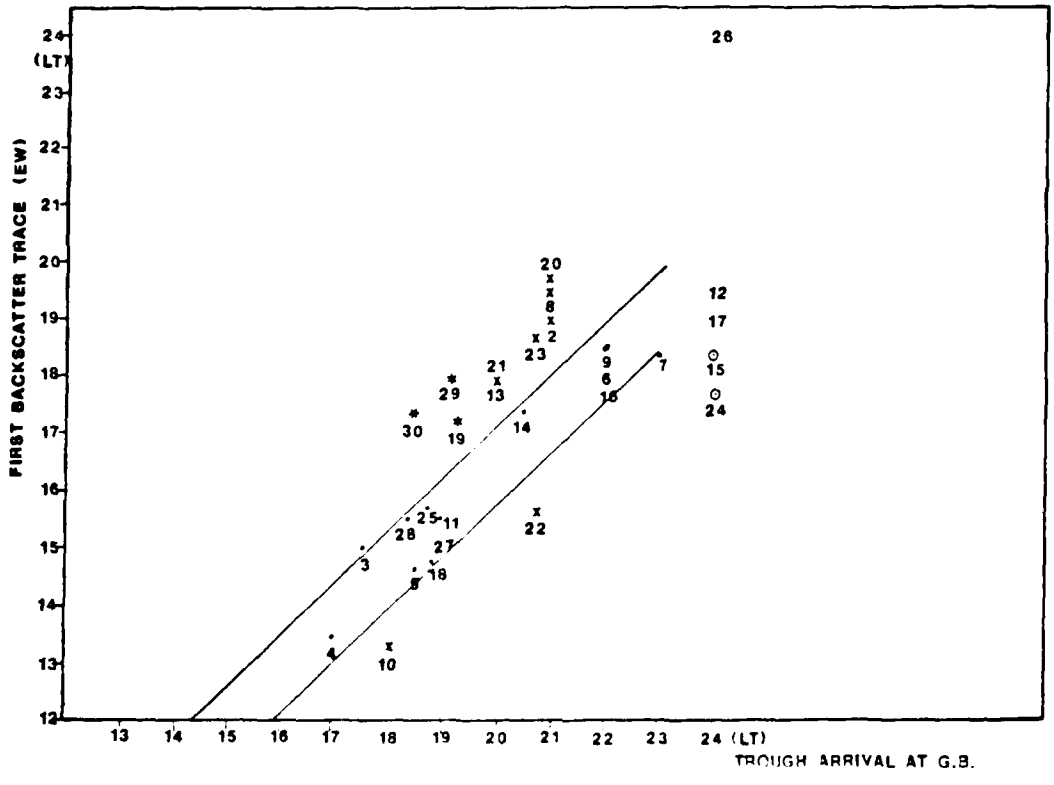

Figure 1. [illegible]
vs. [illegible] at [illegible]

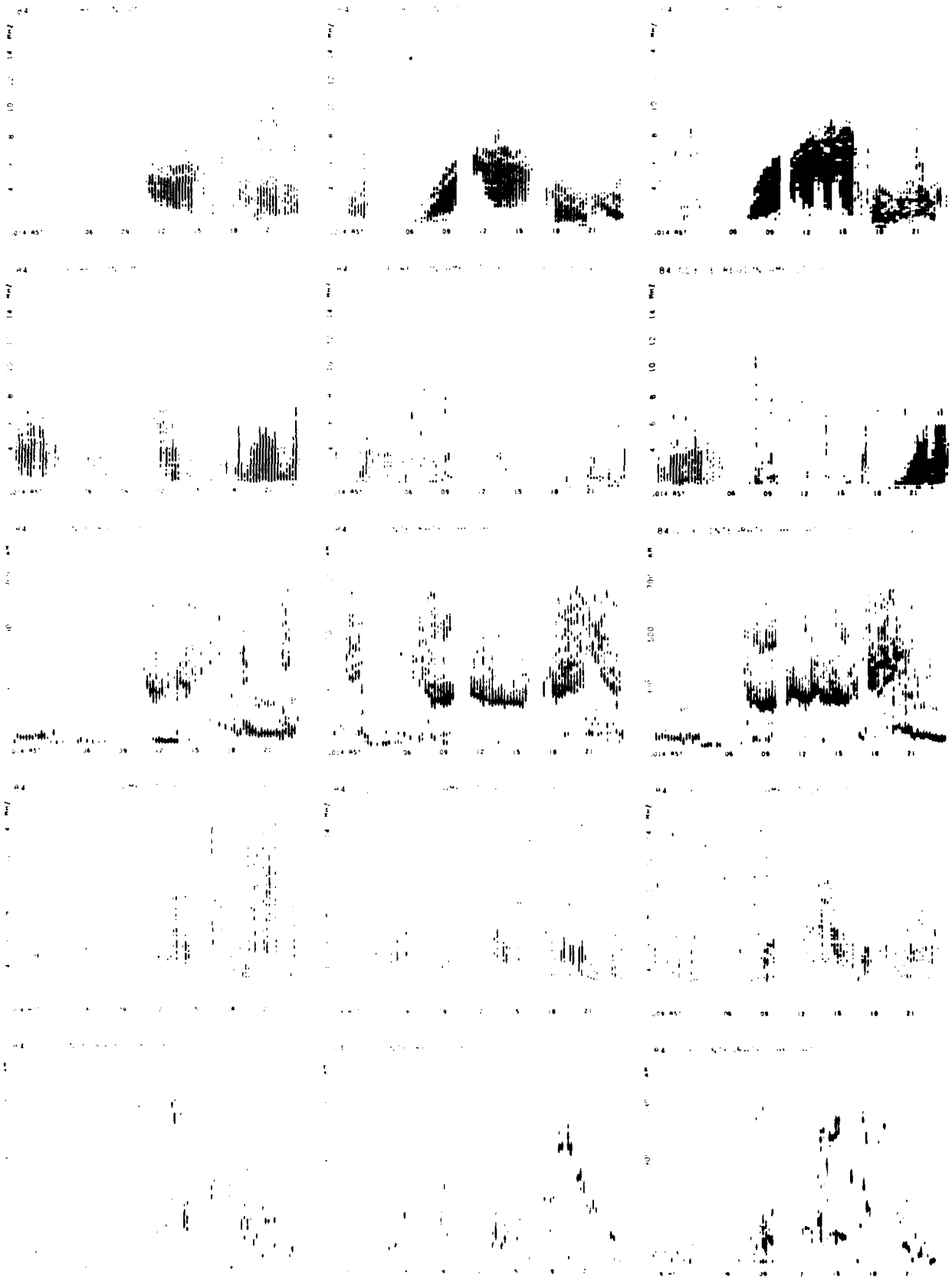

Figure 5.6 Ionospheric Characteristics for 1/3 January 1984

6.0 OBSERVATIONS AT ARGENTIA, NEWFOUNDLAND

Observations of the auroral ionospheric structure and dynamics, the main F-layer trough, and support of the OTH radar operation are the objectives for the new Digisonde installation at Argentia, Newfoundland.

6.1 System Assembly and Installation

ULCAR assembled and tested a complete Digisonde 256 system during the first half year of 1985. The government prepared sounder site did not provide for shelter for the Digisonde equipment. The equipment was therefore installed in a 8' × 16' (interior) trailer in the configuration shown in Figure 6.1. The trailer (Figure 6.2) is equipped with two 8300 BTU air conditioners (providing redundancy if one should fail) and dual axle "RV" suspension to assure smooth over-road transport. At the end of June 1985, the equipment together with the seven receiving loop antennas and the TCI 613F transmit antenna were loaded in the trailer, which was hauled to Argentia by a commercial trucker.

In October 1985, the power lines and the required telephone connections were available on site. The installation of the entire system was completed and the system started its fully automatic operation. Every half hour an ionogram is scanned, automatically scaled and the h'(f) traces converted to an electron density profile. Examples of a nighttime (14 October 1986, 0759 UT = 04:29 LT) and morning (16 October 1986, 1059 UT = 7:29 LT) ionograms are shown in Figures 6.3 and 6.4. The Digisonde ARTIST at Argentia is accessed by three telephone polling links as illustrated in Figure 6.5: the Automated Weather Net (AWN), the remote terminal at Goose Bay, and a dial-up link for use by ULCAR, AFGL

Figure [illegible] Digisonde 256 Electronics as Installed in Shelter at Argentia, Newfoundland

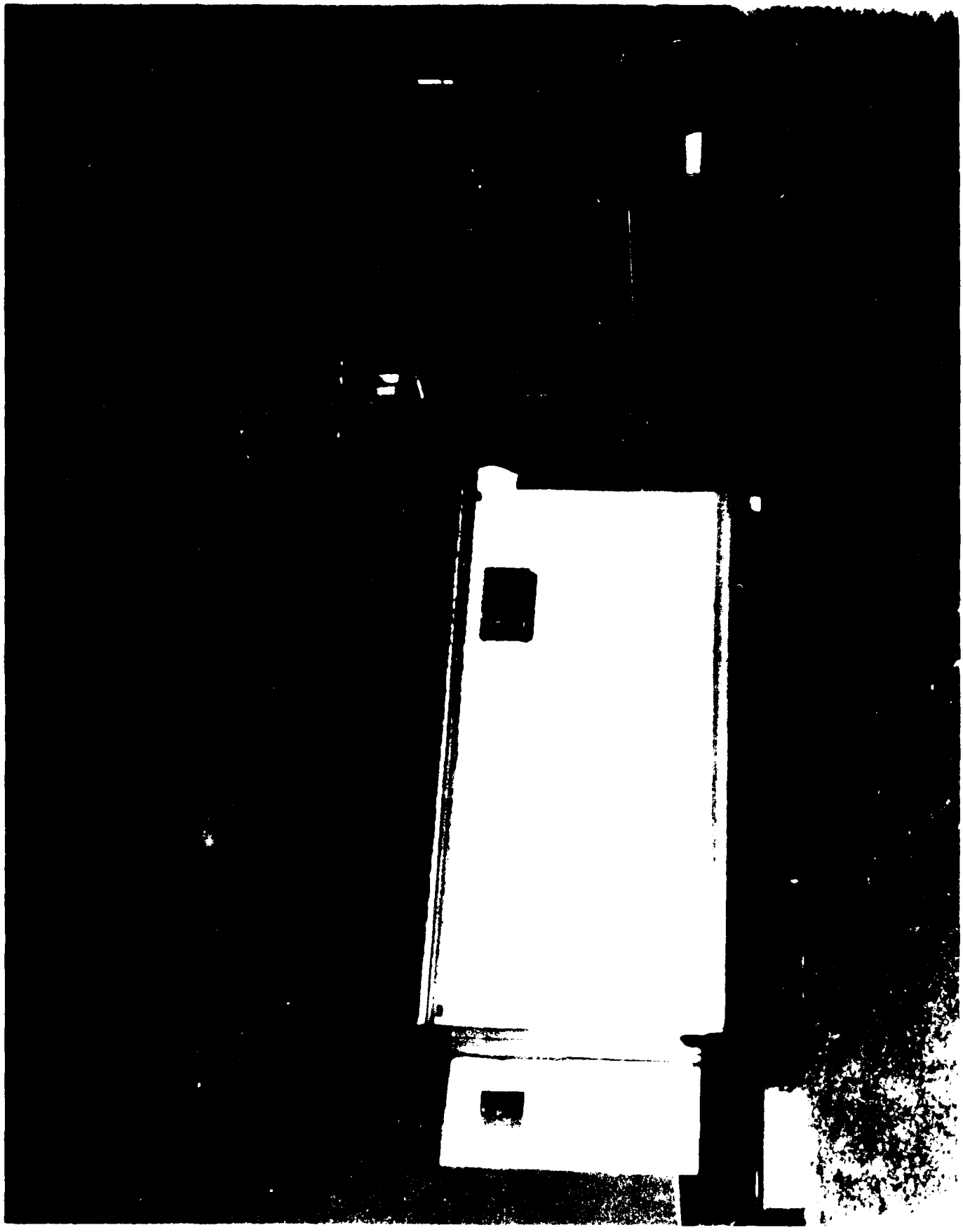

Figure 5.2 Digisonde 256 Field Site, Argentia, Newfoundland; Note Electronics Trailer

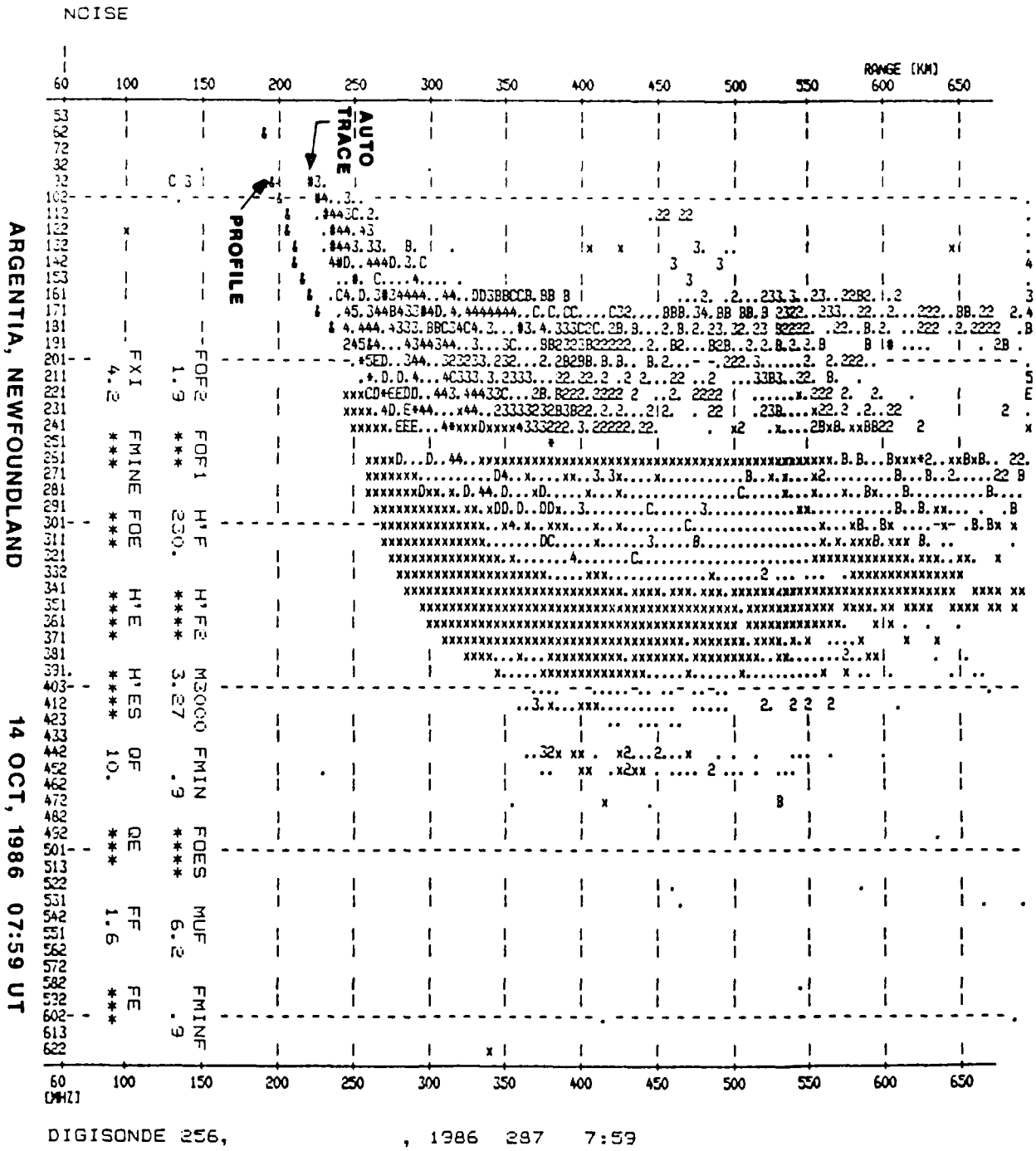
NOISE
RANGE (KM)
60
100
150
200
250
300
350
400
450
500
550
600
650
AUTO TRACE
PROFILE
FXI 4.2
FOF2 1.9
FOF1 ***
H'F 230.
H'F2 ***
M3000 3.27
FMIN .9
FOES ****
MUF 6.2
FMINF .9
FMINE ***
FOE ***
H'E ****
H'ES ****
QF 10.
QE ***
FF 1.6
FE ***
ARGENTIA, NEWFOUNDLAND
14 OCT, 1986 07:59 UT
DIGISONDE 256, , 1986 287 7:59

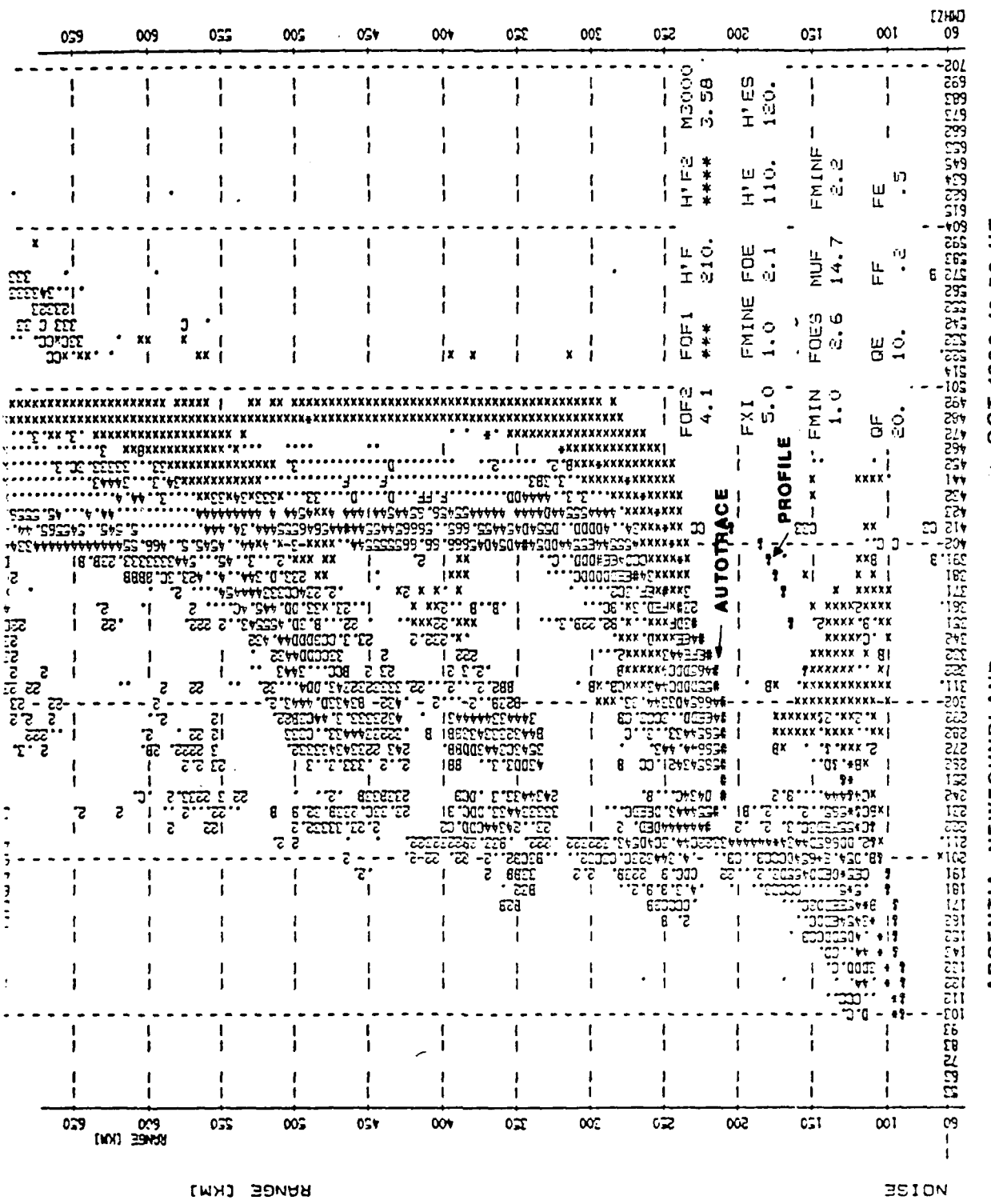

Figure 8.4 ARTIST Scaled Morning Ionogram, Argentia, Newfoundland, 16 October 1986, 1059 UT

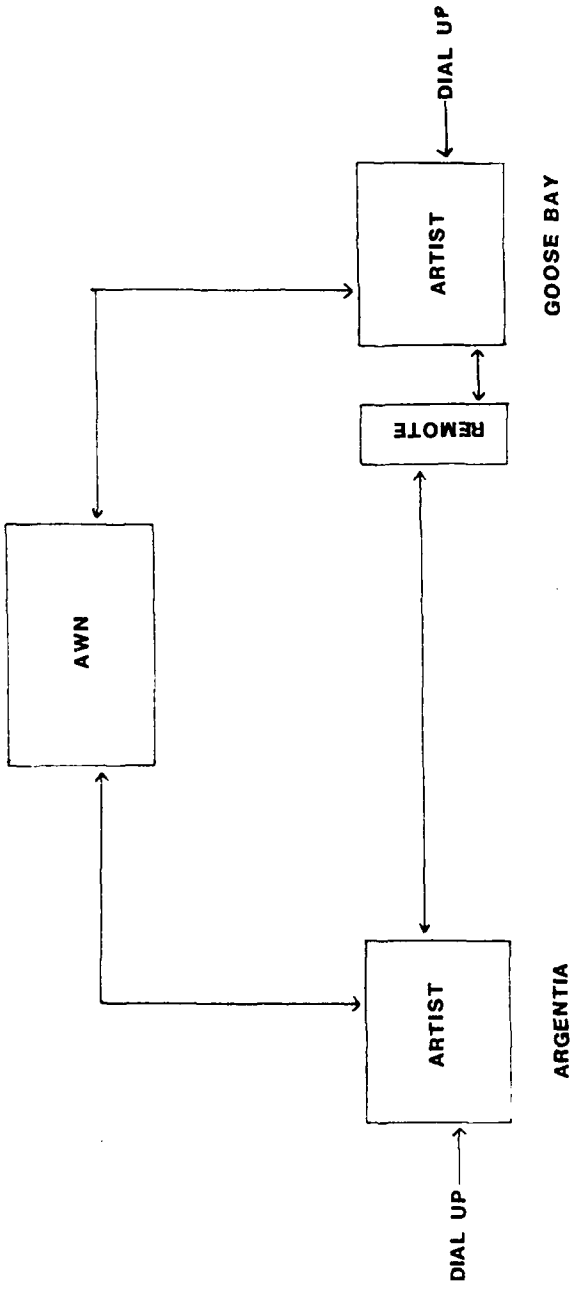

Figure 6.5 Configuration of Telephone Polling Links Between Argentia, AWN and Goose Bay

or other qualified users. Canadian Marconi personnel at the Goose Bay Ionospheric Observatory monitor on their terminal the performance of the Argentia sounder. In case of failure the site representative is called to take appropriate action.

6.2 System Performance

Since October 1985, the system operated continuously with very brief interruptions, mainly caused by power failures. Depending on the type of the power interruptions the Digisonde systems may or may not recover to full operative condition. If it does not recover an on-site manual reset procedure must be executed. An uninterruptible power supply (UPS) with a voltage regulator is needed. Since November 1986 these have been standard in all Digisonde 256 systems. We recommend to retrofit the system with a UPS to prevent the system's computers from getting hung up in illegal states.

Data messages are routed to the AWN port every half hour after the 29 and 59 minute ionograms, independent of whether more ionograms are made inbetween these times. The AWN communication protocol has undergone a number of changes, and although data were successfully transferred for about a year, a final protocol version has yet to be defined, implemented and tested.

On-site data storage on digital magnetic tape (9 tracks, 1600 bytes per inch) permits data playback and computer processing for scientific analysis. Initially, only the scaled data were tape recorded. When ULCAR revisited the site for the first time in February, data were still being written onto the first tape. Currently both the raw ionograms (3 blocks/ionogram) and the scaled data (1 block/ionogram) are written onto tape. For four ionograms per hour, one 2400' tape lasts about three weeks.

6.3 F-Region Drift Studies

As reported in Section 2.1.3 drift observations were made in Argentia in February, April and October 1986. Prior to the October campaign the autodrift routine was implemented and tested in the Digisonde ARTIST computer (see Section 2.2).

7.0 OBSERVATIONS AT THULE, GREENLAND

7.1 Polar Cap Campaigns

In January 1983, December 1983, January 1984, January 1985 and March 1985, ULCAR participated in AFGL's polar cap ionospheric observation campaigns. Radio and optical diagnostics onboard AFGL's Airborne Ionospheric Observatory (AIO) were used to study structure and motion of F region density enhancements in the polar cap (Weber et al, 1984). For the first time, circular polarized receiving antennas were deployed in 1983 when the AIO was on the ground at Thule AB (86° CGL). The Digisonde 128PS onboard the aircraft could now accurately determine foF2, since echoes with ordinary and extraordinary polarization were clearly distinguished. In the polar cap, range and frequency spread F is a permanent feature, making it difficult to scale the critical frequency without polarized antennas in the presence of slightly oblique echoes.

The ground-based and airborne radio/optical observations showed the importance of transport of plasma over large distances from the production or source region across the polar cap. The unique ability of the AIO to monitor specific ionospheric features for extended time periods is illustrated in Figure 7.1. To investigate the structure of drifting F-layer patches as they separate from the dayside cusp region (Weber and Buchau, 1985), the aircraft spent five hours (from 06 to 11 UT) in the dark noon sector. The flight track is plotted in a corrected geomagnetic latitude/local time coordinate system (Figure 7.1). The results of the winter polar cap F region research were published in papers by Buchau et al, 1983, Weber et al, 1984, and Buchau et al, 1985. Reinisch et al, 1987 discusses details of the Digisonde Doppler drift observations at Thule AB.

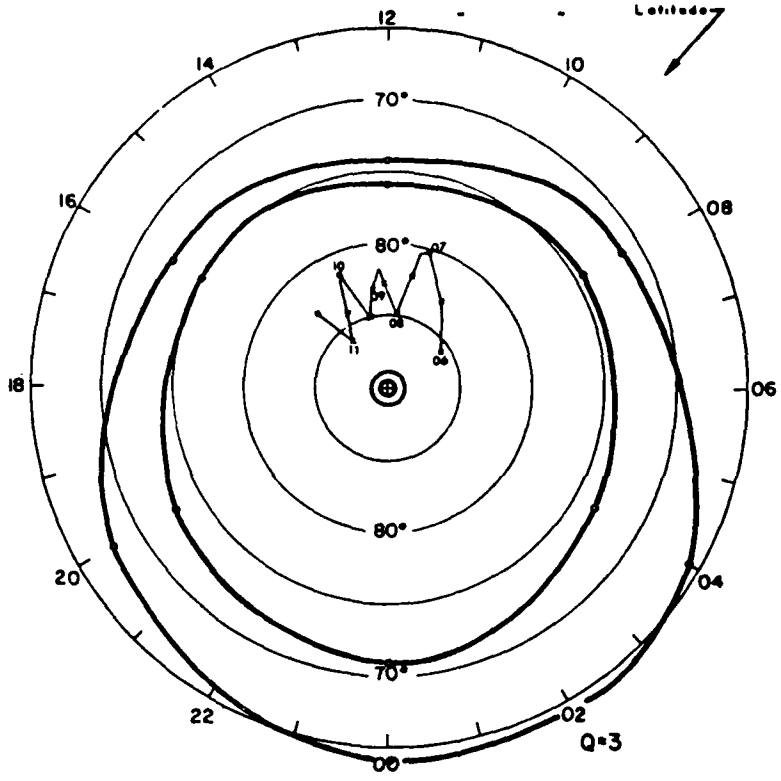

Figure 7.1 Corrected Geomagnetic Latitude/Local Time Plot Showing Aircraft Flight Track on 28 January 1984

7.2 Polar Ionosphere Irregularities Experiment

During the AFGL/NASA Polar Ionosphere Irregularities Experiment in March 1985 two rockets were launched from Sondrestrom, Greenland. The AIO in round-robin flights from Thule AB monitored the Sondrestrom ionosphere using the all-sky imaging photometer (ASIP) and the Digisonde. The ionogram data for AFGL's instrumented rocket launch on 14/15 March 1985 (round-robin flight #3) are summarized in Figure 7.2. At the time of the launch (0205 UT) the auroral oval was at a very close distance and we were unable to identify on the ionogram the F trace corresponding to the arc intersected by the rocket. The oval is first seen at 0130 UT in form of oblique Es echoes. A multitude of Es traces existed after 0150 UT prevailing for the remainder of the flight.

During round-robin #5 for the NASA launch on 20 March 1985, the overhead sporadic E layer had critical frequencies up to about 6 MHz (Figure 7.3). The F region plasma frequencies varied between 3.5 and 2.5 MHz, similar as during RR#3.

7.3 Processing of Polar Cap Ionograms

The Thule ionograms were processed in two ways: data compression to produce ionospheric characteristics and velocity filtering. The ionospheric characteristics show amplitude, frequency and height variations as a function of time, as displayed in Figures 7.4a and 7.4b for 9 January 1983. The integrated height display reveals the approaching F-region ionization between 02 and 04 UT, and the approaching and receding ionization in the disturbed period after 16 UT. The velocities of the moving irregularities were determined using the digital Doppler/range filter developed during the previous contract (Buchau et al, 1983). Figures 7.5a and

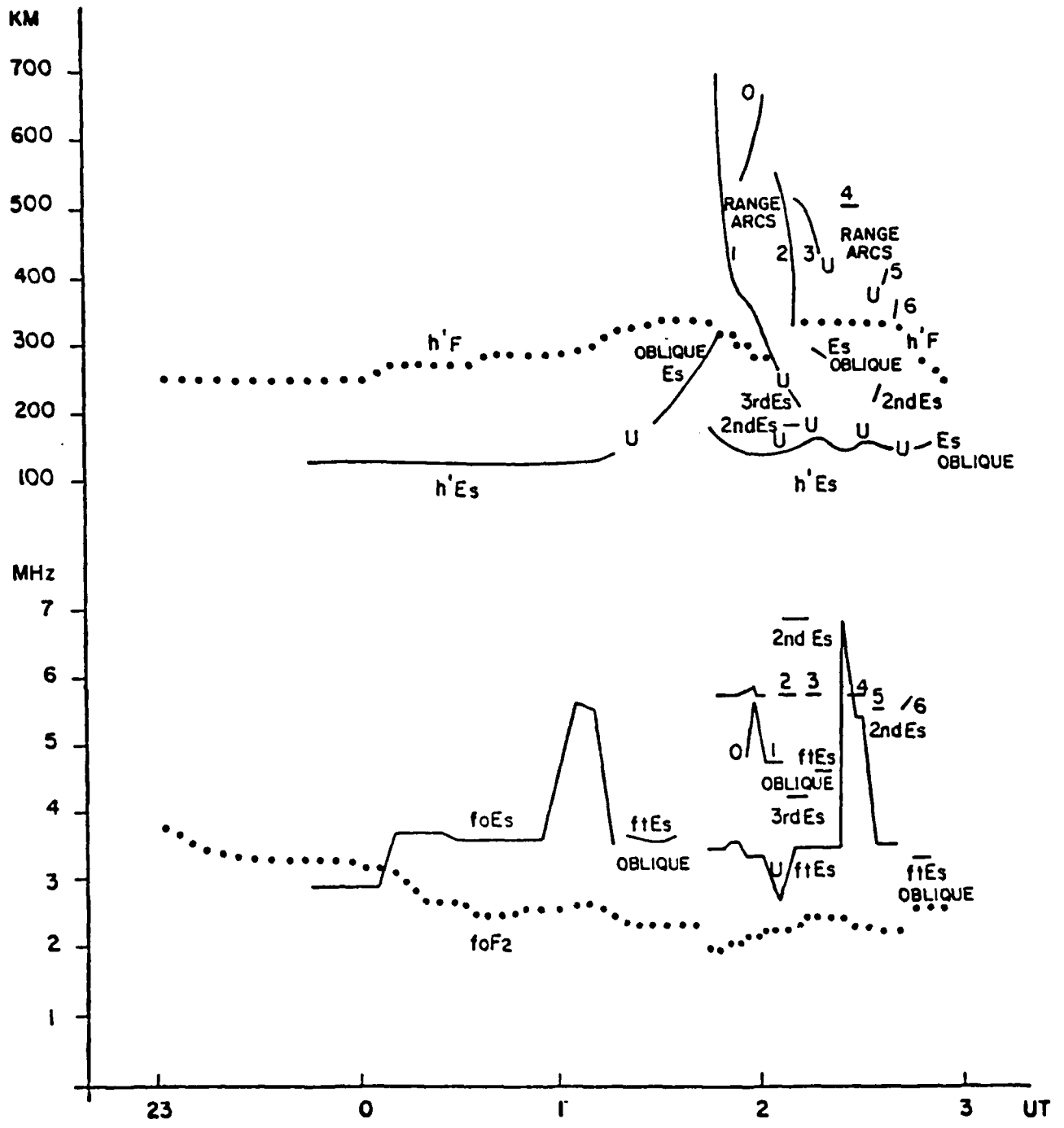

Figure 7.2 Airborne Acquired Ionospheric Data to Support Air Force Geophysics Laboratory Rocket Launch, 14/15 March 1985

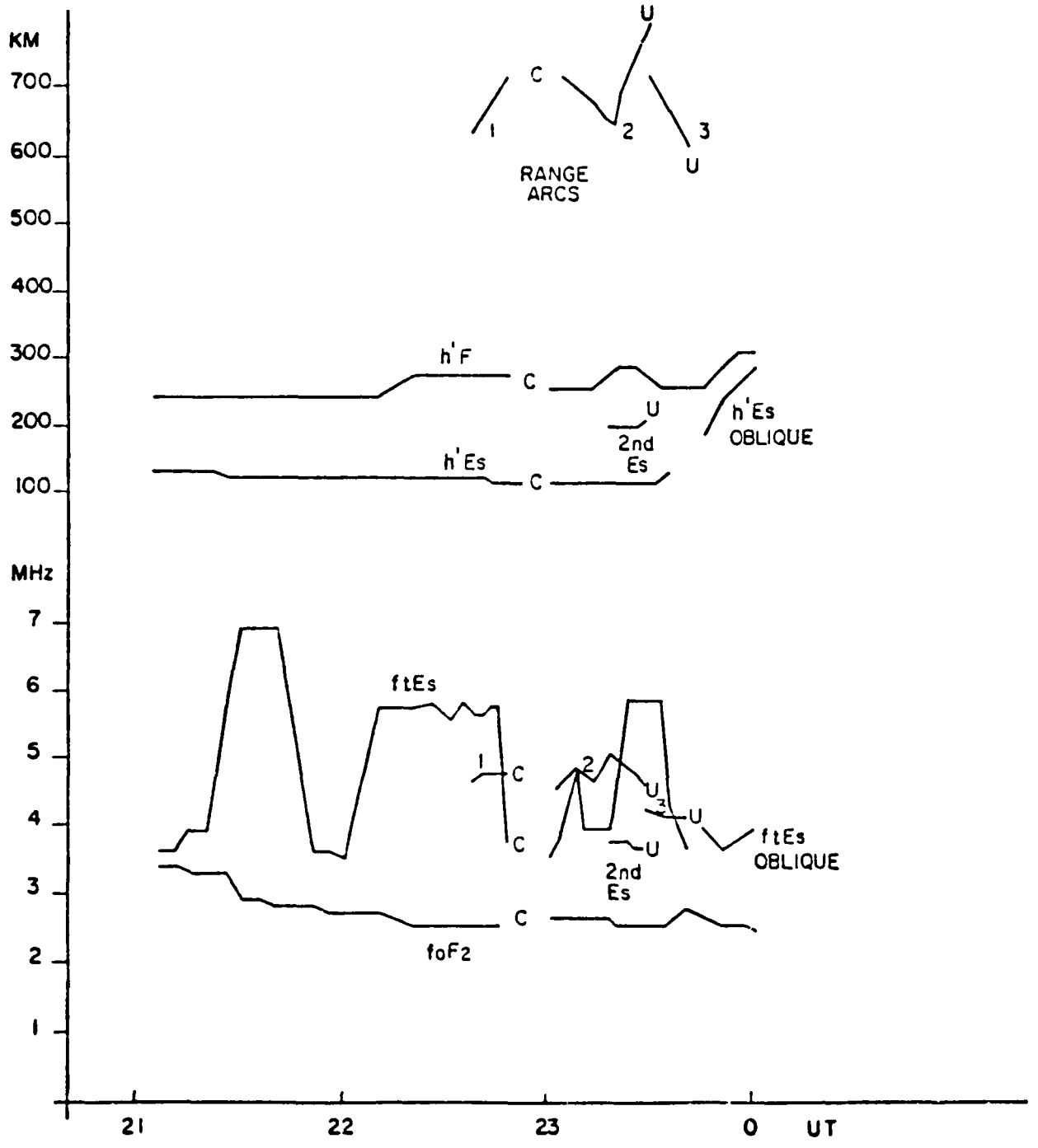

Figure 7.3 Airborne Acquired Ionospheric Data to Support NASA Rocket Launch, 21 March 1985

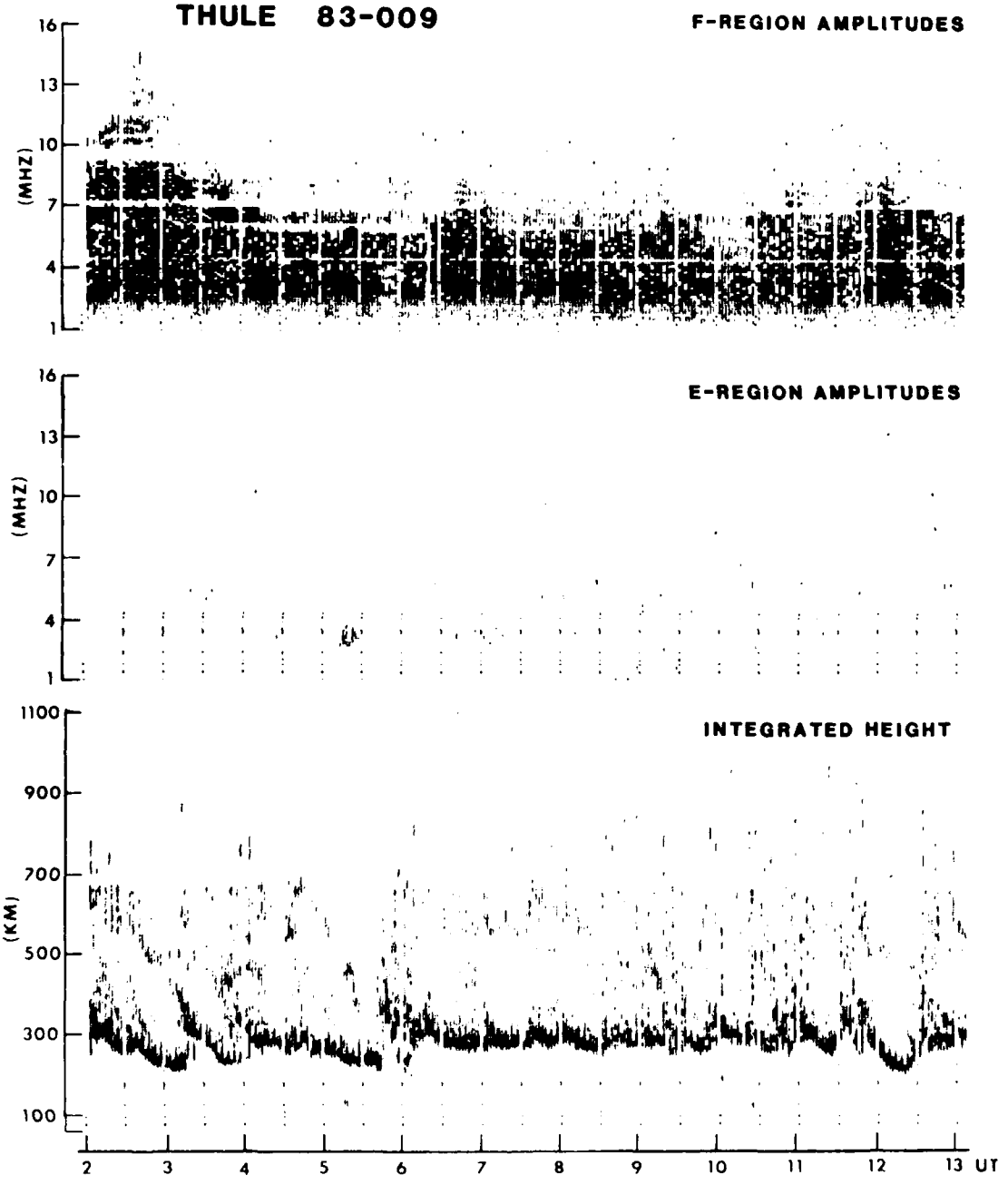

Figure 7.4a Compressed Ionospheric Characteristics, Thule, Greenland, 9 January 1983

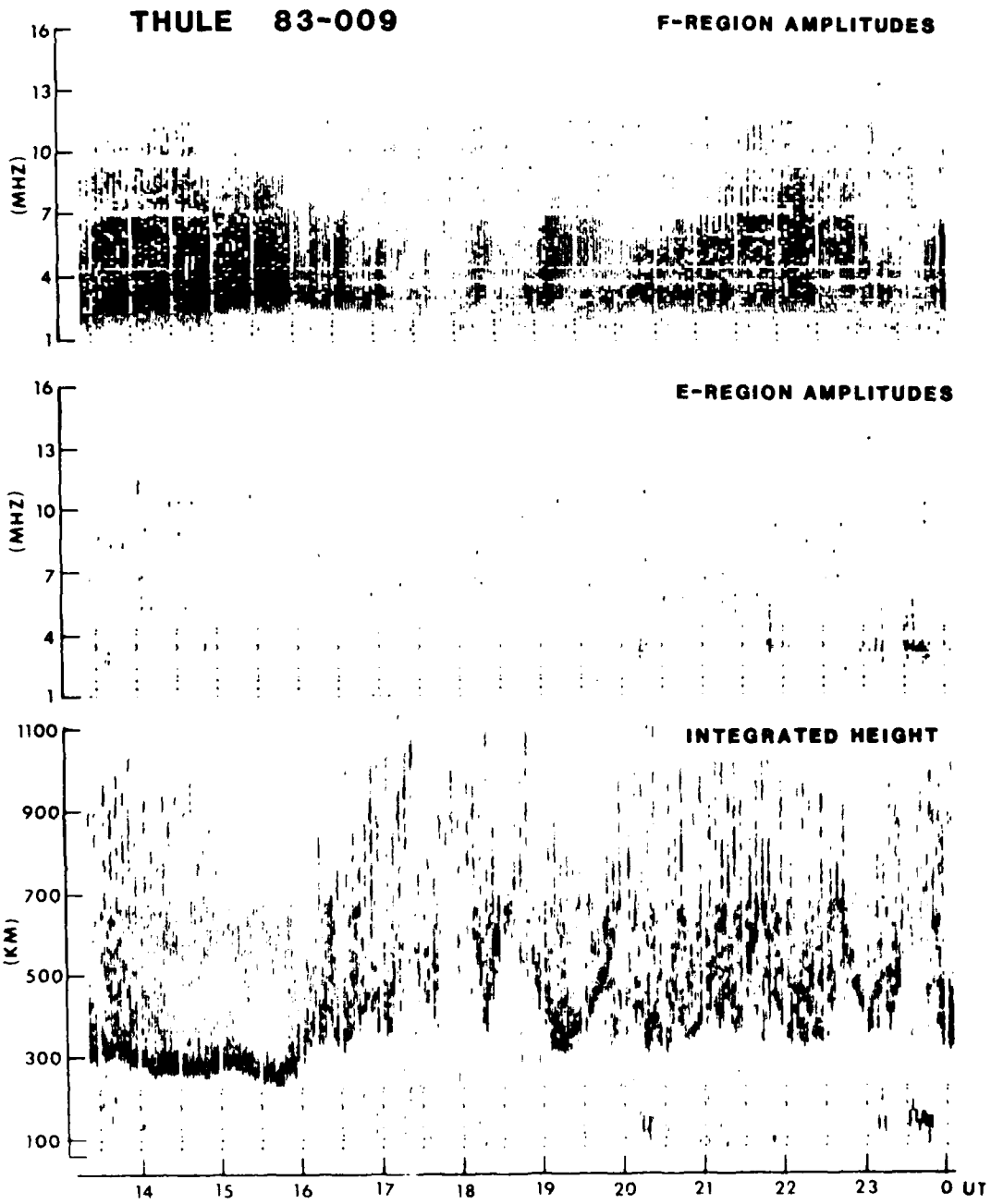

Figure 7.41 Compressed Ionospheric Characteristics, Thule, Greenland, 9 January 1983

7.5b, showing the velocity-filtered data for 9 January 1983, indicate that the predominant plasma drifts on that day were between 200 and 600 m/s. Slower motions, like the front approaching Thule between 03 and 04UT with a velocity of about 100 m/s (Figure 7.4) are suppressed in Figure 7.5. A sequence of rapidly passing irregularities can be seen between 20:00 and 20:30 UT in Figure 7.5b. From the slope of the signal traces, it can be concluded that some of these irregularities moved with velocities between 1000 and 2000 m/s.

ULCAR also participated in the January 1985 AFGL polar cap campaign. The four crossed-loop receiving antennas were deployed again for the Digisonde ground observations, enabling the Digisonde to identify the ordinary and extraordinary wave polarizations, and to measure ionospheric drift.

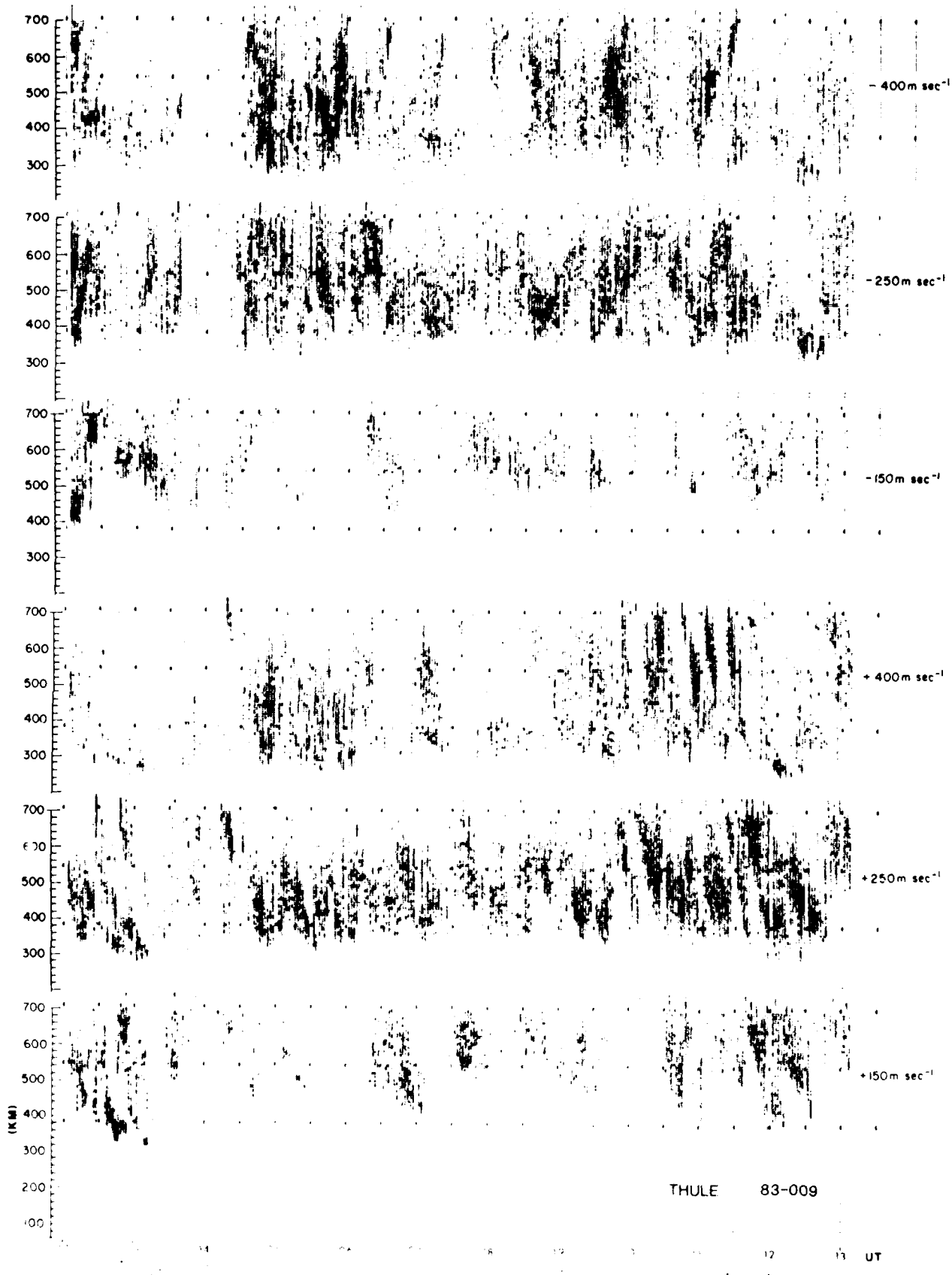
700
600
500
400
300
-400m sec⁻¹
-250m sec⁻¹
-150m sec⁻¹
+400m sec⁻¹
+250m sec⁻¹
+150m sec⁻¹
(KM)
200
100
THULE 83-009
12
13 UT

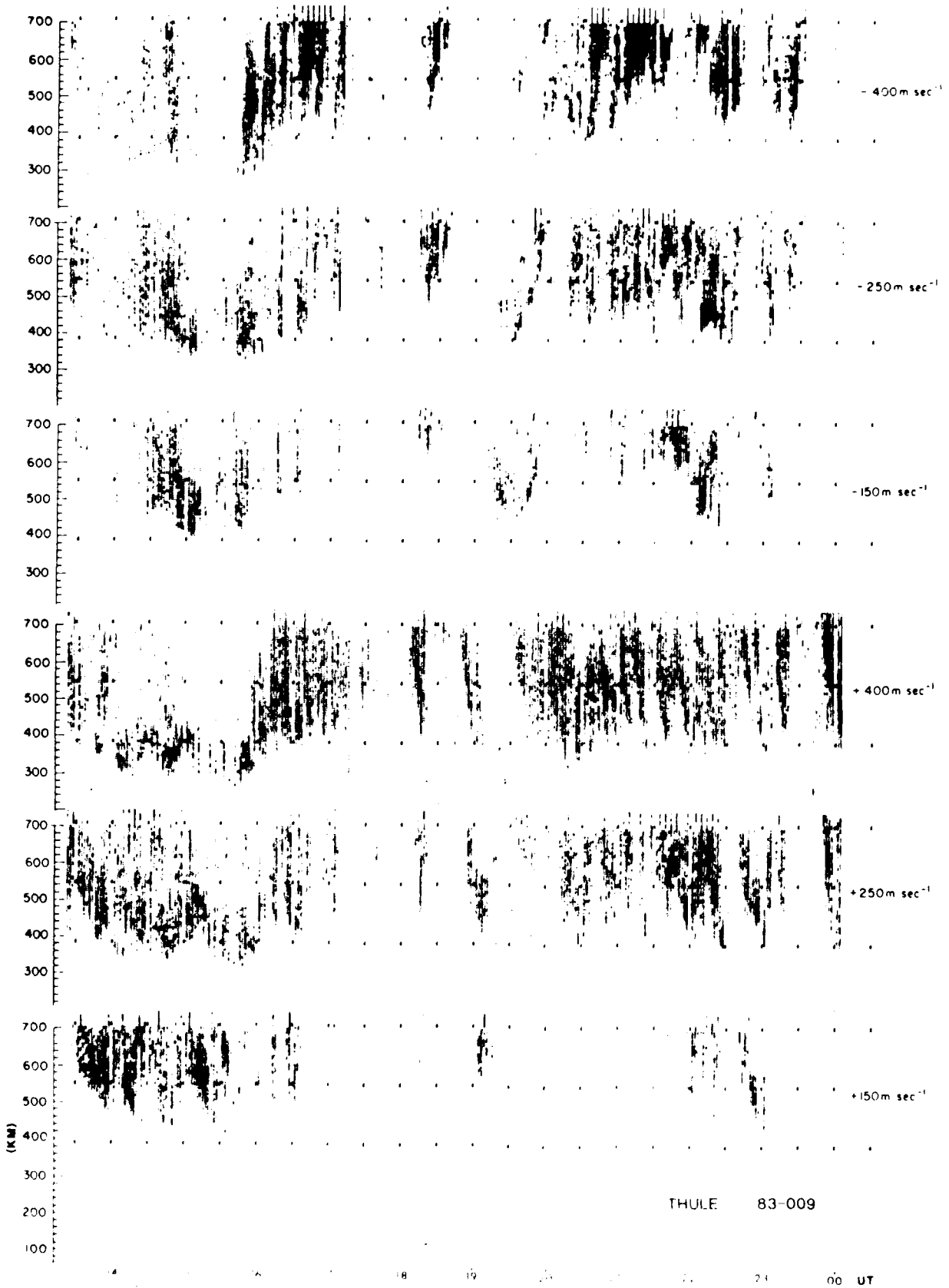
700
600
500
400
300
-400m sec⁻¹
-250m sec⁻¹
-150m sec⁻¹
+400m sec⁻¹
+250m sec⁻¹
+150m sec⁻¹
(KM)
200
100
THULE 83-009
18
19
00 UT

8.0 OBSERVATIONS AT QANAQ, GREENLAND

8.1 Installation of Digisonde 256

Installation of a Digisonde 256 system at the Danish Meteorological Institute (DMI) facilities in Qanaq, Greenland (86.8° CGL) was completed in November 1985. The sounder uses the existing delta antenna (height: 30 m, length: 190 m) for transmission and an array of seven crossed-loop antennas for reception. The antenna site is not level, causing height differences up to 4 m for the individual receiving antennas. To assure phase equality on all antennas for vertical echoes the lengths of the antenna cables were adjusted; for example, the cable for the highest antenna has 4 m of additional cable added.

The distance of the sounder site from DMI's Geophysical Observatory is approximately 3 km. It was, therefore, decided to install a remote terminal with printer at the observatory; a pair of existing telephone wires was used, together with a short-haul modem at each end, to establish the remote control and data link. A dial-up modem at the Digisonde site allows to conduct remote system tests from ULCAR or AFGL.

8.2 Routine Operation

Since November 1985, the Qanaq Digisonde collects ionogram data at a rate of at least four ionograms/hour. The ionograms are automatically scaled in ARTIST and the ionogram data in MMM format together with the scaled data are recorded on 9-track magnetic tape (1600 bytes per inch) and printed on an Okidata printer. Because of malfunctioning, the tape recorder had to be replaced in October 1986. Before that time

the recorder was connected to the Processor, and the scaled data were not recorded on tape.

8.3 ARTIST Performance

For the first time automatic ionogram scaling was applied to polar cap ionograms. We are able to report that the ARTIST performed very well, considering the difficult ionospheric conditions, as illustrated in Figure 8.1. But misscalings occur and one source is the overlapping of ordinary, oblique and extraordinary echo traces in the cusp region, as illustrated in Figure 8.2. The cause for this difficulty lies in the fact that the ARTIST scaling is performed on the MMM'ed ionograms (see Digisonde 256 Manual, p. 57), where each frequency/range bin contains only the amplitude of one signal, selected amongst the ordinary, extraordinary and oblique signals as the strongest. Where the signal traces overlap, the amplitudes become comparable and the MMM process selects the signal in a somewhat arbitrary way, making it difficult for the scaling routine to properly identify a continuous O-trace. The proper remedy would be to simultaneously process three ionograms: one with O-echoes, one with X-echoes, and one with oblique echoes. In the frame of this contract it was not feasible to pursue this approach, since it requires substantial software modifications. Some improvement for the existing problem could be obtained even with the MMM'ed ionograms by forcing the baseline (the preliminary rough trace constructed in the scaling process) to stay in the field of O-echoes and not wander into the X-field. Another source for serious scaling errors is the presence of multiple Es echo traces, when ARTIST mistakes the multiple Es trace as the main F trace. We have identified the reason for this but have not yet corrected it. In the initial phase of constructing the baseline the multiple Es

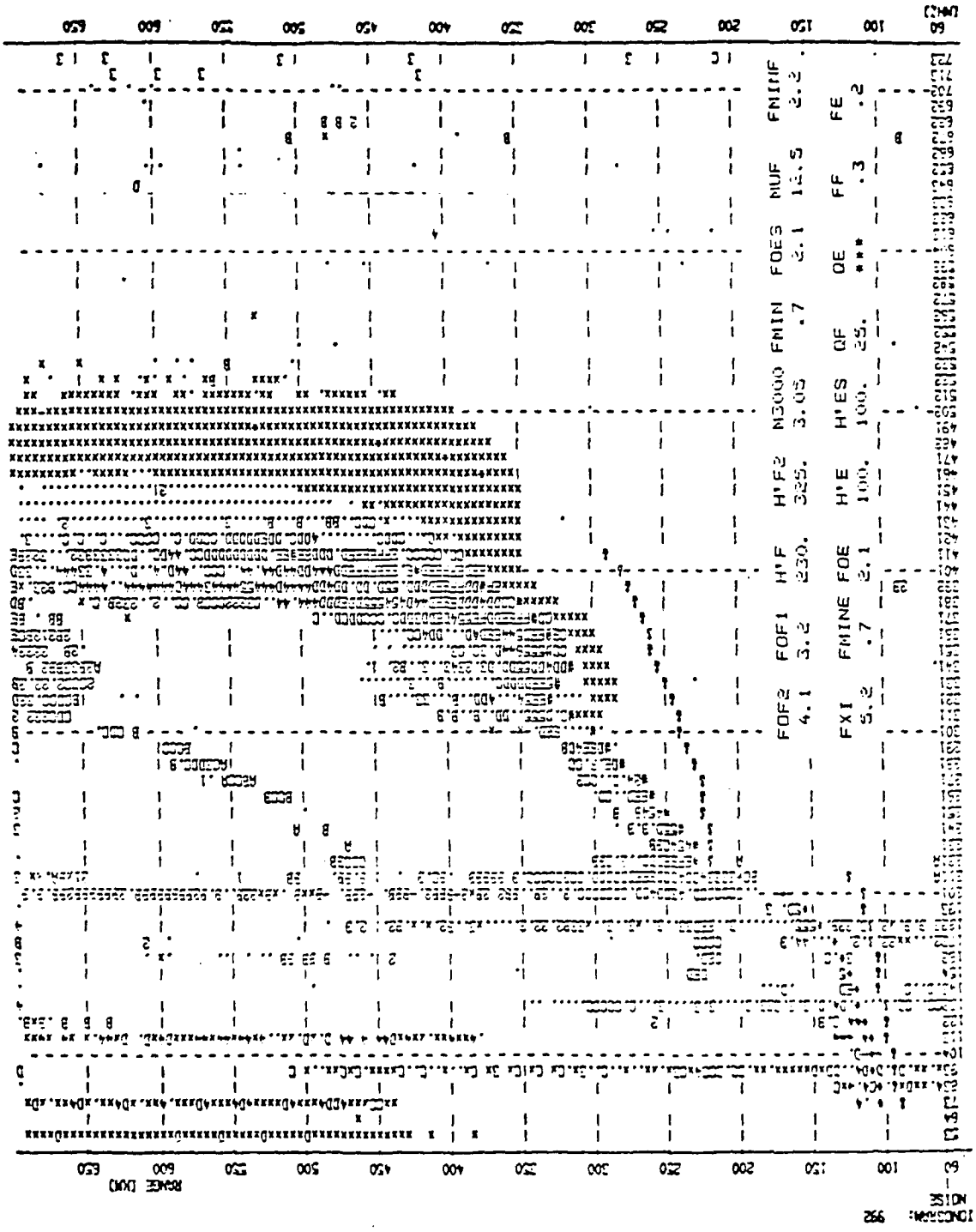

Figure 8.1 ARTIST Scaled Polar Cap Ionogram, Qanaq, Greenland, 3 June 1986, 0200 UT

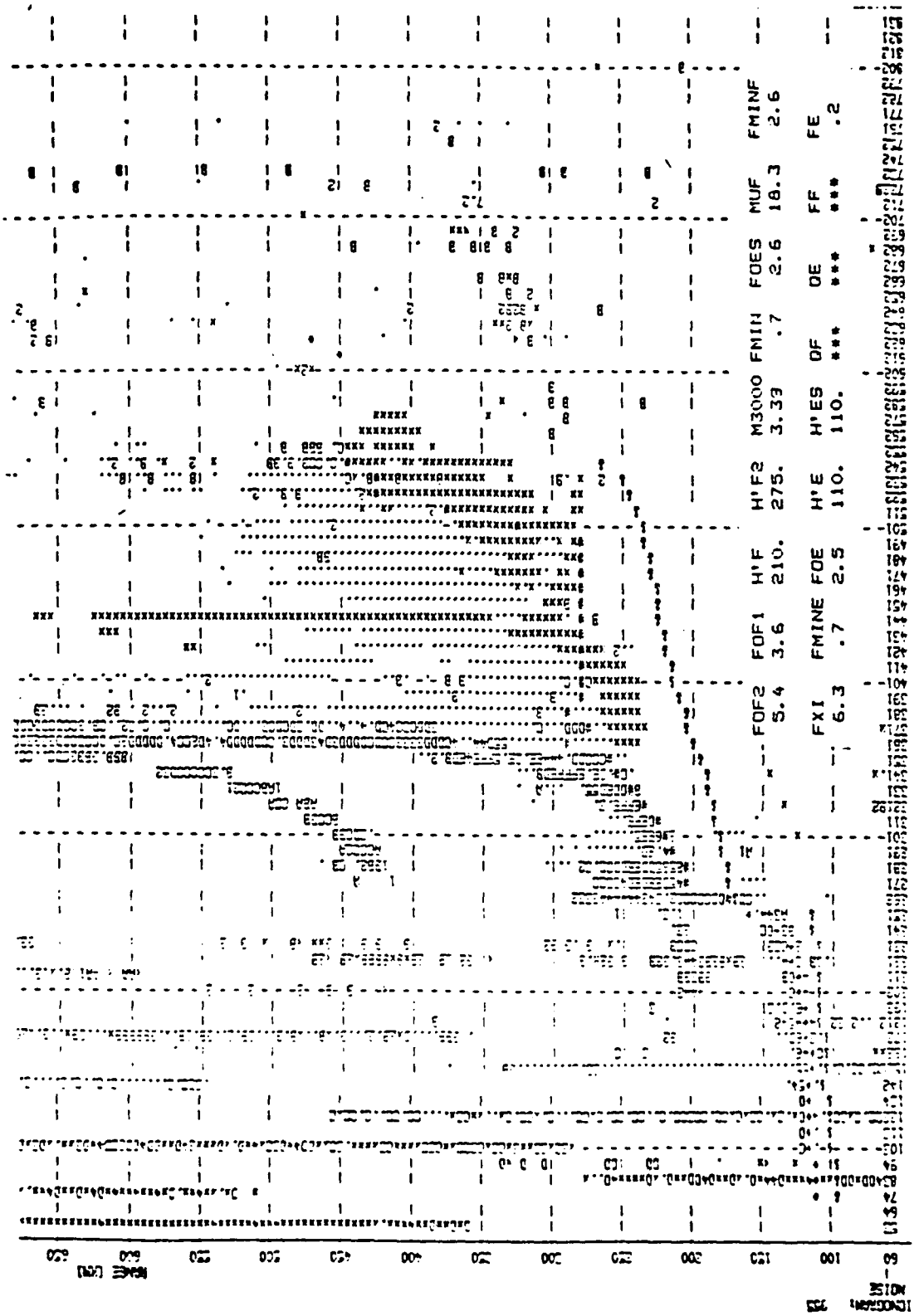

Figure 8.2 ARTIST Scaled Ionogram with Overlapping Ordinary, Oblique, and Extraordinary Traces, Qanaq, Greenland, 1 June 1986, 1300 UT

(as well as E or F) echoes are identified as such, but the echoes are not removed (or clearly labeled) from the ionogram, so they affect the baseline construction at a later stage. The required program modification is of limited extent and should be implemented as soon as possible, benefiting not only the polar cap but also the mid-latitude autoscaling.

8.4 Special Observations

The Digisonde 256 was operated in the drift mode in April and July 1986 monitoring the F region plasma convection for a number of consecutive days. An example of the first drift measurements in the polar cap made under summer/sunlit conditions is shown as Figure 2.6.

In July 1986 a week long campaign was conducted jointly with AFGL and DMI to investigate the phenomena of slant E frequently observed in summer during daytime. Multidirectional ionograms and fixed frequency observations were optimized to obtain good recordings of these oblique echoes. An example of slant E is shown in Figure 8.3, which also illustrates the difficulties of autoscaling.

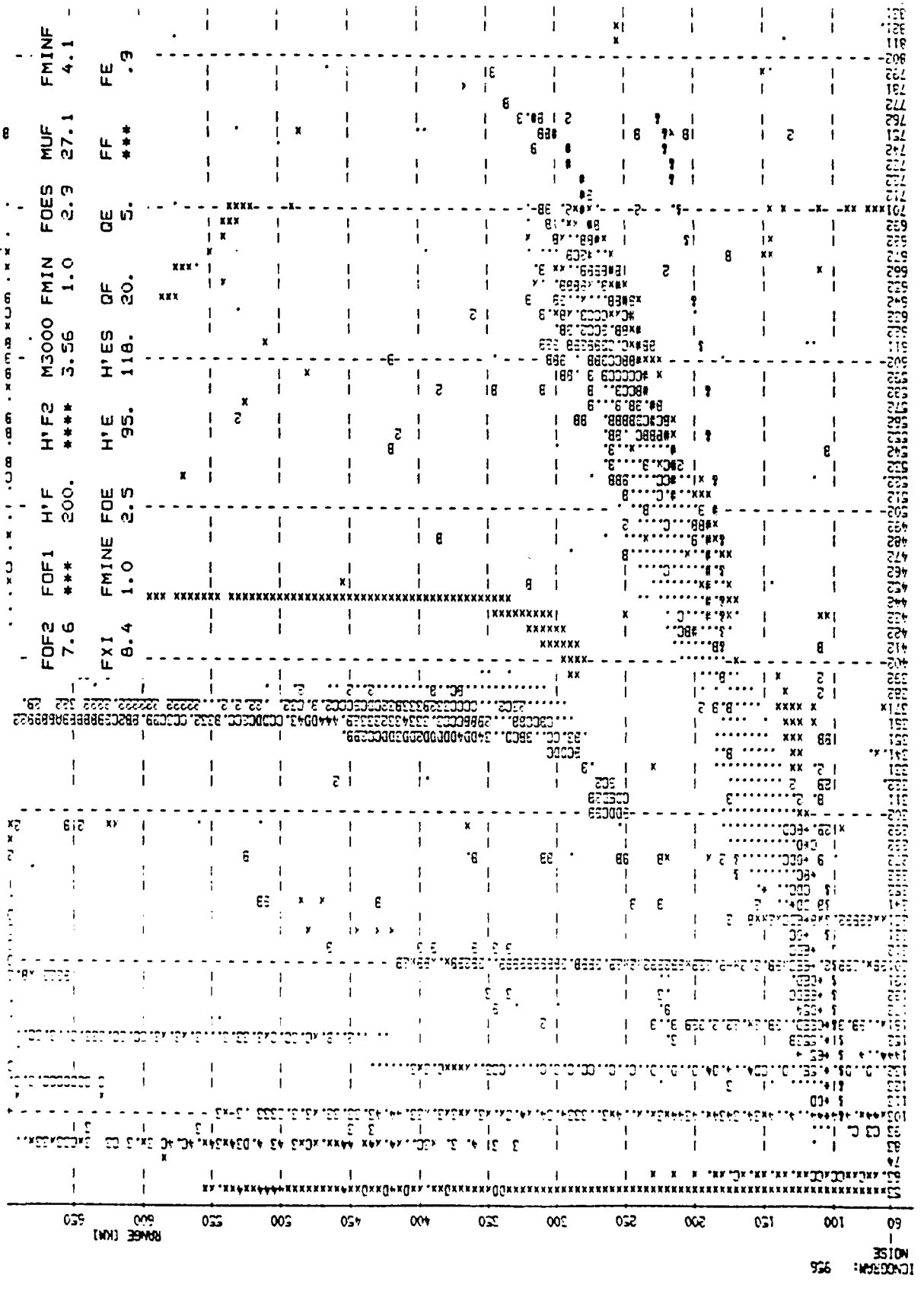

Figure 8.3 ARTIST Scaled Ionogram with Slant Es, Qanaq, Greenland, 1 June 1986, 1400 UT

9.0 OBSERVATIONS AT LOWELL, MASSACHUSETTS

Since ULCAR does not maintain an ionosonde for routine operation, observations of the ionosphere at Lowell are performed on a campaign and opportunistic basis.

9.1 Daytime Mid-Latitude Auroral Event

Observations on 4 February 1983 using a sequence of 5-minute ionograms revealed an unusually early and rapid increase in F-region heights within a 30 minute period. Because the scale height of the F region increased much more than the critical frequency, which in fact decreased on occasion, the increase has been attributed to a vertically accelerated and southward motion of the ionospheric plasma. This suggestion is consistent with ionogram data from Goose Bay (Labrador), Wallops Island (Virginia) and Cape Canaveral Bay (Florida), and with Beacon satellite total electron measurements along three paths. The total electron content measurements at Goose Bay indicate an early decline while the data taken in Hamilton and Cape Kennedy exhibit a substantial increase during the event. The comparison shows the following features:

1. The F-region does not disappear by recombination or otherwise, but is displaced upwards and equatorwards, accelerating with height.
2. The onset is in the north and propagates within one hour towards the equator.
3. The difference in speed and onset time shifts ionization on top of slower moving ionization and thus increases the total electron content for southward inclined Beacon satellite trajectories.

4. The F-region ionization over Goose Bay is displaced toward the south and is partially replaced by aurora E and D-region ionization produced by particle precipitation.

5. Even over Lowell, precipitation ionization produces a second maximum in the scale height for the lower F-region ionization about one-half hour after the main rise. This effect is not seen in Wallops Island.

Figure 9.1 shows an overlay of the time sequence of the lines of constant electron density for three ionospheric stations. To those curves the true height profiles of the four hourly measurements of the Florida station are added.

9.2 AFGL Coordinated Ionospheric Campaign

Ionospheric soundings were taken at Lowell with the Digisonde 128PS from 17 September 1984 to 20 September 1984, in support of an AFGL coordinated ionospheric Energy Budget Campaign which included optical, incoherent and sounder observations. The system was operated continuously, and the ionograms analyzed. Film data from Arecibo were analyzed for hourly parameters: foE, ftEs or foEs, fbEs, foF2, h'minF and h'(2 MHz). The Arecibo data covering the period September 17, 1984, 10:00 AST to September 19, 1984, 12:00 AST, were plotted and the results delivered to AFGL.

9.3 Observations During a Shuttle Burn

A shuttle burn in the F layer occurred at 0324 UT (2224 LT) on 30 July 1985, and the ULCAR Digisonde at Lowell was operated from 0210 UT to 1314 UT, covering the time of the burn and many hours afterwards.

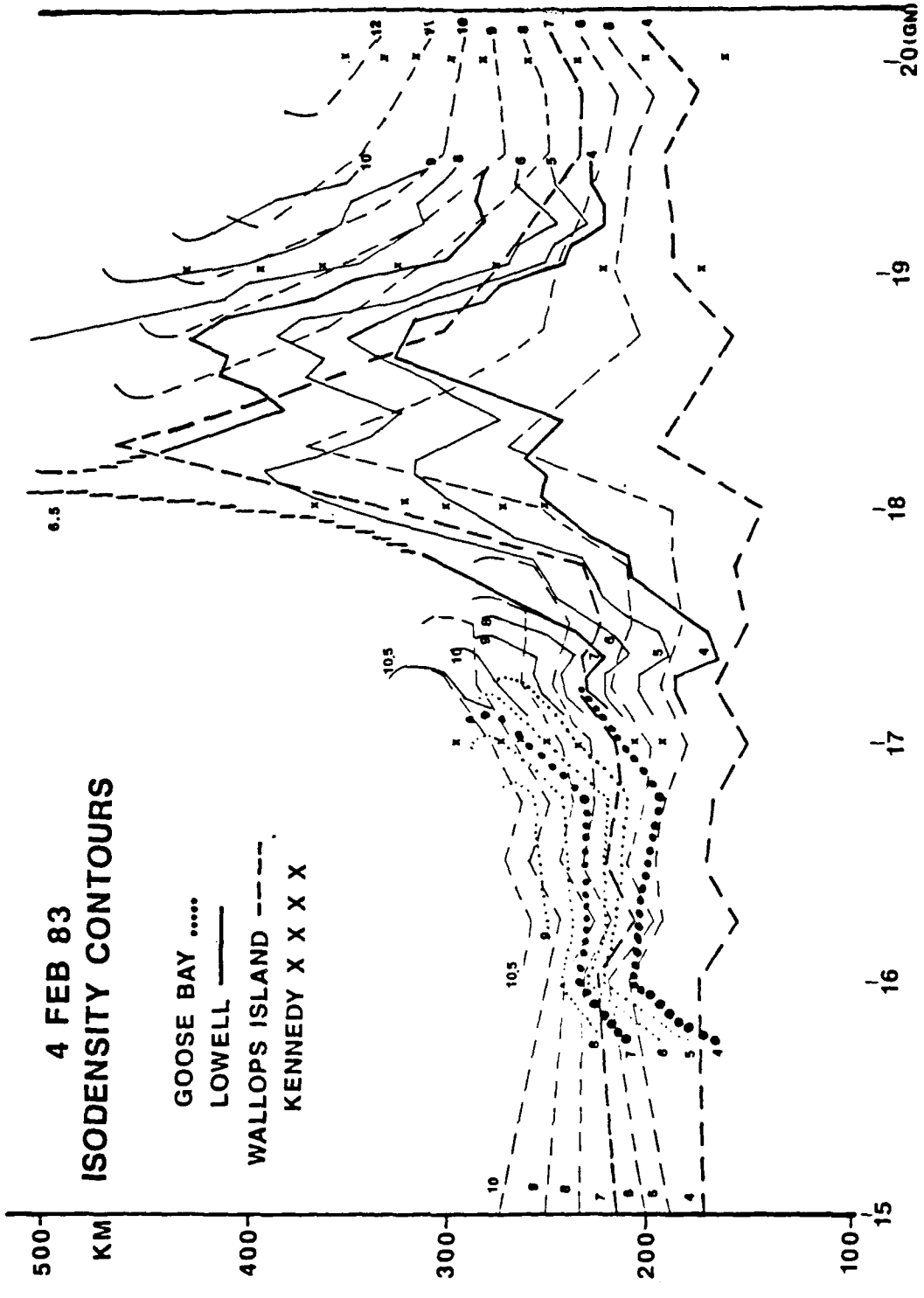

Figure 9.1 Isoelectron Density Contours for Three Ionospheric Stations. Overlaid are the Florida True Height Profiles for Four Observation Periods

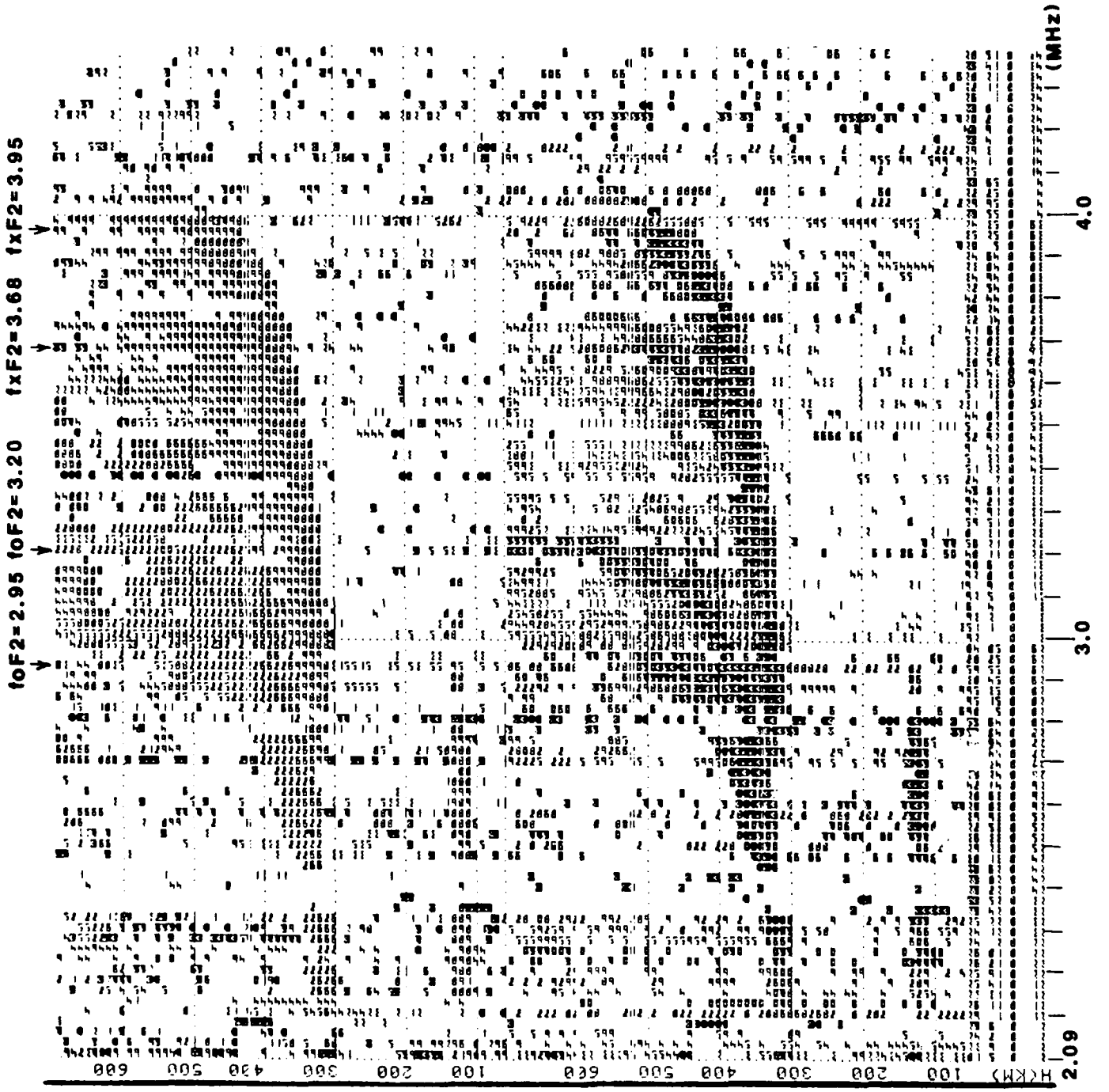

Figure 9.2 Ionogram, Lowell, MA, 30 July 1985, 0514 UT; Note Forking of the E-Region Trace

At the time of the burn, the F layer was completely blanketed by sporadic E, so any effects of the burn on the F layer could not be studied in detail. It was not until 0415 UT (50 minutes after the shuttle burn) that foF2 exceeded ftEs and permitted a study of the F layer. The F trace then showed frequency spreading for about 20 minutes. At 0505, forking of the F trace developed, with two foF2 cusps at 3.1 and 3.5 MHz. This condition (as shown for the time 0514 in Figure 9.2) persisted until 0520 UT, when the cusps merged into a single spread F pattern. The higher foF2 value could have been the result of oblique echoes, possibly from the shuttle burn area. However, this possibility could not be validated because there was no receiving antenna array available at the ionosonde site to allow the determination of the angles of incidence of the separate echoes.

The scaled parameters foF2, h'F, ftEs and h'Es from 03 to 09 UT in 5 minute intervals are listed in Table 9.1. It should be noted that we scaled ftEs rather than foEs. The reason was that the transition from left-hand to right-hand circular polarization (ordinary to extraordinary) was not sharp in the Es traces, and the X trace often extended way beyond the expected 0.7 MHz above the vaguely defined foEs value.

Day	Time UT	foF2	h'F	ftEs	h'Es
211	0300	3.95	290 EA	5.55	100
	05	3.90	280 EA	5.55	100
	10	3.85	270 EA	5.55	100
	15	3.80 UR	270 EA	5.55	100
	20	A	A	5.85	100
	25	3.60 UR	330 EA	5.85	100
	30	3.55	320 EA	5.55	100
	35	3.45 UR	300 EA	5.55	100
	40	A	A	5.55	100
	45	A	A	5.55	100
	50	A	A	5.55	110
	55	A	A	5.20	110
211	0400	A	A	5.00	110
	05	3.40	290 EA	4.35	110
	10	3.30	280 EA	3.75	110
	15	3.25 UF	290 EE	3.10	110
	20	3.30 UF	290 EE	2.95	110
	25	3.30 UF	290 EE	2.90	110
	30	3.30 UF	290 EE	-	-
	35	3.30	290 EE	-	-
	40	3.20	290 EE	-	-
	45	3.15	290 EE	3.30	110
	50	3.15	300 EE	3.15	100
	55	3.15	300 EE	3.15	100
211	0500	3.15	300 EE	3.05	110
	05	3.1/3.5	300 EE	3.10	110
	10	3.0/3.3	300 EE	3.10	110
	15	3.0/3.2	300 EE	2.95	110
	20	2.9/3.1	300 EE	2.90	110
	25	3.00 UF	300 EE	2.55	110
	30	3.00 UF	300 EE	2.55	100
	35	2.95 UF	310 EE	2.90	100
	40	2.90 UF	310 EE	2.85	100
	45	2.8/3.0	310 EE	2.35	100
	50	2.90 UF	310 EE	2.40	100
	55	2.90 UF	310 EE	2.55	100

Day	Time UT	foF2	h'F	ftEs	h'Es
211	0600	2.80 UF	310 EE	3.00	100
	05	2.70	370 EA	2.90	100
	10	2.70	400 EA	2.80	100
	15	2.70	400 EA	2.90	100
	20	2.70	340 EE	2.30	100
	25	2.70	340 EE	-	-
	30	2.70	340 EE	-	-
	35	2.70	340 EE	-	-
	40	2.70	330 EE	-	-
	45	2.70	330 EE	-	-
	50	2.70	320 EE	-	-
	55	2.70	310 EE	-	-
211	0700	2.60	300 EE	-	-
	05	2.60	300 EE	-	-
	10	2.60	300 EE	-	-
	15	2.60	300 EE	-	-
	20	2.50	310 EE	-	-
	25	2.50	310 EE	-	-
	30	2.50	310 EE	-	-
	35	2.50	310 EE	-	-
	40	2.50	310 EE	-	-
	45	2.50	310 EE	-	-
	50	2.50	310 EE	-	-
	55	2.40 UR	300 EE	-	-
211	0800	2.4 UR	300 EE	-	-
	05	2.35	300 EE	-	-
	10	2.30	300 EE	-	-
	15	2.30	320 EE	-	-
	20	2.30	310 EE	-	-
	25	2.30	320 EE	-	-
	30	2.30	320 EE	-	-
	35	2.30	320 EE	-	-
	40	2.30	320 EE	-	-
	45	2.30 UR	320 EE	-	-
	50	2.30 UR	320 EE	-	-
	55	2.30 UR	340 EE	-	-
		2.20	290 EE	-	-

Table 9.1 Ionospheric Parameters, Lowell, 30 July 1985

10.0 PRECISION TARGETING EXPERIMENT

The Precision Targeting Experiment (PTE), described in Scientific Report No. 2 (Sales et al, 1986) was designed primarily to develop a data base for deducing the actual target range (ground range) from the radar range (slant range), for aircraft detections using an over-the-horizon radar. This data base is to be used to evaluate the performance of existing methods for converting radar slant range to ground range, and to provide an estimate of the accuracy with which this transformation can be made.

Three missions of the AFGL aircraft were flown - 5 March 1985, 17 April 1985 and 6 February 1986. The primary purpose of the aircraft was to serve as the target for the OTH-B radar. The frequency management of the radar and the timing of the flights were designed to produce a variety of propagation conditions that would serve to test the accuracy of range conversion under operational conditions.

Attempts to deduce the ground range from the slant range by using a simple model in which reflection occurs at some estimated altitude can be only partly successful. Better knowledge of the structure of the ionosphere is required. Improved results can be obtained by an iterative method which starts with a model of the ionosphere, or through direct ionospheric measurement. Although this direct approach is not always possible for operational radar systems, the method can be applied on an experimental basis to determine the limits set by the ionosphere and the range conversion process.

This direct approach involves the measurement of all relevant ionospheric parameters at a site near the midpoint of the propagation path between the radar and the air-

craft target. The requirement to sound the ionosphere at the midpoint of the radar propagation path from the Wide Aperture Radar Facility (WARF) at Los Banos, CA, could be met only approximately since the range from the radar to the aircraft was always changing. ULCAR operated a Digisonde 256 at the Institute for Telecommunication Sciences site at Erie, CO, for more than a week for each of the three missions, to provide background as well as mission data.

Vertical incidence ionograms were made every five minutes, covering a range 1 to 7 MHz in about 1.5 minutes. The remainder of the 5-minute interval was used to make tilt measurements by operating the Digisonde in the so-called "drift mode" (Bibl et al, 1981).

Periodically, Smith transmission curves appropriate for the range of the aircraft at the particular time were used on each Erie vertical ionogram to deduce the maximum usable frequency (MUF). The value of the MUF was then forwarded to the WARF site as an aid in their frequency management. Two examples are shown in Figure 10.1. The first was made on 5 March 1985 at 1854 UT (1154 LT), and the second on 17 April 1985 at 2109 UT. In both cases the aircraft range was somewhat greater than 3000 km.

There were significant differences between the ionospheric parameters for the first two flight days, particularly for the F2 layer. These differences were clearly related to the level of geomagnetic activity on these days, with 5 March being a "disturbed" day, and 17 April a "quiet" day. Composite plots of the MUF curves and the F2-layer parameters for the first two campaigns are given in Figures 10.2 and 10.3. These data will provide the basis for a comparison between magnetically quiet and disturbed days, and indicate how the radar frequency management and performance might be affected by these changing conditions.

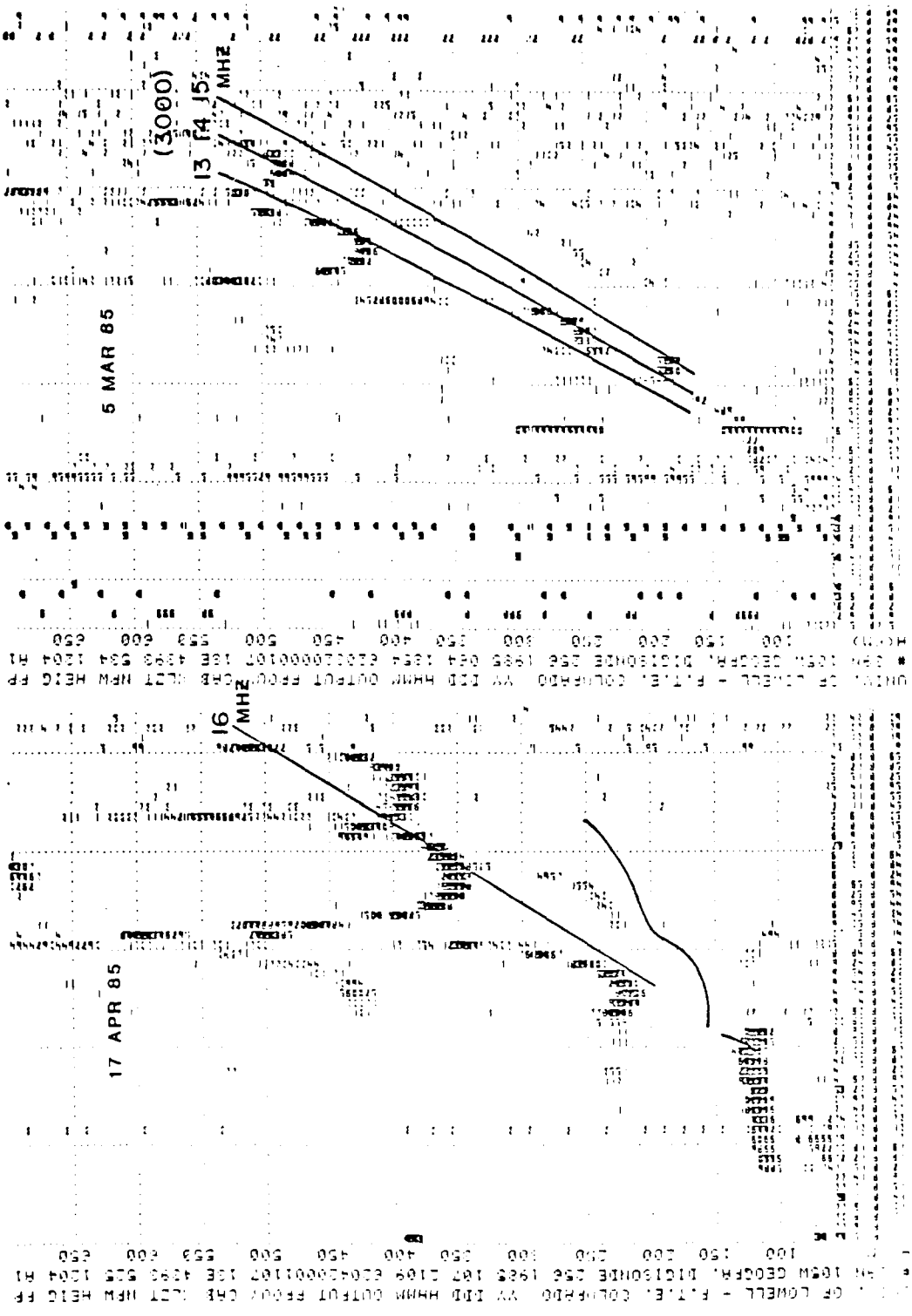

Figure 10.1 Ionograms, Erie, CO, 5 March 1985, 1854 UT and 17 April 1985, 2109 UT; Note the Overlay of the Smith Transmission Curves to Determine the Maximum Usable Frequency

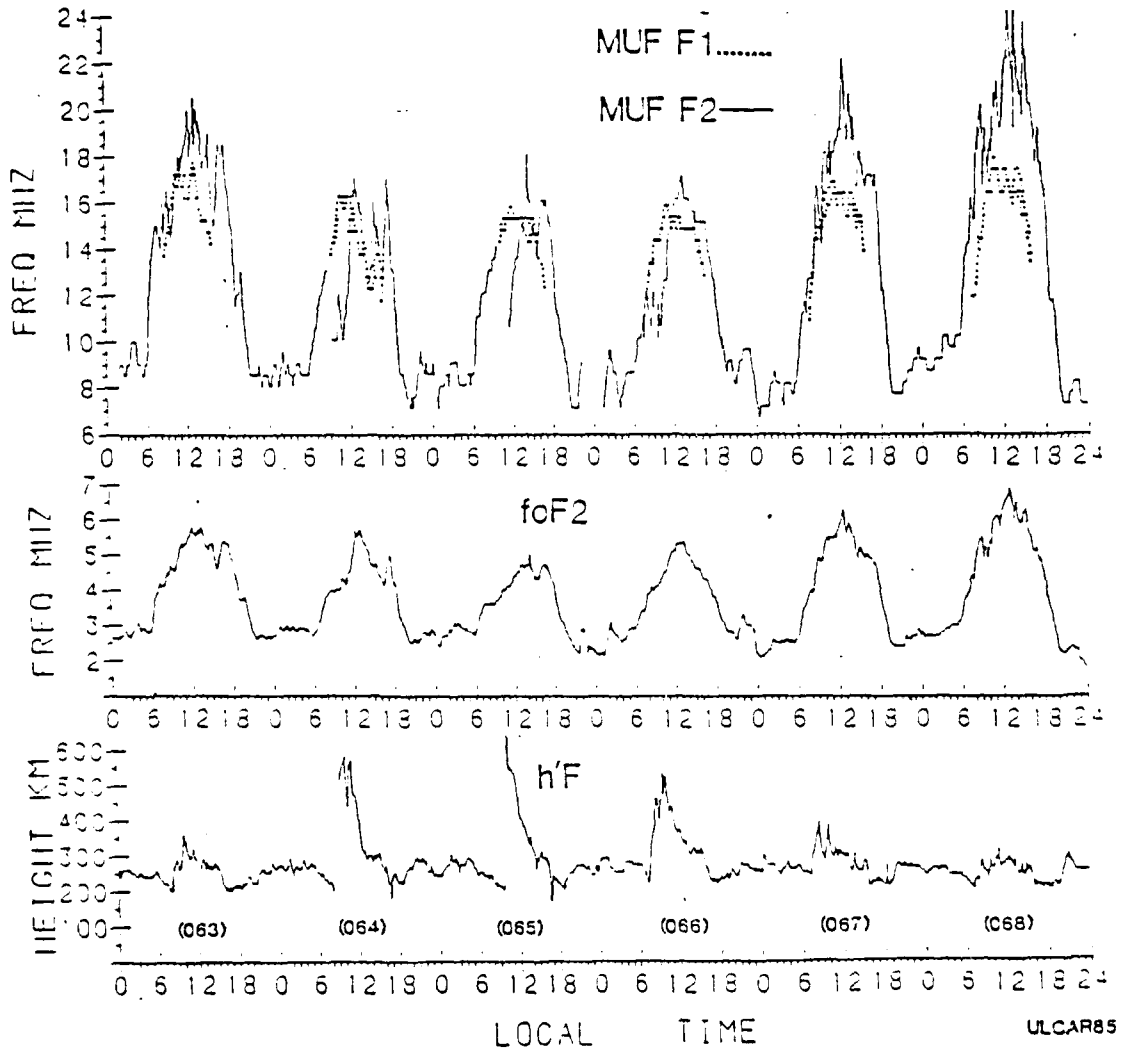

Figure 10.2 Composite Plots of the Maximum Usable Frequencies and the F-Region Parameters, Erie, CO, 4/9 March 1985, 0000 - 2400 MST

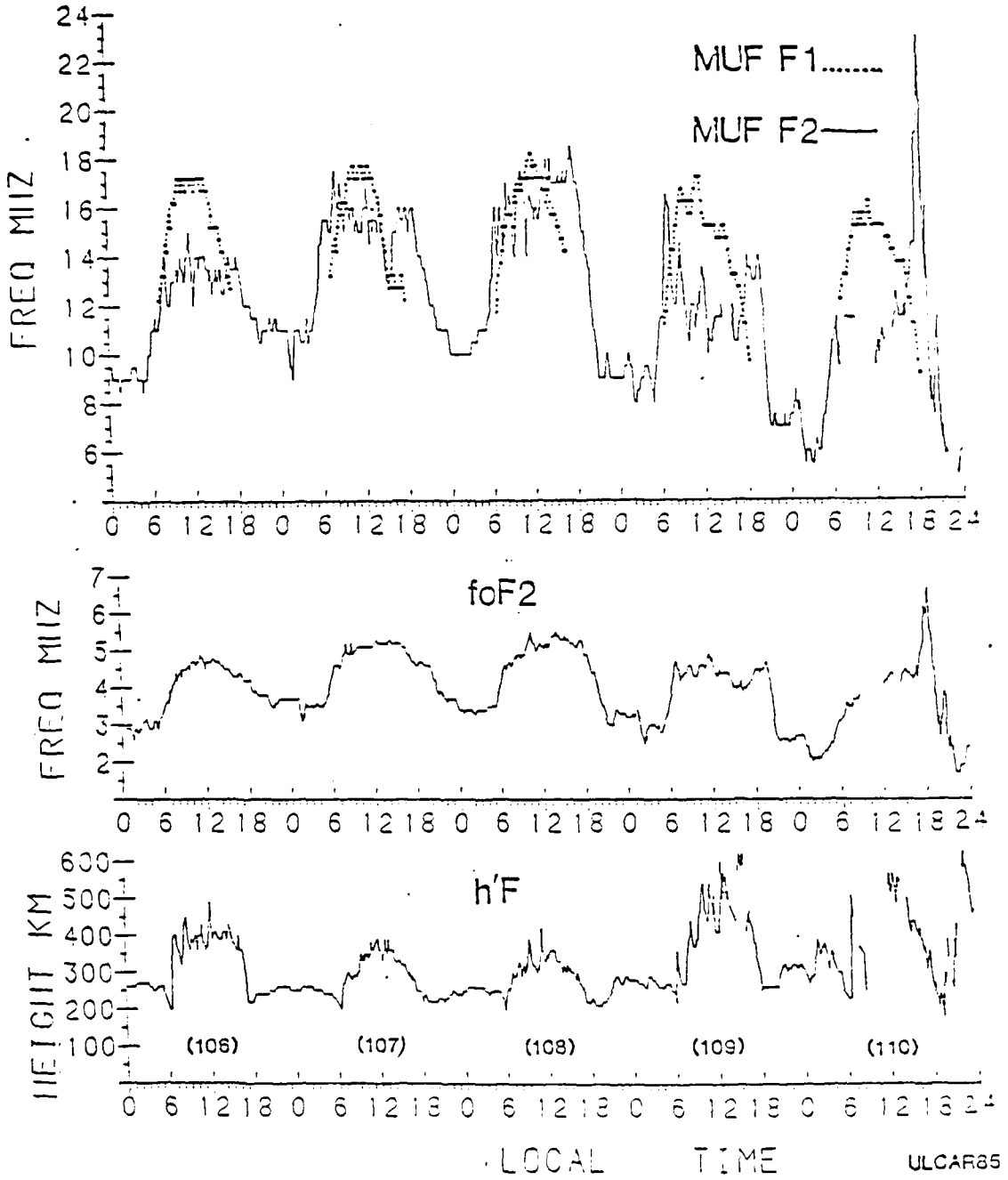

Figure 10.3 Composite Plots of the Maximum Usable Frequencies and the F-Region Parameters, Erie, CO, 16/20 April 1985, 0000 - 2400 MST

Many hours of tilt data were gathered during the three campaigns. The Digisonde 256 can simultaneously sound at four frequencies, and these soundings used to determine the magnitude and direction of the ionospheric tilt. During these particular missions, the system was operated at only two frequencies, each using two different height gates. A complete sky map of the reflecting sources was made at each frequency and each 10 seconds, approximately. This process was repeated about 19 times, filling most of the 5-minute interval between ionograms. The results of the 19 cases can then be superposed to generate a cumulative sky map as shown in Figure 10.4. This figure is very typical of the entire data set for the first two aircraft flights - except for a small number of extraneous points, most sources are clustered very tightly at a particular location in the sky.

The scaled parameter data for the third PTE mission in September 1985 are shown in Figure 10.5. This mission was significantly different from the first two missions, in that the flight began at 01 UT (18 LT), later than the end of either of the first two missions. As indicated in the figure, the flight took place through the sunset transition. No E or F1 layers were present during the flight period. In one respect the analysis of this mission will be simpler, there being only a single ionospheric layer. On the other hand the MUF is continuously changing during the flight and, from that respect, there is no time when the aircraft range change can be simply uncoupled from the ionospheric changes. Figure 10.6 shows a composite of four days around the flight period. All of these days appear relatively normal and geomagnetically quiet.

The F region tilt data from Erie, CO, show an unusual behavior which we have seen before, but not as part of the flight mission. For the other missions in March and

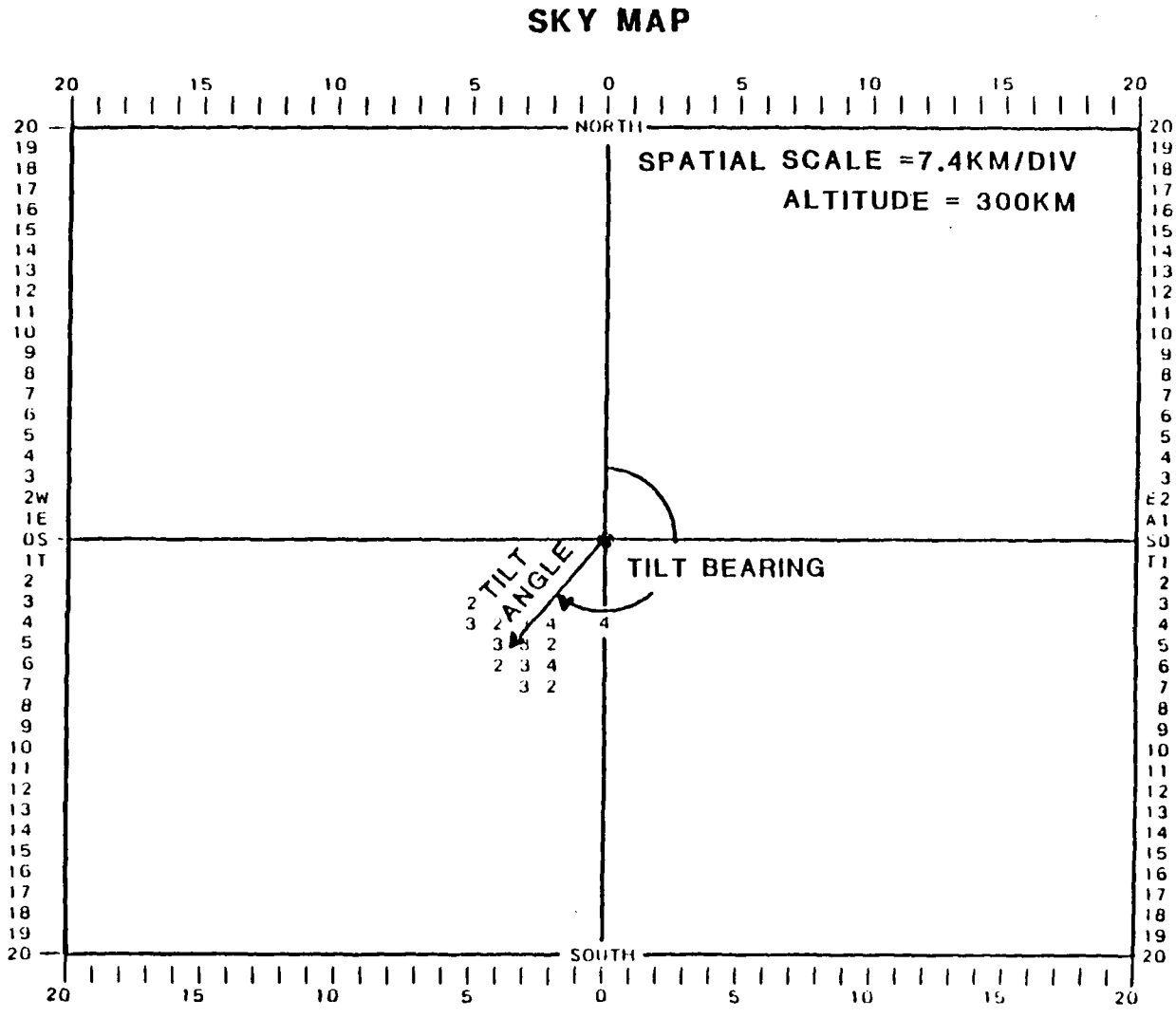

Figure 10.4 Cumulative Sky Map, Erie, CO

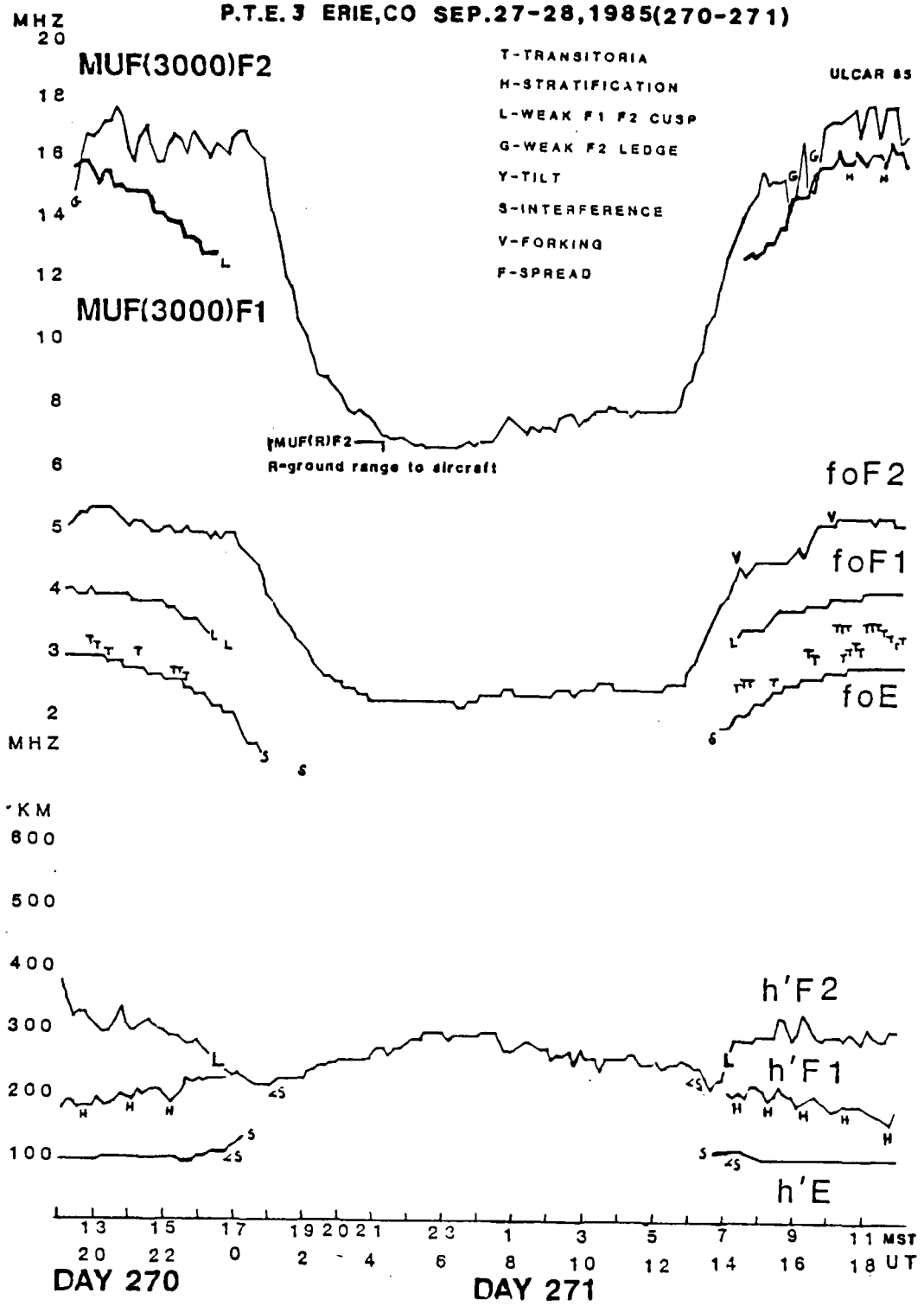

Figure 10.5 Composite Plots of the Maximum Usable Frequencies and Ionospheric Characteristics, ERie, CO, 27-28 September 1985, 1200 - 1100 MST

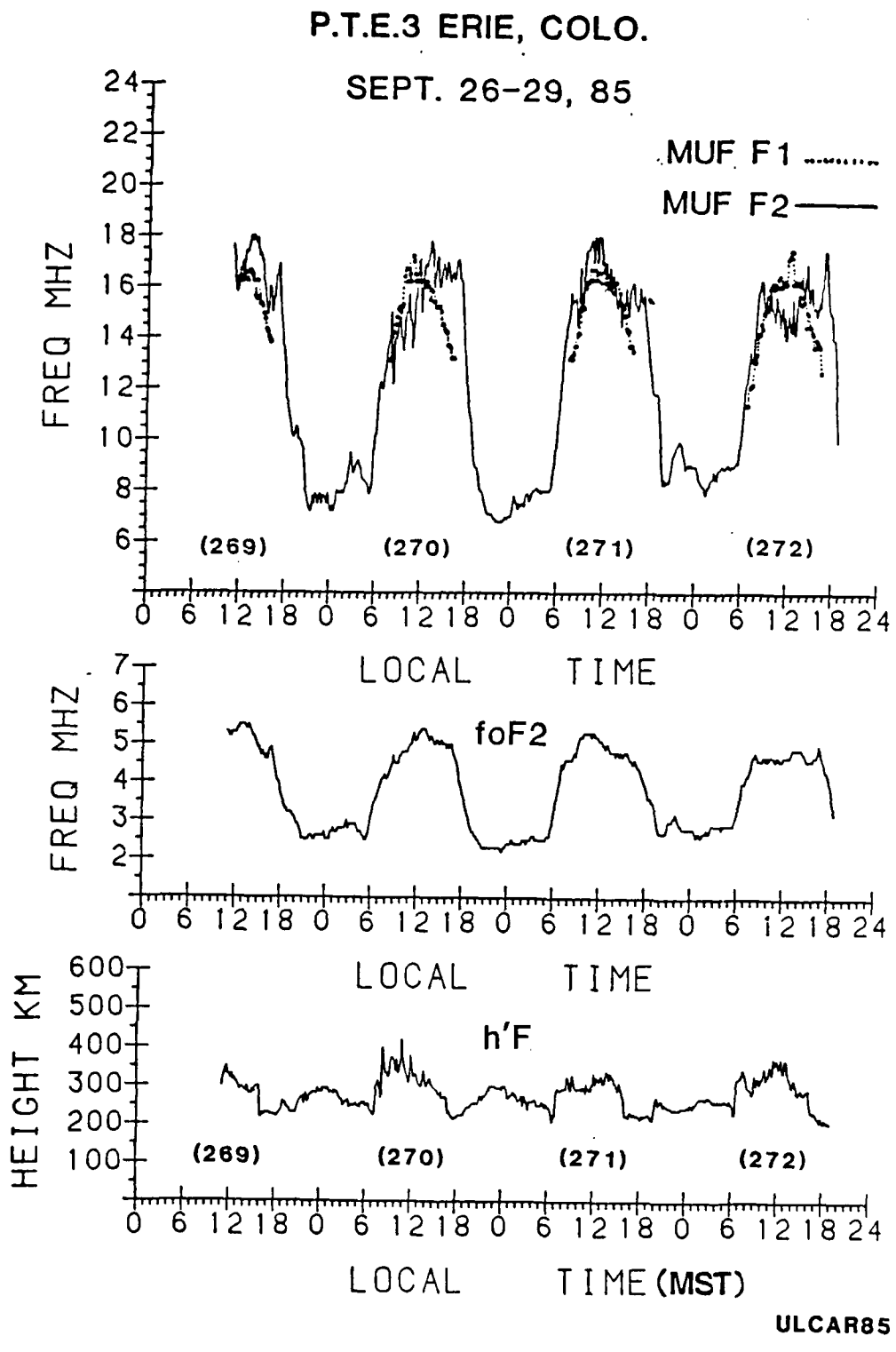

Figure 10.6 Composite Plots of the Maximum Usable Frequencies and F-Region Parameters, Erie, CO, 26/29 September 1985, 1200 - 2400 MST

April 1985 we saw a rather abrupt change in the "roughness" of the F-layer as the ionosphere transitions from day to night and vice versa. These observations were reported at the January 1986 and 1987 URSI Conferences in Boulder, CO (Reinisch et al, 1986; Sales et al, 1987). In these two earlier flights the operation period did not include this transition from the smooth daytime ionosphere to a rough nighttime one. In the September mission the switch occurred relatively abruptly near the middle of the flight at 0241 UT. For the September mission the median tilt angle was 3.2°, with ±1.6° representing the upper and lower decile. For the night period the median tilt increased to 10.0° with the upper and lower decile at ±5°. It is unlikely that this median tilt angle of 10° represents a real tilt. A simple analysis has shown that if the ionosphere were uniformly rough over any significant portion of the sky (sky maps were limited to 15° from zenith) then the median tilt should be 11°. The conclusion here is that the ionosphere has become rough at night with scattering centers located over large areas of the sky.

On the basis of comparison between the operating frequencies of the radar and the measured MUF, the frequency management of the radar was found to be very effective. Naturally this experiment had the advantage of both midpoint vertical incidence soundings, and oblique soundings to the AFGL aircraft. Complete analysis of the propagation modes and the effects of tilts on the coordinate registration process will be performed at a later date.

11.0 OBLIQUE HEATING EXPERIMENT

This experiment was an attempt to modify the ionosphere using high power oblique incidence HF radio waves, and is described in Scientific Report No. 5 (Sales et al, 1986). It ran for a week in May 1984, using the RADC transmitter facility at Ava (Rome), NY, for the oblique heating, and a Digisonde 256 for vertical ionospheric sounding at the projected interaction point, Tullahoma, TN. The sounder was run continuously. Real-time scaling by ARTIST gave the MUF values for the circuit (2000 km), and these were transmitted by telephone to the operations of the Ava transmitter, who modified the transmitter frequency appropriately.

Oblique heating cannot take advantage of the resonance phenomena that make vertical incidence heating such an effective process. Theoretical analysis shows that electron heating is the most likely mechanism for producing changes in the remote ionosphere. Strong electric fields are predicted in the caustic region near the reflection point, as illustrated in Figure 11.1. These intense fields are responsible for the ionospheric heating and, when combined with heat conduction, can produce a modified region of sufficient size to affect other radio waves incident on this region. Figure 11.2 shows the calculated contours of electron temperature for the specified conditions. The available transmitter had an effective radiated power of 20 MW, but it was recognized at the outset that the configuration was probably underpowered and not likely to induce detectable changes in the ionosphere at Tullahoma.

No changes in the ionosphere were in fact detected. This was partly due to the low power used, which must be increased by at least a factor of four to ensure any chance of

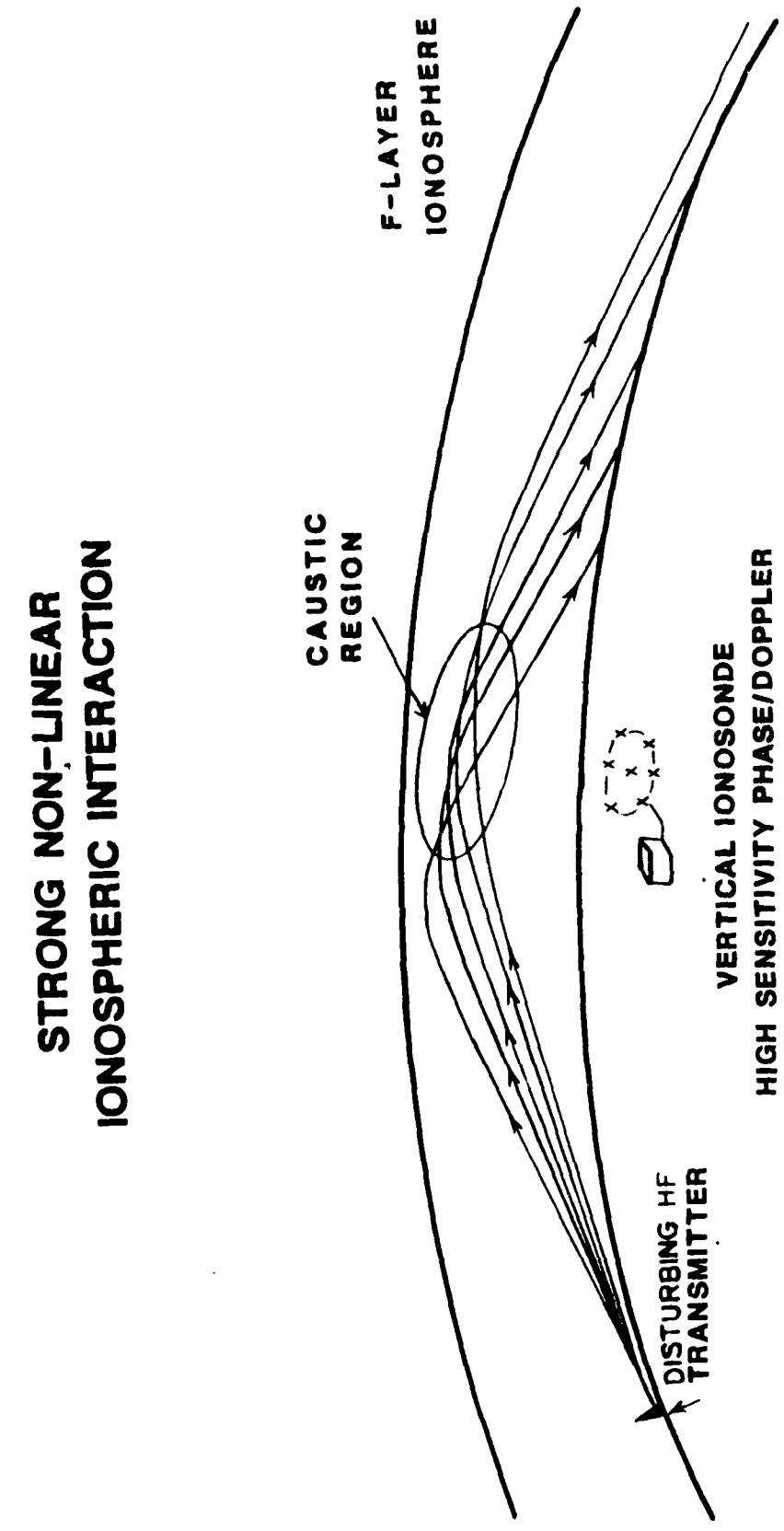

Figure II.1 Oblique Heating Experimental Setup Showing Caustic Region

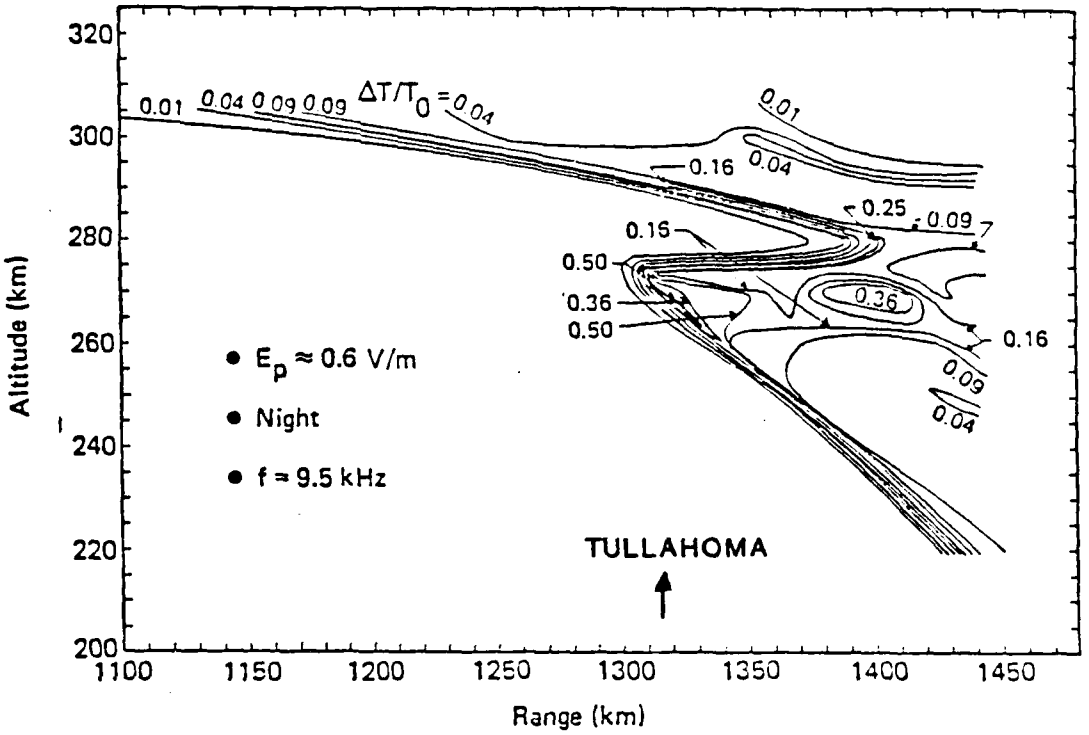

Figure 11.2 Calculated Contours of Electron Temperature in the Caustic Region

success. Analysis of the data obtained also indicated that inappropriate choices had been made for the heater cycling time. Theoretical studies had shown that approximately 120 seconds would be required to develop the heated region, so it was decided to use a 10-minute heating cycle, i.e. 8 minutes on, and 2 minutes off. However, it was found that the background noise had high spectral densities near the chosen 10-minute period, obscuring any wanted signal.

Plans are in hand to repeat the experiment, perhaps on a different circuit and using a different transmitter, taking advantage of the experience gained to date. In particular, the heater cycle time will be reduced to 5 minutes.

12.0 AWS OTH RADAR TRAINING MANUAL

The ULCAR contribution to the proposed Air Weather Service (AWS) Over-the-Horizon Radar Training Manual is the chapter on propagation. The manual will be used by AWS personnel responsible for the environmental assessment (EA) function of the OTH-B system in Maine.

The chapter on propagation is close to completion. ULCAR has developed the software necessary to synthesize backscatter ionograms as would be seen at the site. Figure 12.1 shows a synthesized backscatter ionogram, compared with an actual backscatter ionogram made at the ERS site during the winter of 1980. The synthesized ionogram shows the mode structure and signal strength that will serve to train the AWS EA operators to recognize the structure of the backscatter ionograms.

A new method has been developed which allows the IONOCAP prediction code to be used to compute the orthogonality condition for simulating ionospheric clutter. The calculated clutter will form part of the synthesized backscatter ionogram.

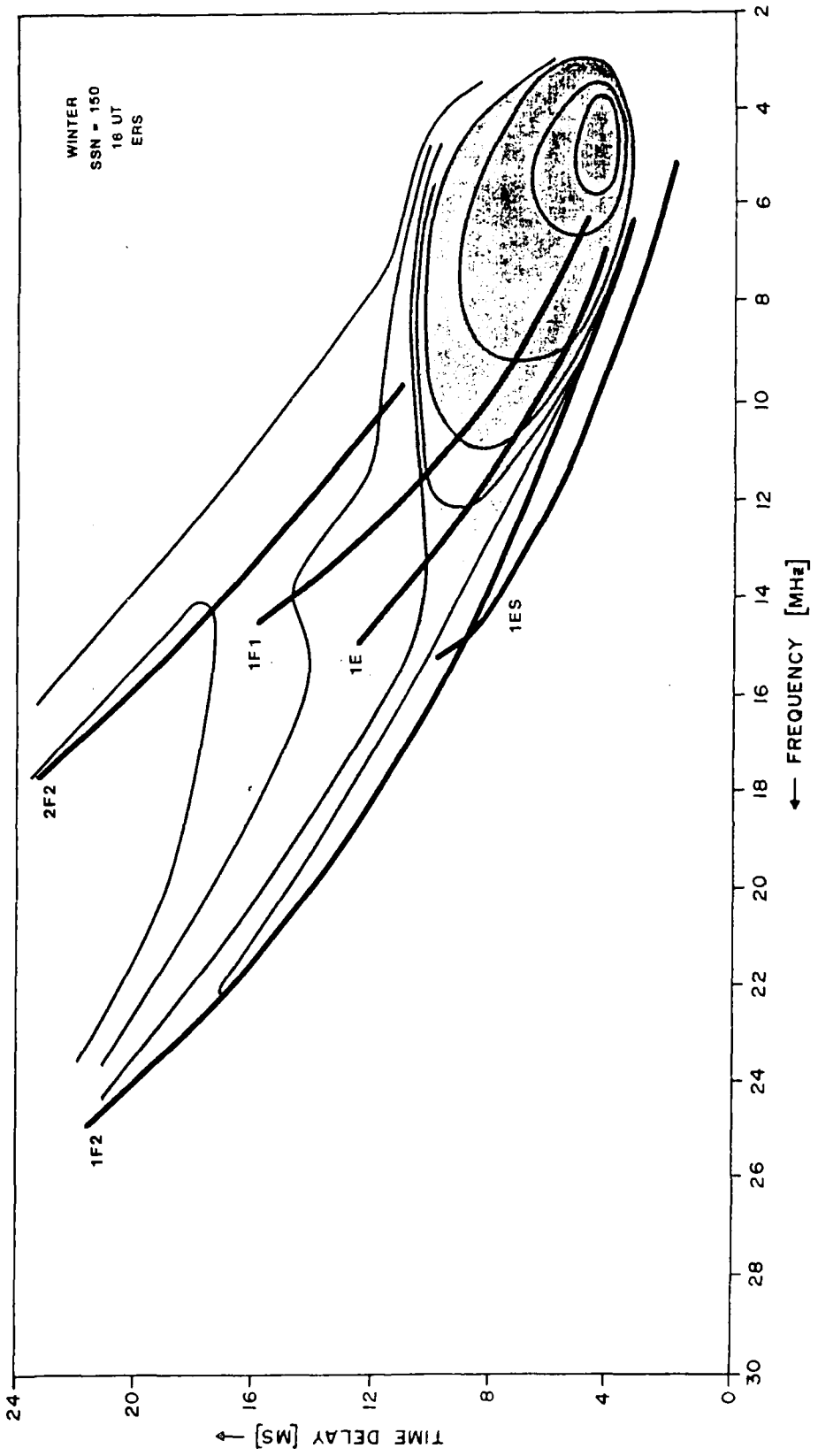

Figure 12.1 Synthesized Backscatter Ionogram Compared to an Actual Backscatter Ionogram, OTH-B Experimental Radar System, Winter 1980, Sunspot Number of 150

13.0 COMPRESSED DATA AND MICROFICHE

New techniques for the further processing or compression of Digisonde data have been developed.

13.1 Ionospheric Characteristics on Microfiche

A computer program has been written for use on the AFGL computer which stores ionospheric characteristics on microfiche. Amplitude, frequency and height variations as a function of time, and velocity filtered characteristics are displayed with appropriate scales and titles. Digisonde tapes can now be processed at AFGL, with the options of either printing by Versatec or displaying on microfiche, or both. Figure 13.1 shows examples of the microfiche presentation for 36 hours of data recorded at Goose Bay during 3-4 December 1983. The top two panels are the F and E frequency characteristics (f plots) from the vertical ionograms, while the third panel is the integrated virtual height. The bottom two panels are the frequency and height characteristics from the backscatter ionograms.

Improved backscatter characteristics were obtained by removing the vertical echoes from the backscatter characteristics. Since the Goose Bay Digisonde records alternately vertical and backscatter ionograms, the program first records the height bins with echoes as either O or X for each vertical ionogram, then erases the echoes for the same height and frequency in the following oblique ionogram. Figures 13.2 and 13.3 are the ionospheric characteristics for Goose Bay on January 1-3, 1984. In Figure 13.2, the backscatter characteristics include overhead echoes, while in Figure 13.3, the overhead echoes have been removed from the backscatter characteristics.

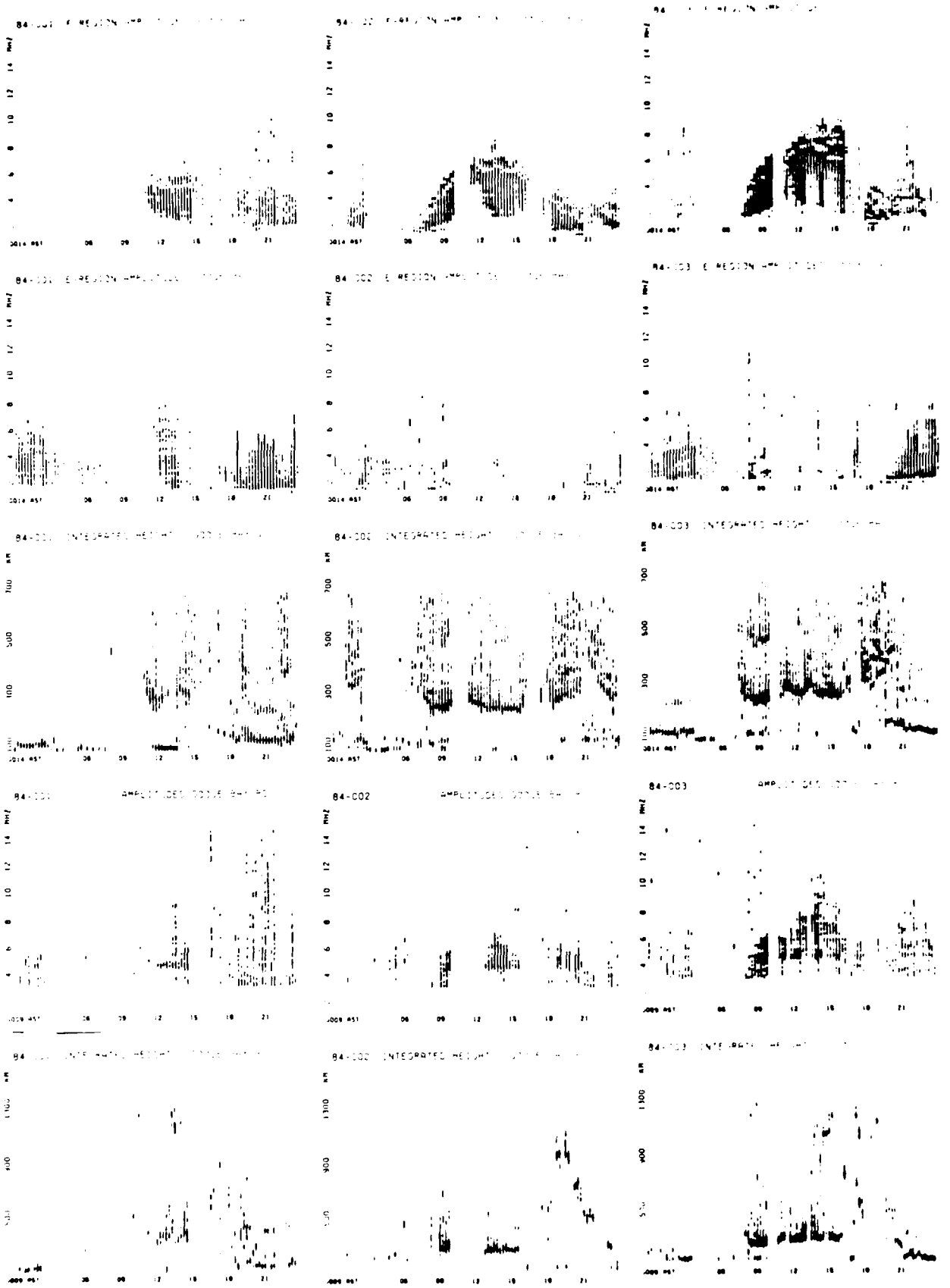

Figure 13.2 Ionospheric Characteristics from Backscatter Ionograms, Goose Bay, Labrador, 1-3 January 1984

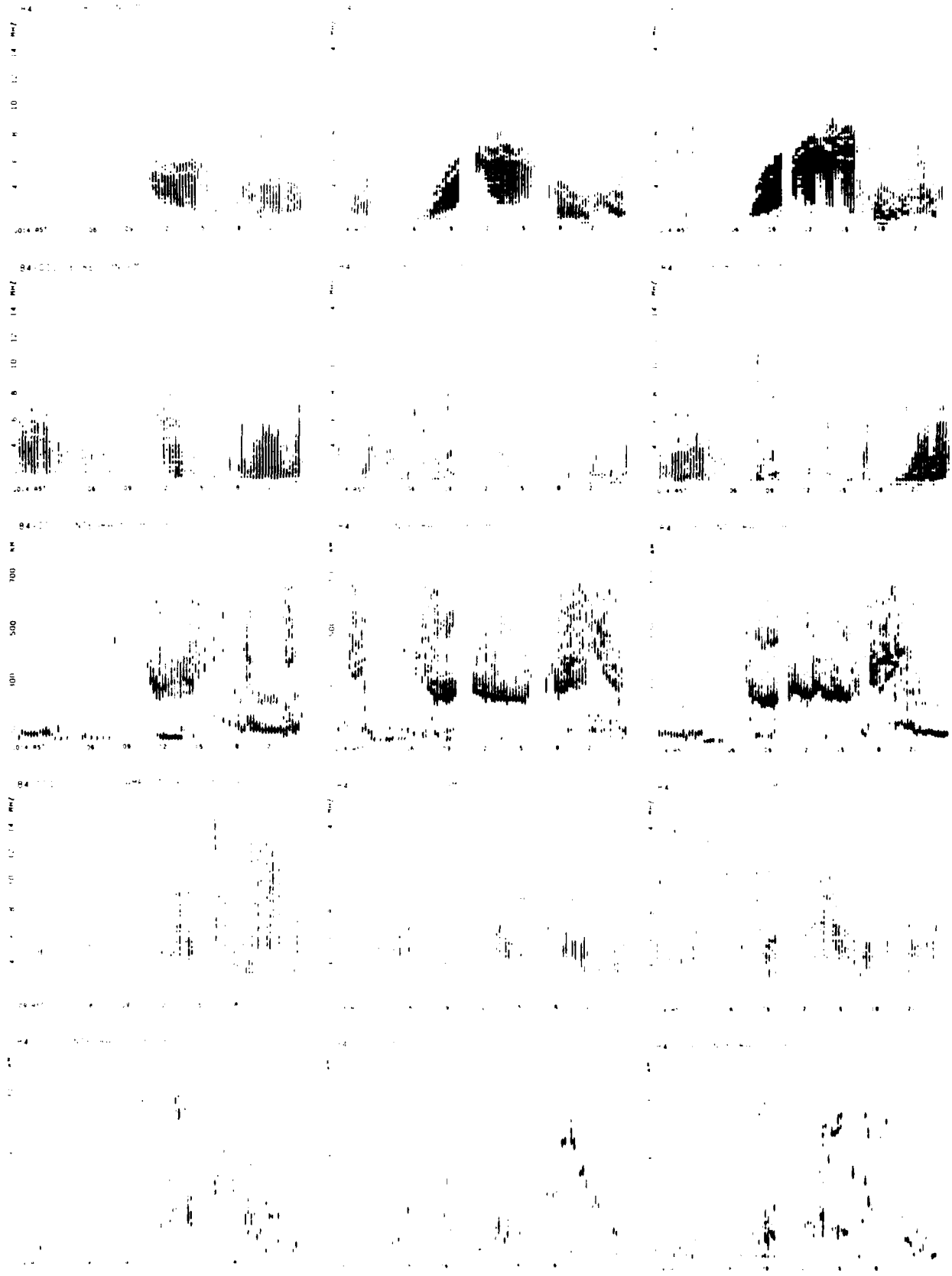

Figure 13.3 Ionospheric Characteristics Data Collected at Goose Bay
Ionograms (Vertical Echoes Removed), Goose
Bay, Labrador, 1-5 January 1984

13.2 Directional Ionograms on Microfiche

The 1984 Thule ionograms alternately scanned the north-south direction in one ionogram and the east-west direction in the next. A computer program was developed to merge each ionogram with the preceding ionogram, with the status value of each echo in the merged ionogram indicating the direction of signal arrival, and the O and X polarization for the vertical echoes. The resulting ionograms are displayed on microfiche. A sequence of five directional ionograms from Thule on 3 February 1984, starting at 23:09 UT and spaced by 2.5 minutes, is shown in Figure 13.4. The ionogram type (status) from top to bottom is north, east, south, west directions, ordinary and extraordinary vertical. At 23:14, ionization approaches (indicated by the positive Doppler shifts) from the north (top panel). At 23:29 (not shown), the ionization moves away (negative Doppler shifts) toward the south.

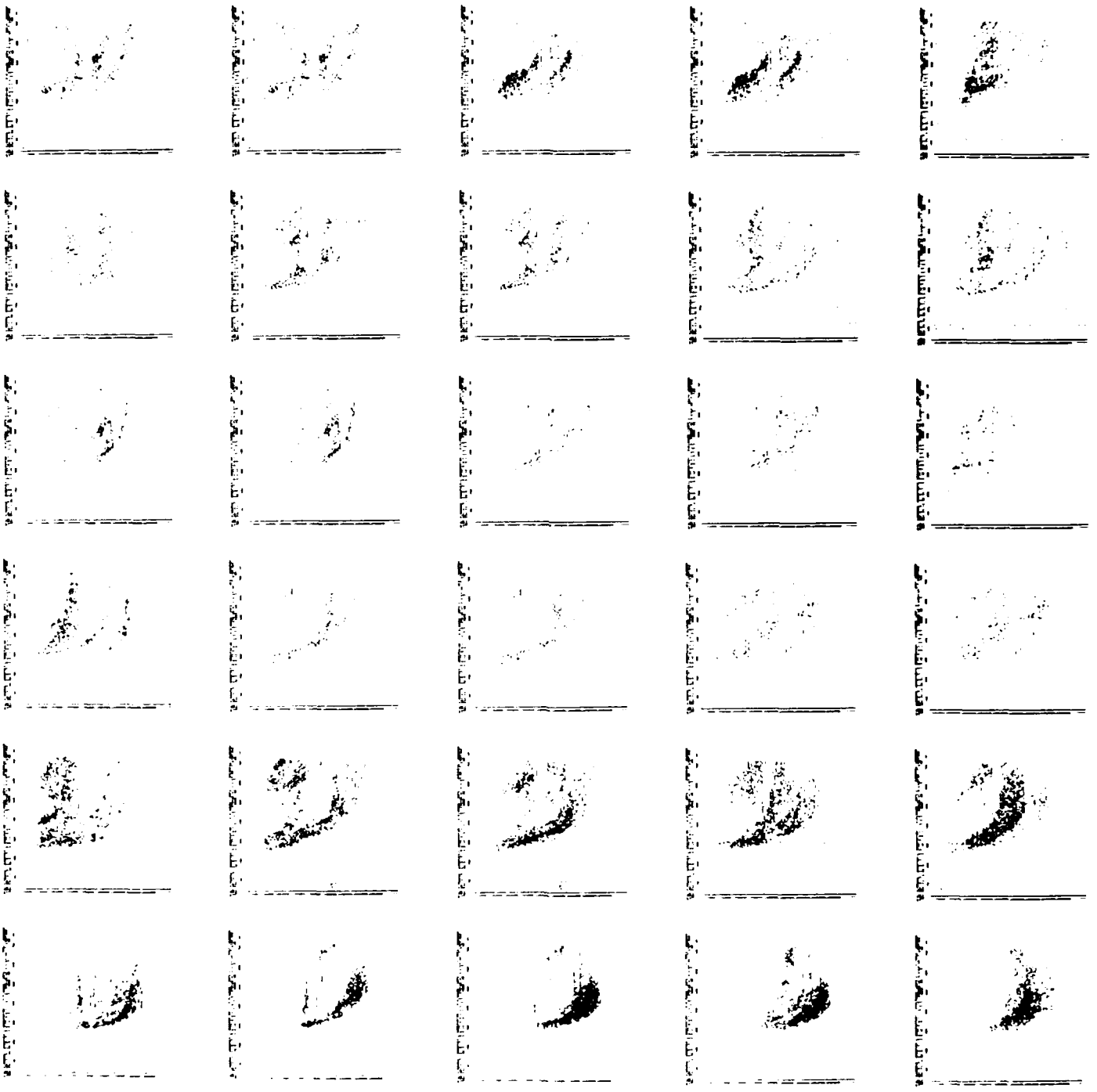

Figure 3.3.4 Directional Ionograms, Thule, Greenland,
3 February 1984, 2304 - 2319 UT

14.0 BATTLE-TOAD EXPERIMENTS IN UTAH

Project BATTLE-TOAD was an HF experiment conducted in October 1984 to test the concept of employing cooperative beacons to improve the accuracy of HF time-of-arrival-difference (TOAD) geolocation systems. The experiment involved continuous transmission of HF signals from ten transmitting sites (taken two at a time) to five receiver sites. Vertical incidence ionosondes were operated at Boulder, Colorado; Los Alamos, New Mexico; and Richfield, Utah. The observations were used to provide real-time information about the ionospheric structure in the vicinity of the experiment. The ionosonde information was used in conjunction with propagation predictions obtained from the program IONCAP to provide quasi-real time frequency management for all the circuits. Acceptable communications, i.e. hearability, was achieved for over 90% of the duration of the experiment.

ULCAR installed a Digisonde 256 system with a TCI wideband dipole transmitting antenna and four receiving crossed-loop antennas at Richfield, Utah, to serve as an ionospheric reference station for the TOAD experiments.

Observations commenced on 7 October 1984, with a five-minute sequence of vertical incidence ionograms for 12 hour test periods each day through 18 October 1984. Hourly ionograms were recorded in between these test periods. The data were recorded on magnetic tape and printed on a local printer. The ARTIST-scaled data were automatically transmitted by telephone line to Boulder every five minutes, where the data were used to make propagation predictions to validate the overall project concept. An example of the ARTIST data is shown in Figure 14.1 for October 13, 1984 at 19:59 UT. A report on the project was presented by Rush et al (1985) at the URSI meeting in Vancouver, Canada.

```
+-------------------------------------------------------------+
+  T.O.A.D. - RICHFIELD. UTAH - LAT 39N LONG 112W - OCTOBER 1984  +
+  DIGISONDE 256 - UNIVERSITY OF LOWELL - CEN. FOR ATMOS. RSCH.   +
+-------------------------------------------------------------+

STATION YEAR DAY H  M      OUT OPT B  E  G CAB XLZT NRW HEIG PROGRAM
  891   1984 287 19:59 UT 1484300 01-11 1 12E 4463 534 1205.  A1

FOF2  FOF1  H'F   H'F2  M1000 FMIN  FOES  MUF   FMINF
 7.9   4.4  203.  278.  1.64   1.9   3.0  13.0   3.2

FXI   FMINE FOE   H'E   H'ES  QF    QE    FF    FE
 8.7   1.9   3.0  103.  103.  ***   ***   ***    .3

AUTOSCALED TRACES [KM]:
-----------------------
 3.  *****  *****  ****.  ****.  ****.  ****.  ****.  ****.  ****.  ****.
 4.   630.   645.  ****.  ****.  ****.  ****.  ****.  ****.  ****.  ****.
 5.   277.   277.  ****.  ****.  ****.  ****.  ****.  ****.  ****.  ****.
 6.   282.   287.  ****.  ****.  ****.  ****.  ****.  ****.  ****.  ****.
 7.   307.   312.  ****.  ****.  ****.  ****.  ****.  ****.  ****.  ****.
 1.  *****  *****  *****  *****  *****  *****  *****  *****  *****   95.
 2.   100.   100.   100.   100.   105.   105.   105.   110.   115.   120.
 3.   130.

NORMALIZED AMPLITUDE AS AT REFLECTION HEIGHT 100KM IN [DB]
      TOPF     2.     3.     4.     5.     6.     7.
 F     33.    30.     0.    56.    65.    69.    64.
 E     19.    37.
ES     19.    37.
```

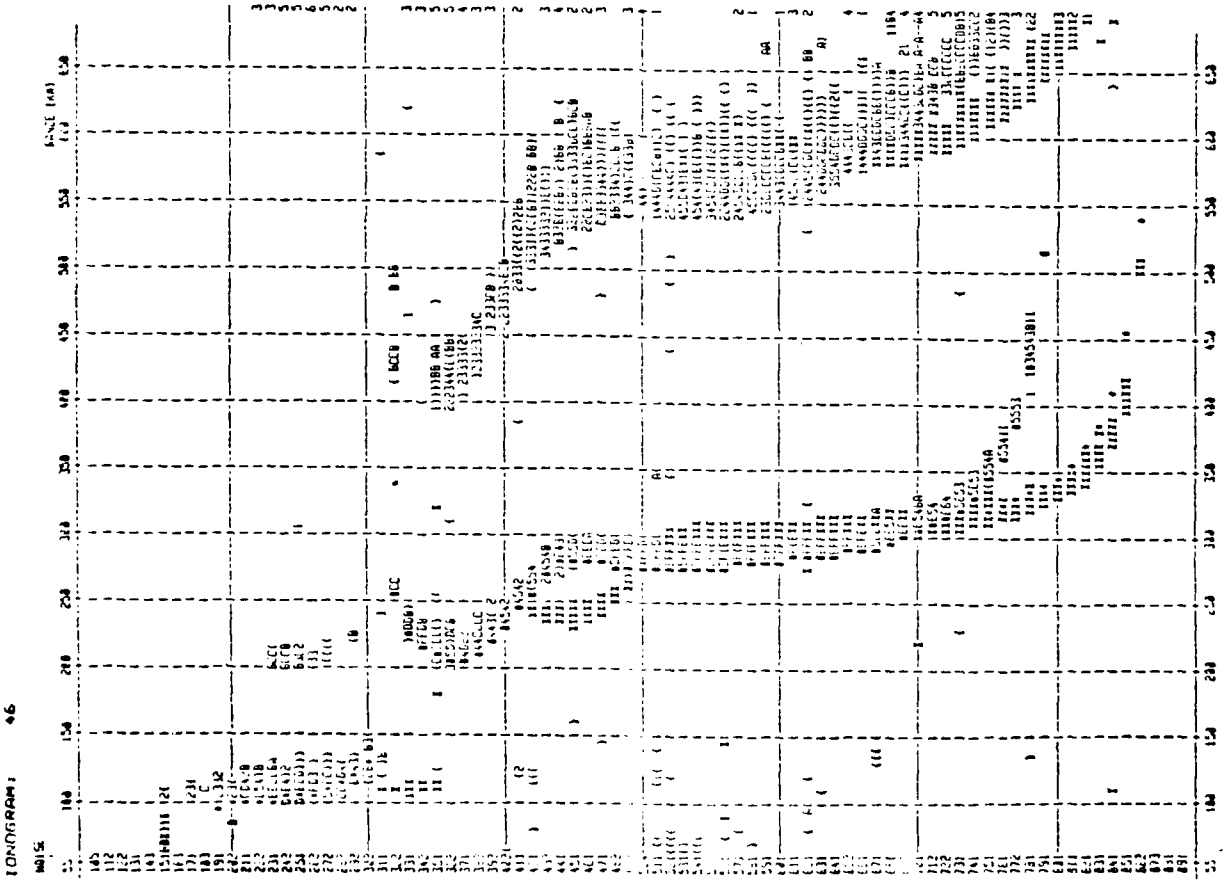

Figure 14.1 ARTIST Scaled Ionogram Data; Example of Automatically Transmitted Information from Richfield, Utah, 13 October 1984, 1959 UT

15.0 CHEMICAL RELEASES AT WALLOPS ISLAND

Upper atmospheric chemical release experiments were carried out from Wallops Island (Virginia) during October and November 1983. The AFGL airborne ionospheric observatory was used to monitor the ionosphere at optical and radio wavelengths. ULCAR personnel operated the Digisonde on board the aircraft, to observe the effects of the chemical releases. Ionograms were recorded on paper and magnetic tape every 2.5 minutes.

A small depletion was observed for about ten minutes after the night release (0520 UT) on 9 November. ULCAR also operated a Digisonde 256 in Lowell, Massachusetts during the rocket campaign, using a log-periodic antenna pointing towards Wallops Island. No rocket related signatures were detected with the Lowell sounder.

16.0 DIGISONDE 256 RF POWER TESTS AT WALLOPS ISLAND

A Digisonde 256, built for operation at Bermuda, with a 7-element array of crossed-loop receiving antennas was deployed at the NASA Wallops Flight Facility, Wallops Island, Virginia on 16 June 1986. A programmable attenuator was inserted between the Digisonde 256 Processor's RF output and the 10 kW final amplifier to provide control of the transmitter output power. Four power levels were used with nominal output power of 7 kW, 1 kW, 170 W and 30 W (actual measured outputs versus frequency are plotted in Figure 16.1). These levels were achieved using 0 dB, 22 dB, 28 dB and 34 dB of in-line attenuation under automatic control of the Processor's input computer. The transmitter could be operated into either of two antennas, a TCI (Technology for Communications International) 613 or TCI 613T antenna. These were also selected under automatic control of the Processor's input computer via a coaxial relay. Therefore, a total of eight operational configurations were employed, four power levels into each of two antennas. The eight configurations were operated once every 30 minutes throughout the day and night from 20 June 1986 to 4 July 1986.

Using the Digisonde performanc at a 7 kW transmit power level as a reference, the degradation of data quality as a function of reduced transmit power levels was determined for two antennas, the TCI 613T and TCI 613 models.

The statistics of median error, mean error and standard deviation of foF2 and M3000 parameters showed an acceptable degradation for the 1 kW transmit power level on the 613T antennas. Surprisingly accurate results were obtained at the 170 W transmit level on the 613 antenna. The 613 antenna consistently resulted in a 4 to 6 dB stronger echo than

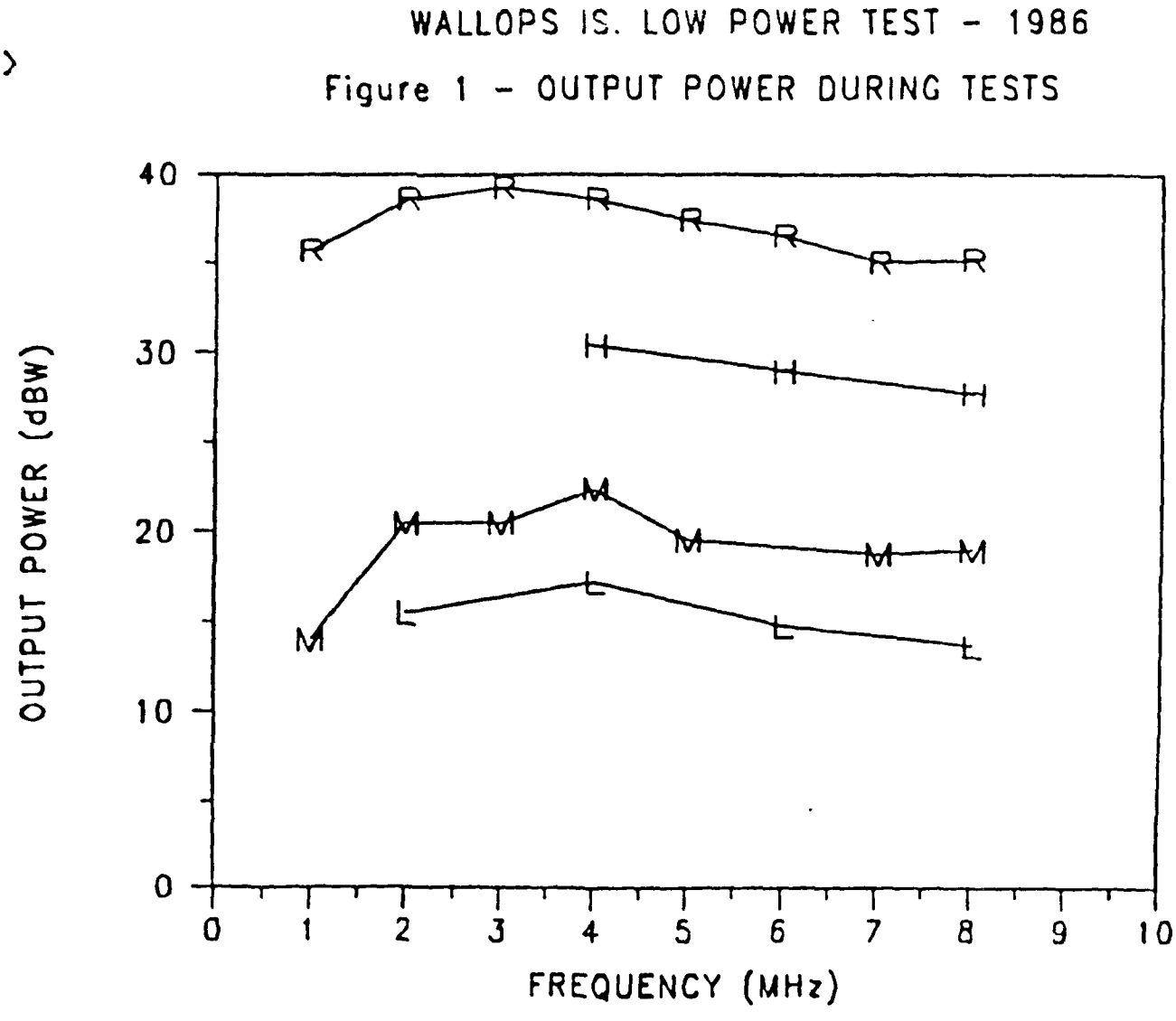

Figure 16.1 Digisonde Output Power Levels vs. Frequency for 0, 22, 28 and 34 dB Attenuation, Wallops Island, VA, 16 June 1986

those obtained using the 613T antenna. This is reflected by similarities between percentage scaled from the 613 at 170 Watts and the 613T at 1 kW. Either of these two configurations maintains a low to mid 90's percentage of being able to automatically scale the ionograms with an occasional slip into the 80's. We consider this acceptable for general purpose data to support propagation predictions or radar frequency management.

As best compromise, we recommend the use of the 613 antenna with an RF power of 500-1000 Watts. The Test and Evaluation Report by Haines (1986) describes the measurements in full detail.

17.0 PAPERS, PRESENTATIONS AND REPORTS

Papers

"F-Layer Ionization Patches in the Polar Cap," B. W. Reinisch, E. J. Weber, J. Buchau, J. G. Moore, J. R. Sharber, R. C. Livingston and J. D. Winningham, J. Geophys. Res., Vol. 89, No. A3, pp. 1683-1694, March 1984.

"Ionospheric Structures in the Polar Cap: Their Origin and Relation to 250 MHz Scintillation," B. W. Reinisch, J. Buchau, D. N. Anderson, E. J. Weber, H. C. Carlson, J. C. Moore and R. C. Livingston, Radio Science, Vol. 20, No. 3, pp. 325-338, May-June 1985.

"New Techniques in Ground-Based Ionospheric Sounding and Studies," Radio Science, Vol. 21, No. 3, pp. 331-341, May-June 1986.

"Digital Ionosonde Observations of the Polar Cap F Region Convection," B. W. Reinisch, J. Buchau and E. J. Weber, Proceedings of the STP-International Symposium on Solar Terrestrial Physics, XXVI COSPAR, Toulouse, France, June 30-July 12, 1986.

Presentations

"Ionospheric Drift Measurements with Digital Ionosondes," B. W. Reinisch, K. Bibl and C. G. Dozois, International Symposium on Space Physics, November 10-14, 1986, Beijing, The People's Republic of China.

"Digital Ionosonde Observations of the Polar Cap F Region Convection," B. W. Reinisch, J. Buchau and E. J. Weber, XXVIth COSPAR Meeting, June 30-July 12, 1986, Toulouse, France.

Reports

"Electron Density Profiles from Automatically Scaled Digital Ionograms. The ARTIST's Valley Solution," R. R. Gamache, W. T. Kersey and B. W. Reinisch, Scientific Report No. 1, AFGL-TR-85-0181, ULRF-434/CAR, 1985. ADA180990

"Ionospheric Propagation Studies During the Precision Targeting Experiments," B. W. Reinisch, G. S. Sales, K. Bibl and C. G. Dozois, Scientific Report No. 2, AFGL-TR-86-0030, ULRF-431/CAR, ADA172316, 1986.

"Quality Control of True Height Profiles Obtained Automatically from Digital Ionograms," L. F. McNamara, Scientific Report No. 3, AFGL-TR-86-0098, ULRF-432/CAR, ADA171328, 1986.

"Ionosonde Studies of Field-Aligned Irregularities During High-Power HF Heating at Arecibo," B. W. Reinisch, L. F. McNamara and J. Buchau, Scientific Report No. 4, AFGL-TR-86-0168, ULRF-434/CAR, 1986.

"Digisonde 256 RF Power Tests at Wallops Island. Test Evaluation Report," D. M. Haines, Scientific Report No. 5, AFGL-TR-86-0185, ADA173831, August 1986.

"Preliminary Investigation of Ionospheric Modification Using Oblique Incidence High Power HF Radio Waves," G. S. Sales, B. W. Reinisch and C. G. Dozois, Scientific Report No. 6, AFGL-TR-86-0203, ULRF-435/CAR, September 1986. ADA179174

"High Latitude F-Region Drift Studies," Bodo W. Reinisch, Jurgen Buchau, Edward J. Weber, Claude G. Dozois and Klaus Bibl, Scientific Report No. 7, ULRF-436/CAR, AFGL-TR-87-0154 , December 1986. ADA184466

18.0 REFERENCES

Bibl, K., B. W. Reinisch and D. F. Kitrosser, "Digisonde 256: General Description of the Compact Digital Ionospheric Sounder," University of Lowell, First Edition, December 1981; Revised.

British Antarctic Survey Scientific Report 88 or JATP 40, pp. 629-640, 1983.

CCIR, "Propagation Prediction Methods for High Frequency Broadcasting," Report 894, International Radio Consultative Committee, International Telecommunications Union, Geneva, Switzerland,

CCIR, "Second CCIR Computer-Based Interim Method for Estimating Skywave Field Strength and Transmission Loss at Frequencies Between 2 and 30 MHz," Supplement to Report 252,

Dozois, C. G., "A High Frequency Radio Technique for Measuring Plasma Drifts in the Ionosphere," Scientific Report No. 6, AFGL-TR-83-0202, ULRF-424/CAR, ADA140509, 1983.

Dudeney, J. R., "The Accuracy of Simple Methods for Determining the Height of the Maximum Electron Concentration of the F2 Layer from Scaled Ionospheric Characteristics," J. Atmos. Terr. Phys., 45, 629-640 (1983).

Gamache, R. R., W. T. Kersey and B. W. Reinisch, "Electron Density Profiles from Automatically Scaled Digital Ionograms. The ARTIST's Valley Solution," Scientific Report No. 1, AFGL-TR-85-0181, Air Force Geophysics Laboratory (1985). ADA180990

Haines, D. M., "Digisonde 256 RF Power Tests at Wallops Island. Test Evaluation Report," Scientific Report No. 5, AFGL-TR-86-0185, ADA173831, August 1986.

Huang, X. and B. W. Reinisch, "Automatic Calculation of Electron Density Profiles from Digital Ionograms. 2. True Height Inversion of Topside Ionograms with the Profile-Fitting Method," Radio Science, 17, 4, 837 (1982).

McNamara, L. F., "A Comparative Study of Methods of Electron Density Profile Analysis," World Data Center A for Solar-Terrestrial Physics Report, UAG-68, Boulder, CO, 1979.

McNamara, L. F., "Model Starting Heights for N(h) Analysis of Ionograms," J. Atmos. Terr. Phys. 41, 543-548, 1979.

McNamara, L. F., B. W. Reinisch and J. Tang, "Values of hmF2 Deduced from Automatically Scaled Ionograms," Space Research XV, Proceedings of COSPAR Meeting in Toulouse, France, June 1986.

Paul, A. K., "Processing of Digital Ionograms," NOSC TD 529, 1982.

Reinisch, B. W. and K. Bibl, "Ionospheric Research Using Digital Ionosondes," Final Report, March 1980-April 1983, AFGL-TR-83-0184, ADA140012, July 1983.

Reinisch, B. W., J. Buchau, E. J. Weber, C. G. Dozois and K. Bibl, "High Latitude F-Region Drift Studies," Scientific Report No. 7, ULRF-436/CAR, AFGL-TR-87-0154 , December 1986. ADA184466

Reinisch, B. W. and X. Huang, "Automatic Calculation of Electron Density Profiles from Digital Ionograms. 3. Processing of Bottomside Ionograms," Radio Science, 18, 477 (1983).

Sales, G. S., B. W. Reinisch and C. G. Dozois, "Preliminary Investigation of Ionospheric Modification using Oblique Incidence High Power HF Radio Waves," Scientific Report No. 6, AFGL-TR-86-0203, ULRF-435/CAR, September 1986. ADA179174

Shimazaki, T., "World-Wide Daily Variations in the Height of the Maximum Electron Density in the Ionospheric F2 Layer," J. Radio Res. Labs., Japan, 2(2), 86-97 (1955).

Snyder, M. A., "Chevyshev Methods in Numerical Approximation," Prentice Hall, New Jersey (1966).

Titheridge, J. E., "The Generalized Polynomial Analysis of Ionograms," Technical Report No. 78/1a, Radio Research Centre, the University of Aukland, New Zealand.

Titheridge, J. E., "Ionogram Analysis with the Generalised Program POLAN," World Data Center A for Solar-Terrestrial Physics, Report UAG-93, December 1985.

END

DATE

FILMED

6-1988

DTIC